NASA Contractor Report 2919

A Two-Scale Scattering Model With Application to the JONSWAP '75 Aircraft Microwave Scatterometer Experiment

Frank J. Wentz

CONTRACT NAS1-14330
DECEMBER 1977

NASA

NASA Contractor Report 2919

A Two-Scale Scattering Model With Application to the JONSWAP '75 Aircraft Microwave Scatterometer Experiment

Frank J. Wentz
Frank J. Wentz & Associates
Cambridge, Massachusetts

Prepared for
Langley Research Center
under Contract NAS1-14330

National Aeronautics
and Space Administration

**Scientific and Technical
Information Office**

1977

TABLE OF CONTENTS

SUMMARY

In the first part of this report, we treat the general problem of bistatic scattering from a two-scale surface. The treatment is entirely two-dimensional and is in a vector formulation independent of any particular coordinate system. The two-scale scattering model is then applied in the second part to backscattering from the sea surface. In particular, the model is used in conjunction with the JONSWAP '75 aircraft scatterometer measurements to determine the sea surface's two-scale roughness distributions, namely the probability density of the large-scale surface slope and the capillary wavenumber spectrum. Best fits yield, on the average, a 0.7 dB rms difference between the model computations and the vertical polarization measurements of the normalized radar cross section. Correlations between the distribution parameters and the wind speed are established from linear, least-squares regressions.

NORMALIZED RADAR CROSS SECTION OF A TWO-SCALE SURFACE

Introduction

In the first part of this report we extend the two-scale scattering model developed by Wentz [1975] to include an anisotropic wavenumber spectrum for the small-scale roughness. The original notation is modified so that the formulation is completely in vector form with no reference to a particular coordinate system. Also, the scattering pattern is expressed in terms of the normalized radar cross section (NRCS) rather than in terms of a scattering coefficient. An asterisk superscript to an equation number indicates that the equation is from Wentz [1975]. The correspondence of the original notation to that used herein is detailed in Appendix A, which lists important quantities in terms of both notations.

Rice's [1951] perturbation theory for small-scale scattering is a fundamental part of the two-scale model. It should be noted that he required the small-scale wavenumber spectrum to be symmetric about the plane of incidence. We remove this requirement, and as a result, two cross-polarization terms appear in the expressions for the radiation reflected in the specular direction from the surface.

The author is grateful to W. L. Jones of NASA Langley for his support and assistance throughout this research. He also wishes to thank L. C. Schroeder of NASA Langley and J. L. Mitchell of LTV Aerospace Corporation for providing the summary data and plots on which the analysis is based, Professor K. Hasselman of the Max Planck Institute for Meteorology and the JONSWAP Experiment Team for supplying the wind-field analysis, and R. C. Roy for help in the preparation of the report.

Two-Scale Scattering Equation

The two-scale scattering model is based on the assumption that the NRCS for a surface can be represented by a weighted sum of the NRCS for finite regions on the surface. This weighted sum is expressed in integral form by the two-scale scattering equation that is derived in this section. In particular the two-scale surface consists of small-scale roughness superimposed onto a large-scale surface Σ_ℓ. The rms height variation of the small-scale roughness is small compared to the radiation wavelength λ, the radius of curvature at all points on Σ_ℓ is much larger than λ. The surface Σ_ℓ is divided into subregions $\Delta\Sigma_\ell$ that have dimensions large compared to λ and that are nearly flat in the respect that the variation of the surface normal is small compared to unity. The assumption is then made that these regions scatter radiation as if they were a collection of independent targets, i.e., the radiation scattered from one region does not interfere with the radiation scattered from another. Finally, the scattered radiation is assumed to escape the surface without experiencing multiple scattering.

We define the surface scattering coefficient $\Gamma(\vec{k}_i,\vec{E}_i;\vec{k}_s,\vec{E}_s;\vec{N})$ as follows:

$$P_s/P_i = \Gamma(\vec{k}_i,\vec{E}_i;\vec{k}_s,\vec{E}_s;\vec{N})\ (\vec{k}_s\cdot\vec{N})\ d\vec{k} \tag{1}$$

where P_i (P_s) is the time-averaged power of radiation that is incident onto (scattered from) the surface, that has a unit propagation vector in the

differential solid angle $d\vec{k}$ centered on $\vec{k}_i$ ($\vec{k}_s$), and that has a unit polarization vector $\vec{E}_i$ ($\vec{E}_s$), which may be complex. The argument $\vec{N}$ denotes the unit normal to the mean scattering surface. The definition of the NRCS $\sigma^o(\vec{k}_i,\vec{E}_i;\vec{k}_s,\vec{E}_s;\vec{N})$ given by Ruck [1970] is

$$\sigma^o(\vec{k}_i,\vec{E}_i;\vec{k}_s,\vec{E}_s;\vec{N}) = (4\pi/A) \lim_{r\to\infty} r^2 \langle |\vec{E}\cdot\vec{E}_s|^2 \rangle \qquad (2)$$

The scattered electric field $\vec{E}$ is the field at position $r\vec{k}_s$ (letting the surface be at the origin) produced by an incident plane wave that has unit intensity, that has a unit propagation vector $\vec{k}_i$, and that has a unit polarization vector $\vec{E}_i$. The brackets $\langle \cdot\,\cdot \rangle$ denote a time-average, and A is the area of the mean scattering surface that is subtended by the incident radiation. Poynting's relationship between the electric field and the power gives

$$P_s/P_i = \{d\vec{k}/[A(-\vec{k}_i\cdot\vec{N})]\} \lim_{r\to\infty} r^2 \langle |\vec{E}\cdot\vec{E}_s|^2 \rangle \qquad (3)$$

Combining (1), (2), and (3) gives

$$\sigma^o(\vec{k}_i,\vec{E}_i;\vec{k}_s,\vec{E}_s;\vec{N}) = 4\pi\ (-\vec{k}_i\cdot\vec{N})\ (\vec{k}_s\cdot\vec{N})\ \Gamma(\vec{k}_i,\vec{E}_i;\vec{k}_s,\vec{E}_s;\vec{N}) \qquad (4)$$

Equation (4) is used to rewrite the original formulation in terms of the NRCS. Substituting (4) into (11*) gives

$$\sigma^{o}(\vec{k}_i,\vec{E}_i;\vec{k}_s,\vec{E}_s;\vec{N}) = 4\pi\ (\vec{k}_s\cdot\vec{N})\ \chi(\vec{k}_i,\vec{N})$$

$$\int_{4\pi} d\vec{n}\ u(-\vec{k}_i\cdot\vec{n})\ u(\vec{k}_s\cdot\vec{n})\ (\vec{n}\cdot\vec{N})^{-1}\ pdf(\vec{n})\ (-\vec{k}_i\cdot\vec{n})\ \Gamma_{\Delta}(\vec{k}_i,\vec{E}_i;\vec{k}_s,\vec{E}_s;\vec{n}) \qquad (5)$$

where $\Gamma_{\Delta}(\vec{k}_i,\vec{E}_i;\vec{k}_s,\vec{E}_s;\vec{n})$ is the scattering coefficient for $\Delta\Sigma_{\ell}$ and $u(\cdots)$ is the unit step function. The quantity $pdf(\vec{n})\ d\vec{n}$ is the probability that a point on Σ_{ℓ} has a unit normal within the differential solid angle $d\vec{n}$ centered on $\vec{n}$. An additional term $u(\vec{k}_s\cdot\vec{n})$ is included in the integral and prohibits radiation from passing through the surface and into the upper hemisphere. In terms of the new notation, the shadowing function previously given by (9*) is

$$\chi(\vec{k}_i,\vec{N}) = (-\vec{k}_i\cdot\vec{N}) \Big/ \int_{4\pi} d\vec{n}\ u(-\vec{k}_i\cdot\vec{n})\ (\vec{n}\cdot\vec{N})^{-1}\ pdf(\vec{n})\ (-\vec{k}_i\cdot\vec{n}) \qquad (6)$$

For situations in which shadowing is insignificant, such as smooth surfaces or near-nadir scattering, $\chi(\vec{k}_i,\vec{N}) = 1$.

The scattering coefficient for $\Delta\Sigma_{\ell}$ is defined by

$$P_s/P_i = \Gamma_{\Delta}(\vec{k}_i,\vec{E}_i;\vec{k}_s,\vec{E}_s;\vec{n})\ (\vec{k}_s\cdot\vec{N})\ d\vec{k} \qquad (7)$$

where, in this instance, P_i and P_s refer to radiation that is incident onto and scatter from $\Delta\Sigma_{\ell}$. The NRCS $\sigma_{\Delta}(\vec{k}_i,\vec{E}_i;\vec{k}_s,\vec{E}_s;\vec{n})$ for $\Delta\Sigma_{\ell}$ is given

by (2) in which A is now the area of $\Delta\Sigma_\ell$. The relationship between the electric field and the power is still given by (3), except that $\vec{n}$ replaces $\vec{N}$, and hence

$$\sigma^o_\Delta(\vec{k}_i,\vec{E}_i;\vec{k}_s,\vec{E}_s;\vec{n}) = 4\pi\ (-\vec{k}_i\cdot\vec{n})\ (\vec{k}_s\cdot\vec{N})\ \Gamma_\Delta(\vec{k}_i,\vec{E}_i;\vec{k}_s,\vec{E}_s;\vec{n}) \tag{8}$$

Substituting (8) in (5) yields the two-scale scattering equation.

$$\sigma^o(\vec{k}_i,\vec{E}_i;\vec{k}_s,\vec{E}_s;\vec{N}) =$$
$$\chi(\vec{k}_i,\vec{N})\ \int_{4\pi}\!\!d\vec{n}\ u(-\vec{k}_i\cdot\vec{n})\ u(\vec{k}_s\cdot\vec{n})\ (\vec{n}\cdot\vec{N})^{-1}\ \mathrm{pdf}(\vec{n})\ \sigma^o_\Delta(\vec{k}_i,\vec{E}_i;\vec{k}_s,\vec{E}_s;\vec{n}) \tag{9}$$

Formulas for Bistatic Scattering

The NRCS for a region $\Delta\Sigma_\ell$ is taken to be the same as that for an infinite, random, small-scale surface Σ_s of the type defined by Rice [1951]. The surface Σ_s is tilted such that its mean surface has a normal equal to $\vec{n}$. Applying perturbation theory to Maxwell's equations, Rice found that the scattering depends upon the following implicit arguments:

1) the wavenumber k of the incident and the scattered radiation
2) the ratio ε of the surface permittivity to the permittivity of the upper medium containing the incident and the scattered radiation
3) the two-dimensional wavenumber spectrum $F(\vec{\kappa},\vec{n})$ of Σ_s.

The upper medium is assumed to be non-conducting and to have the same permeability as the surface. The spectrum $F(\vec{\kappa},\vec{n})$ is normalized such that its integral over all roughness wavenumbers $\vec{\kappa}$ equals the mean squared height variation ζ^2 on Σ_s, where $k\zeta << 1$. The argument $\vec{n}$ accounts for the fact that the spectrum in general depends on the tilt of the underlying large-scale surface.

The NRCS for Σ_s consists of a delta function pointing in the direction of specular reflection and a background of Bragg scattered power of order

$k^2\zeta^2$. Performing the integration indicated by (9), we obtain

$$\sigma^o(\vec{k}_i,\vec{E}_i;\vec{k}_s,\vec{E}_s;\vec{N}) = \pi\,\chi(\vec{k}_i,\vec{N})\,(\vec{n}_r\cdot\vec{N})^{-1}\,\mathrm{pdf}(\vec{n}_r)\,S^r(\vec{k}_i,\vec{E}_i;\vec{k}_s,\vec{E}_s;\vec{n}_r) \qquad (10)$$
$$+\,\chi(\vec{k}_i,\vec{N})\int_{4\pi}d\vec{n}\;u(-\vec{k}_i\cdot\vec{n})\;u(\vec{k}_s\cdot\vec{n})\;(\vec{n}\cdot\vec{N})^{-1}\,\mathrm{pdf}(\vec{n})\;\sigma_b^o(\vec{k}_i,\vec{E}_i;\vec{k}_s,\vec{E}_s;\vec{n})$$

$$\sigma_b^o(\vec{k}_i,\vec{E}_i;\vec{k}_s,\vec{E}_s;\vec{n}) = 16\pi k^4\;(-\vec{k}_i\cdot\vec{n})^2(\vec{k}_s\cdot\vec{n})^2\;F(\vec{\kappa}_b,\vec{n})\;S^b(\vec{k}_i,\vec{E}_i;\vec{k}_s,\vec{E}_s;\vec{n}) \qquad (11)$$

The first term in (10) is the result of integrating over the delta function, and $\sigma_b^o(\vec{k}_i,\vec{E}_i;\vec{k}_s,\vec{E}_s;\vec{n})$ is the NRCS of the remaining Bragg component. The unit vector $\vec{n}_r$ is the surface normal that produces specular reflections and is given by

$$\vec{n}_r = (\vec{k}_s - \vec{k}_i)/|\vec{k}_s - \vec{k}_i| \qquad (12)$$

The roughness wavenumber $\vec{\kappa}_b$ that is responsible for Bragg scattering in direction $\vec{k}_s$ is

$$\vec{\kappa}_b = k\,\vec{n}\times[(\vec{k}_s - \vec{k}_i)\times\vec{n}] \qquad (13)$$

The scattering function $S^m(\vec{k}_i,\vec{E}_i;\vec{k}_s,\vec{E}_s;\vec{n})$, m = r or b, is the squared absolute value of four terms that correspond to the combinations of two orthogonal incident polarizations and two orthogonal scattered polarizations.

In terms of horizontal and vertical polarizations, the scattering function is

$$S^m(\vec{k}_i,\vec{E}_i;\vec{k}_s,\vec{E}_s;\vec{n}) = \left| \sum_{\substack{\mu=h,v \\ \nu=h,v}} [\vec{E}_i \cdot \vec{e}_\mu(\vec{k}_i,\vec{n})]\ \alpha^m_{\mu\nu}\ [\vec{E}^*_s \cdot \vec{e}_\nu(\vec{k}_s,\vec{n})] \right|^2 \tag{14}$$

where * indicates complex conjugate and the $\alpha^m_{\mu\nu}$ are the scattering matrix elements for the reflected (m = r) and the Bragg scattered (m = b) radiation. The vector functions $\vec{e}_h(\vec{k},\vec{n})$ and $\vec{e}_v(\vec{k},\vec{n})$ correspond to the horizontal and vertical polarization vectors with respect to the surface normal $\vec{n}$.

$$\vec{e}_h(\vec{k},\vec{n}) = \vec{k}\times\vec{n}/|\vec{k}\times\vec{n}| \tag{15}$$

$$\vec{e}_v(\vec{k},\vec{n}) = \vec{k}\times\vec{e}_h(\vec{k},\vec{n}) \tag{16}$$

The scattering matrix elements to order $k^2\zeta^2$ for the reflected radiation are

$$\alpha^r_{hh} = \rho_h(\theta_r)\ \left(1 - 2k\cos\theta_r \int d\vec{\kappa}\ F(\vec{\kappa},\vec{n}_r)\ Q_{hh}(\vec{k}_i,\vec{k}_s,\vec{n}_r,\vec{\kappa})\right) \tag{17}$$

$$\alpha^r_{hv} = 2k\cos\theta_r \int d\vec{\kappa}\ F(\vec{\kappa},\vec{n}_r)\ Q_{hv}(\vec{k}_i,\vec{k}_s,\vec{n}_r,\vec{\kappa}) \tag{18}$$

$$\alpha^r_{vh} = -\alpha^r_{hv} \tag{19}$$

$$\alpha^r_{vv} = \rho_v(\theta_r)\ \left(1 - 2k\cos\theta_r \int d\vec{\kappa}\ F(\vec{\kappa},\vec{n}_r)\ Q_{vv}(\vec{k}_i,\vec{k}_s,\vec{n}_r,\vec{\kappa})\right) \tag{20}$$

where the integrals are over all vector wavenumbers $\vec{\kappa}$. The local incidence angle θ_r is given by

$$\cos \theta_r = -\vec{k}_i \cdot \vec{n}_r \tag{21}$$

The Fresnel reflection coefficients, $\rho_h(\theta_r)$ and $\rho_v(\theta_r)$, for horizontal and vertical polarization are

$$\rho_h(\theta_r) = [\cos \theta_r - \xi(\theta_r)]/[\cos \theta_r + \xi(\theta_r)] \tag{22}$$

$$\rho_v(\theta_r) = [\varepsilon \cos \theta_r - \xi(\theta_r)]/[\varepsilon \cos \theta_r + \xi(\theta_r)] \tag{23}$$

The Q functions in the integrands come from a second-order perturbation expansion and are somewhat complicated.

$$Q_{hh}(\vec{k}_i, \vec{k}_s, \vec{n}_r, \vec{\kappa}) = k\, \xi(\theta_r) - (c - b)(p^2 + bc)/D \tag{24}$$

$$Q_{hv}(\vec{k}_i, \vec{k}_s, \vec{n}_r, \vec{\kappa}) = -\Xi_h(\theta_r)\, \Xi_v(\theta_r)\, [(c - b)\, \xi(\theta_r)\, pq - \varepsilon k^2 \sin \theta_r\, q]/D \tag{25}$$

$$Q_{vv}(\vec{k}_i, \vec{k}_s, \vec{n}_r, \vec{\kappa}) = \{\varepsilon k\, \xi(\theta_r)\, (D - 2k \sin \theta_r\, p)$$

$$-(c - b)[\xi^2(\theta_r)\, (q^2 + bc) - \varepsilon \sin^2\theta_r\, (p^2 + q^2)]\}/[D(\varepsilon \cos^2\theta_r - \sin^2\theta_r)] \tag{26}$$

The supplementary equations are

$$\Xi_h(\theta_r) = (\varepsilon - 1)^{\frac{1}{2}}/[\cos \theta_r + \xi(\theta_r)] \tag{27}$$

$$\Xi_v(\theta_r) = (\varepsilon - 1)^{\frac{1}{2}}/[\varepsilon \cos \theta_r + \xi(\theta_r)] \tag{28}$$

$$\xi(\theta_r) = (\varepsilon - \sin^2\theta_r)^{\frac{1}{2}} \tag{29}$$

$$D = p^2 + q^2 + bc \tag{30}$$

$$b = (k^2 - p^2 - q^2)^{\frac{1}{2}} \tag{31}$$

$$c = (\varepsilon k^2 - p^2 - q^2)^{\frac{1}{2}} \tag{32}$$

$$p = \vec{n}_r \times \vec{e}_h(\vec{k}_i, \vec{n}_r) \cdot \vec{\kappa} + k \sin \theta_r \tag{33}$$

$$q = -\vec{e}_h(\vec{k}_i, \vec{n}_r) \cdot \vec{\kappa} \tag{34}$$

where $i = \sqrt{-1}$ and b is either a positive real or a negative imaginary number.

The scattering matrix elements to order $k\zeta$ for the Bragg scattered radiation [Ruck, 1970] are

$$\alpha^b_{hh} = \Xi_h(\theta_i)\ \Xi_h(\theta_s)\ \cos\Phi \tag{35}$$

$$\alpha^b_{hv} = -\Xi_h(\theta_i)\ \Xi_v(\theta_s)\ \xi(\theta_s)\ \sin\Phi \tag{36}$$

$$\alpha^b_{vh} = -\Xi_v(\theta_i)\ \Xi_h(\theta_s)\ \xi(\theta_i)\ \sin\Phi \tag{37}$$

$$\alpha^b_{vv} = \Xi_v(\theta_i)\ \Xi_v(\theta_s)\ [\varepsilon \sin\theta_i \sin\theta_s - \xi(\theta_i)\ \xi(\theta_s)\ \cos\Phi] \tag{38}$$

where the angles θ_i, θ_s, and Φ are given by

$$\cos\theta_i = -\vec{k}_i \cdot \vec{n} \tag{39}$$

$$\cos\theta_s = \vec{k}_s \cdot \vec{n} \tag{40}$$

$$\cos\Phi = \vec{e}_h(\vec{k}_i, \vec{n}) \cdot \vec{e}_h(\vec{k}_s, \vec{n}) \tag{41}$$

$$\sin\Phi = \vec{e}_h(\vec{k}_i, \vec{n}) \times \vec{e}_h(\vec{k}_s, \vec{n}) \cdot \vec{n} \tag{42}$$

DETERMINATION OF THE SEA SURFACE'S TWO-SCALE ROUGHNESS DISTRIBUTIONS FROM JONSWAP '75 SCATTEROMETER MEASUREMENTS

Introduction

We now apply the two-scale scattering model presented in the first part to the problem of backscattering from the sea surface. The backscattering is a function of the probability density $\text{pdf}(\vec{n})$ of the large-scale surface normal $\vec{n}$ and the wavenumber spectrum $F(\vec{\kappa},\vec{n})$ of the small-scale roughness superimposed on the large-scale surface ($\vec{\kappa}$ = vector wavenumber). The radiation frequency to be considered is 13.9 GHz, and as a consequence the spectrum $F(\vec{\kappa},\vec{n})$ corresponds to the capillary region of the sea wavenumber spectrum. The expressions for the two distributions, $\text{pdf}(\vec{n})$ and $F(\vec{\kappa},\vec{n})$, contain a number of unspecified parameters. Our object is to determine the distribution parameters from aircraft scatterometer measurements taken during JONSWAP '75. This is accomplished by varying the parameters and finding the values that give a best fit, in the least-squares sense, to the measurements. In particular, separate fits are done for a number of different wind speeds ranging from 4 to 13 m/s. The wind speeds are found from a wind field analysis based on sea-surface anemometer measurements. The best-fit parameters are then correlated with the logarithm of the wind speed by performing linear, least-squares regressions. The results are compared with those obtained from previous scatterometer experiments, with Cox and Munk's sea-surface slope pdf, and with Phillips' idealized capillary spectrum.

Description of JONSWAP '75 Experiment

During the August and September '75 portion of JONSWAP, aircraft scatterometer measurements of the sea-surface NRCS were conducted over the North Sea. For each flight the aircraft flew an assortment of straight lines and circles. The azimuth viewing angle ϕ for the line measurements remained fixed while the nadir viewing angle θ was incremented from 0° to 50° in 10° steps. In the case of the circles, θ was held approximately constant, and ϕ ranged from 0° to 360° in 10° steps. These two viewing angles are defined in Figure 1 relative to the viewing vector $\vec{k}_i$. For the five flights we consider, 13, 14, 16, 17, and 19, there are three circles and at least two orthogonal lines. The nadir angles for the circles are 20°, 40°, and 65°, except Flight 13 for which the largest nadir angle is 50°.

Throughout the measurements the polarization was continuously being switched between horizontal and vertical. The vertical polarization measurements are used to determine the distribution parameters from least-squares fits. These parameters characterize the sea-surface roughness and should be independent of polarization. As a check on this independence, we compute the NRCS for horizontal polarization using the best-fit parameters and compare the results with the measurements.

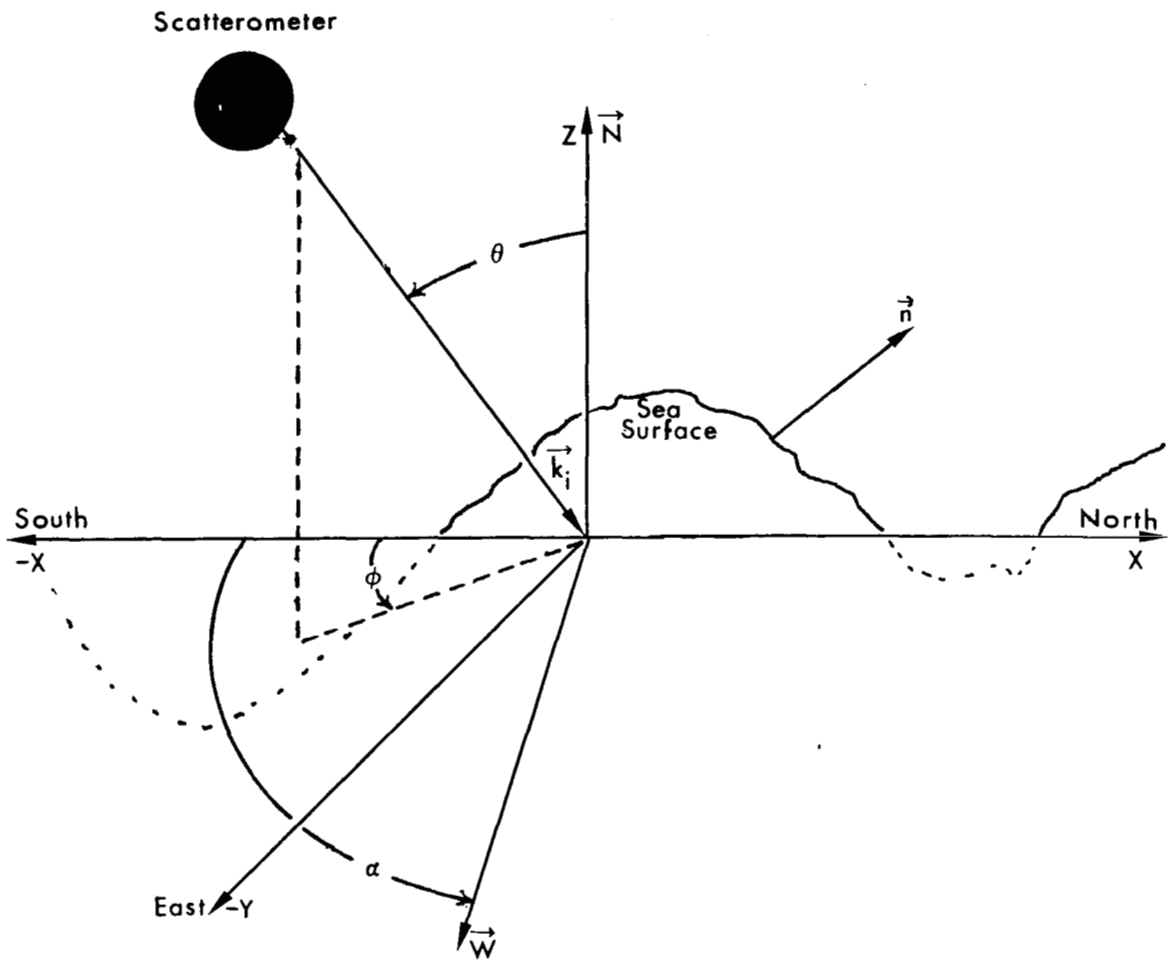

Fig. 1. Geometry for backscattering.

Probability Density of the Large-Scale Surface Normal

The form for the probability density $\mathrm{pdf}(\vec{n})$ of the large-scale surface normal $\vec{n}$ is based on Cox and Munk's [1956] observations of the sun glitter on rough seas. Their data were reduced in terms of the probability density $\mathrm{pdf}(S_u,S_c)$ of the upwind and crosswind surface slopes, S_u and S_c. The relationship between $\mathrm{pdf}(\vec{n})$ and $\mathrm{pdf}(S_u,S_c)$ is

$$\mathrm{pdf}(\vec{n}) = (\vec{n}\cdot\vec{N})^{-3}\,\mathrm{pdf}(S_u,S_c) \tag{43}$$

$$S_u = \vec{n}\cdot\vec{W}/(\vec{n}\cdot\vec{N}) \tag{44}$$

$$S_c = \vec{n}\cdot\vec{N}\times\vec{W}/(\vec{n}\cdot\vec{N}) \tag{45}$$

where $\vec{N}$ is the unit normal to the mean sea surface and $\vec{W}$ is the unit vector pointing downwind and orthogonal to $\vec{N}$. The factor $(\vec{n}\cdot\vec{N})^{-3}$ is the Jacobian relating the differential area $dS_u\,dS_c$ to the differential solid angle $d\vec{n}$. The vectors in the above equations are shown in Figure 1.

Cox and Munk found that $\mathrm{pdf}(S_u,S_c)$ is close to Gaussian and can be fitted to the following Gram-Charlier series:

$$\mathrm{pdf}(S_u,S_c) = [1 + T(\mu,\nu)]\,\exp[-\tfrac{1}{2}(\mu^2+\nu^2)]/(2\pi\langle S_u^2\rangle^{\frac{1}{2}}\langle S_c^2\rangle^{\frac{1}{2}}) \tag{46}$$

$$\mu = S_u/\langle S_u^2\rangle^{\frac{1}{2}} \tag{47}$$

$$\nu = S_c / \langle S_c^2 \rangle^{\frac{1}{2}} \tag{48}$$

The quantities $\langle S_u^2 \rangle$ and $\langle S_c^2 \rangle$ are the upwind and crosswind slope variances, and the function $T(\mu,\nu)$ accounts for deviations from a Gaussian distribution. We retain moments up to fourth order, and $T(\mu,\nu)$ is then

$$T(\mu,\nu) = c_1\mu(\nu^2-1) + c_2(\mu^3-3\mu) + c_3(\nu^4-6\nu^2+3)$$

$$+ c_4(\nu^2-1)(\mu^2-1) + c_5(\mu^4-6\mu^2+3) \tag{49}$$

where c_1 and c_2 are the skewness coefficients and c_3, c_4, and c_5 are the peakedness coefficients. The large-scale parameters $\langle S_u^2 \rangle$, $\langle S_c^2 \rangle$, c_1, c_2, c_3, c_4, and c_5 are to be determined from the least-squares fits.

Wavenumber Spectrum of the Small-Scale Roughness

The Fourier expansion for the wavenumber spectrum $F(\vec{\kappa},\vec{n})$ of the small-scale roughness is

$$F(\vec{\kappa},\vec{n}) = \sum_{m} a_m(\kappa,\vec{n}) \cos 2m\Psi + b_m(\kappa,\vec{n}) \sin 2m\Psi \tag{50}$$

The quantity κ is the magnitude of the vector wavemumber $\vec{\kappa}$, and Ψ is the angle between $\vec{\kappa}$ and the projection $\vec{w}$ of the unit wind vector $\vec{W}$ onto the plane orthogonal to $\vec{n}$.

$$\cos \Psi = \vec{\kappa}\cdot\vec{w}/(\kappa w) \tag{51}$$

$$\sin \Psi = \vec{\kappa}\cdot(\vec{n}\times\vec{w})/(\kappa w) \tag{52}$$

$$\vec{w} = \vec{n}\times(\vec{W}\times\vec{n}) \tag{53}$$

where w is the magnitude of $\vec{w}$.

In order to simplify (50), we assume that the spectral coefficients are independent of $\vec{n}$ and that the spectrum is symmetric about the wind projection $\vec{w}$. Furthermore, we retain only the first two terms of the expansion and approximate the spectrum by

$$F(\vec{\kappa},\vec{n}) = a_0(\kappa) + a_1(\kappa) \cos 2\Psi \tag{54}$$

The spectrum $F(\vec{\kappa},\vec{n})$ refers to regions on the sea surface having dimensions L large compared to the radiation wavelength λ. Waves longer than L do not contribute to $F(\vec{\kappa},\vec{n})$. To be definite, we let $L = 10\lambda$, and the spectrum is then zero for $\kappa < k/10$. Also the spectral components for roughness wavenumbers greater than 2k do not contribute to the Bragg scattering. Hence, the spectral band of interest is $k/10 < \kappa < 2k$. For the radiation wavenumber under consideration, $k = 2.9\ cm^{-1}$, this spectral band corresponds to the capillary region of the sea spectrum. Wind-wave tunnel measurements [Pierson and Stacy, 1973] indicate that in the region from $0.1\ cm^{-1}$ to $6\ cm^{-1}$ the coefficient $a_0(\kappa)$ has the form

$$a_0(\kappa) = h\ \kappa^{-q(\kappa)} \tag{55}$$

The function $q(\kappa)$ slowly varies with κ and ranges from 3 to 4.

The ratio a_r of $a_0(\kappa)$ to $a_1(\kappa)$ is assumed independent of κ, and our final approximation for the small-scale spectrum is

$$F(\vec{\kappa},\vec{n}) = h\ \kappa^{-q}\ (1 + a_r \cos 2\Psi)\ u(\kappa - \kappa_c) \tag{56}$$

The unit step function $u(\kappa - \kappa_c)$ satisfies the requirement that the spectrum is zero for $\kappa < k/10$. The wavenumber κ_c at which the cutoff to zero occurs is between k/10 and 2k. The exponent q represents the mean value of $q(\kappa)$ over the region $\kappa_c < \kappa < 2k$. The small-scale parameters h, q, a_r, and κ_c are to be determined from the least-squares fits.

Inputs for the Scattering Model

The scattering model requires a number of inputs in addition to the large-scale and small-scale distribution parameters mentioned in the previous two sections. For the special case of backscattering of like polarizations, these inputs are the following:

1) the radiation wavenumber k
2) the complex ratio ε of the sea water permittivity to the permittivity of free space
3) the unit propagation vector $\vec{k}_i$ of the incident radiation
4) the unit polarization vector $\vec{E}_i$ of the incident radiation
5) the unit normal $\vec{N}$ to the mean sea surface
6) the unit vector $\vec{W}$ pointing downwind

The JONSWAP '75 aircraft scatterometer operated at 13.9 GHz. The wavenumber k corresponding to this frequency is 2.91 cm^{-1}, and the permittivity ratio ε is 40.1 - 39.3 i [Porter and Wentz, 1971]. In order to specify the vectors, we choose the coordinate system that has the mean sea surface lying in the z = 0 plane and the x axis pointing north. The vectors are then given by

$$\vec{k}_i = [\cos\phi \sin\theta, \sin\phi \sin\theta, -\cos\theta] \tag{57}$$

$$\vec{E}_i = \begin{cases} \vec{k}_i \times \vec{N} / |\vec{k}_i \times \vec{N}| & \text{horizontal polarization} \\ \vec{k}_i \times (\vec{k}_i \times \vec{N}) / |\vec{k}_i \times \vec{N}| & \text{vertical polarization} \end{cases} \tag{58}$$

$$\vec{N} = [0,\ 0,\ 1] \tag{59}$$

$$\vec{W} = [-\cos \alpha,\ -\sin \alpha, 0] \tag{60}$$

The nadir and azimuth viewing angles, θ and ϕ, were recorded for each scatterometer measurement. The wind direction angle α is found from a harmonic analysis of scatterometer measurements taken while the aircraft flew circles, as is discussed in the next section.

Determination of Wind Direction

Before the distribution parameters can be found, the wind direction angle α must be specified. The assumption is made that the sea surface is in equilibrium with the prevailing wind. The NRCS measurements $\sigma^\circ(\theta,\phi)$ are then symmetric about the wind vector and can be expressed by the following Fourier expansion:

$$\sigma^\circ(\theta,\phi) = \sum_m A_m(\theta) \cos m(\phi-\alpha) \tag{61}$$

The measurements taken during circle flights for the two larger nadir angles display a dominant second-order harmonic. An analysis of this harmonic yields α to within an ambiguity of π, and sea-surface anemometer data allow for the removal of the ambiguity. Table 1 compares the wind direction determined from the scatterometer measurements with the value given by the anemometer data. The average discrepancy of approximately 10° is consistent with the error inherent in the anemometer data.

TABLE 1. Wind Direction Determination

	Wind Direction Measured East from North	
Flight No.	Scatterometer Data	Anemometer Data
13	157°	149°
14	49°	60°
16	204°	202°
17	211°	192°
19	245°	230°

POWER REFLECTIVITY

The small-scale wavenumber spectrum $F(\vec{\kappa},\vec{n})$ given in the previous section applies to wavenumbers between 0.1 cm^{-1} and 6 cm^{-1}. The computation of the scattering function for the reflected radiation, which is given by (14), requires integrating $F(\vec{\kappa},\vec{n})$ over all spectral wavenumbers. For backscattering, the scattering function represents the power reflectivity R for nadir incidence. To avoid having to specify $F(\vec{\kappa},\vec{n})$ for all $\vec{\kappa}$, we let R be an additional parameter to be found from least-squares fits.

Determination of Parameters

A list of the parameters to be determined appears in Table 2. The small-scale parameter h is listed in terms of $a_0(\kappa_m)$, the zeroth-order harmonic of the wavenumber spectrum at the minimum phase speed. The wavenumber κ_m for the minimum phase speed equals 3.64 cm^{-1}. The relationship between h and $a_0(\kappa_m)$ is

$$a_0(\kappa_m) = h\ \kappa_m^{-q} \tag{62}$$

The parameter $\langle S^2 \rangle^{\frac{1}{2}}$ is the rms slope of the large-scale waves and is given by

$$\langle S^2 \rangle^{\frac{1}{2}} = (\langle S_u^2 \rangle + \langle S_c^2 \rangle)^{\frac{1}{2}} \tag{63}$$

All other parameters in Table 2 have been defined in the previous sections.

The first eight parameters in Table 2 are contained within the probability density of the large-scale surface slope and are termed large-scale parameters. To determine these parameters, we increment each one over the range of possible values and find the combination of values that minimize the variance between the computed NRCS and the measurements for $\theta < 20°$ taken during a single flight. The restriction is placed on the nadir angle because in this angular region the NRCS is most sensitive to variations in the large-scale parameters. The small-scale anisotropy ratio a_r is found from a harmonic analysis of circle measurements for the two larger nadir angles.

	Mean	RMS	b_0	b_1	r^2
$\langle S_u^2 \rangle^{\frac{1}{2}}$	1.32×10^{-1}	1.30×10^{-2}	7.18×10^{-2}	6.99×10^{-2}	8.34×10^{-1}
$\langle S_c^2 \rangle^{\frac{1}{2}}$	1.24×10^{-1}	1.14×10^{-2}	7.28×10^{-2}	5.95×10^{-2}	7.91×10^{-1}
$\langle S^2 \rangle^{\frac{1}{2}}$	1.81×10^{-1}	1.70×10^{-2}	1.02×10^{-1}	9.16×10^{-2}	8.39×10^{-1}
c_1	-2.20×10^{-2}	5.62×10^{-2}	9.28×10^{-3}	-3.63×10^{-2}	1.21×10^{-2}
c_2	-5.00×10^{-3}	1.46×10^{-2}	2.63×10^{-3}	-8.86×10^{-3}	1.07×10^{-2}
c_3	8.00×10^{-3}	1.25×10^{-2}	2.61×10^{-2}	-2.10×10^{-2}	8.12×10^{-2}
c_4	3.90×10^{-2}	3.45×10^{-2}	1.81×10^{-2}	2.42×10^{-2}	1.43×10^{-2}
c_5	9.00×10^{-3}	1.85×10^{-2}	-6.51×10^{-3}	1.80×10^{-2}	2.75×10^{-2}
a_r	6.14×10^{-1}	8.26×10^{-2}	5.64×10^{-1}	5.80×10^{-2}	1.43×10^{-2}
q	$4.94\times10^{+0}$	$1.48\times10^{+0}$	$8.71\times10^{+0}$	$-4.39\times10^{+0}$	2.26×10^{-1}
κ_c †	$1.93\times10^{+0}$	5.02×10^{-1}	$1.83\times10^{+0}$	1.18×10^{-1}	1.43×10^{-3}
R	4.13×10^{-1}	4.58×10^{-2}	3.33×10^{-1}	9.31×10^{-2}	1.05×10^{-1}
$\log a_0(\kappa_m)$ ††	$-5.65\times10^{+0}$	4.42×10^{-1}	$-7.92\times10^{+0}$	$2.64\times10^{+0}$	9.10×10^{-1}

† κ_c in unit of cm^{-1}

†† $a_0(\kappa_m)$ in units of cm^4

A determination of the remaining parameters in Table 2 is done for each line and for the set of three circles. The computed NRCS for $\theta < 20°$ is approximately proportional to the power reflectivity R. For intermediate nadir angles, $20° < \theta < 30°$, the NRCS is sensitive to the choice of the cutoff wavenumber κ_c. At the larger angles, $30° < \theta < 65°$, the NRCS is approximately proportional to the zeroth-order harmonic $a_0(\kappa_m)$. The values for R, κ_c, and $a_0(\kappa_m)$ are chosen so as to minimize the variance between the computed NRCS and the measurements within the respective angular regions. Finally, the spectrum exponent q is found by requiring that the slope of the computed NRCS versus θ curve equals the measurement curve in the region $40° < \theta < 65°$.

The best-fit values for the parameters appear in Appendix B along with plots of the computed NRCS and the JONSWAP '75 measurements. The plots for the lines show the NRCS in terms of decibels versus the nadir angle θ (termed incidence angle on the plots). The calculated values are indicated by the solid curve, and the measurements, by diamonds or squares. The curve is a computer-generated interpolation based on computations every 5°, and any discontinuities in the slope of the curve are due to the interpolation routine. The plots for the circles show the NRCS in terms of decibels versus the flight direction angle $\beta = \phi - \alpha$. Hence $\beta = 0$ corresponds to an upwind observation. In these plots the calculated NRCS is indicated by triangles, and the measurements, by squares. The small dips at upwind and downwind shown by the computed circle data for $\theta = 20°$ are due to the non-Gaussian part of the probability density for the large-scale slopes. The measurements show no such dips, and it appears that the determination of the non-Gaussian parameters c_1 through c_5 is not entirely satisfactory.

Table 3 gives for each flight the rms variance between the computed NRCS and the measurements. The average rms variance for vertical polarization is 0.7 dB. Having determined the model parameters from the best fits, we then compute the NRCS for horizontal polarization. The rms variance between these computations and the horizontal polarization measurements is 2.4 dB. The larger rms variance for horizontal polarization is due in part to the model predicting a greater separation between the two polarizations at the larger nadir angles than is shown by the measurements. Further investigation is required to resolve this discrepancy between the model and the measurements.

TABLE 3. RMS Variance Between Computed NRCS and Measurements

	RMS Variance (dB)	
Flight Number	Vertical Polarization	Horizontal Polarization
13	0.7	1.6
14	0.6	3.4
16	1.0	2.6
17	0.4	3.2
19	0.6	1.3
Average	0.7	2.4

Regressions for Parameters Versus Wind Speed

In this section we investigate the correlation between the parameters and the wind speed. During the JONSWAP '75 flights, sea-surface anemometer measurements were made at the Pisa Tower in the North Sea. A wind-field analysis was done based on these measurements in conjunction with weather maps and anemometer data from other sites. The results are contained in Appendix B, which gives a wind speed for each line, for each set of circles, and for the overall flight. The wind speeds are adjusted so as to correspond to an anemometer height of 19.5 m in a neutral atmosphere.

Linear least-squares regressions of the parameters versus the logarithm of wind speed W are then found. The regressions have the form

$$p = b_1 \log W + b_0 \tag{64}$$

where p denotes the parameter under consideration. The regression coefficients b_0 and b_1 appear in Table 2 along with the coefficient of determination r^2 . A value of r^2 near unity indicates a high correlation between p and W. Also included in Table 2 are the means and the rms variations of the parameters, irrespective of wind speed. Line 3, Run 1 of Flight 13 is omitted from the regressions and the averages because of the small value of $a_0(\kappa_m)$ (a factor of 5 below the rest of the Flight 13 data). We feel that in this case the friction velocity at the sea surface may have been less than the critical velocity required to ruffle the surface.

The only parameters that show a high correlation with wind speed are

the large-scale rms slopes, $\langle S_u^2 \rangle^{\frac{1}{2}}$, $\langle S_c^2 \rangle^{\frac{1}{2}}$, and $\langle S^2 \rangle^{\frac{1}{2}}$, and the logarithm of the zeroth-order harmonic of the small-scale wavenumber spectrum, $\log a_0(\kappa_m)$. Figures 1 and 2 show $\langle S^2 \rangle^{\frac{1}{2}}$ and $\log a_0(\kappa_m)$ plotted versus log W. The best-fit values determined from the JONSWAP '75 data are indicated by the circles. The regressions are shown by the solid straight lines. The two dashed curves in Figure 1 come from Cox and Munk's [1956] expressions for a clean and an oil-slick surface. The curves nicely bound the data. The stars represent the best-fit values deduced from scatterometer measurements taken during the spring of 1973 over the Gulf of Mexico (3.0 and 6.5 m/s stars) and over the Atlantic Ocean near the Chesapeake Light Tower (15 m/s star). The additional data agree well with the JONSWAP '75 data except in Figure 2 at the lower wind speeds. The cause of the disagreement has not yet been resolved.

The other parameters seem reasonably independent of the wind speed. The rms variation of the non-Gaussian parameters c_1 through c_5 is approximately equal to or less than their mean value. This fact suggests setting c_1 through c_5 to zero, thereby eliminating the unrealistic dips that occur at upwind and downwind in the circle plots. The remaining wind-independent parameters have a rms variation small compared to their mean value. The mean value of 0.61 for the ratio a_r indicates a strong anisotropy for the small-scale wavenumber spectrum. The spectrum exponent q has a mean value equal to 4.9, which compares favorably to Phillips' [1966] value of 4 for an idealized capillary spectrum. The mean value of 1.9 cm^{-1} for the cutoff wavenumber κ_c is roughly half the radiation wavenumber k. Finally, the mean value of the power reflectivity R is 0.41 compared to a value of 0.61 for the Fresnel power reflectivity. It thus appears that the small-scale roughness reduces the reflected power by one third.

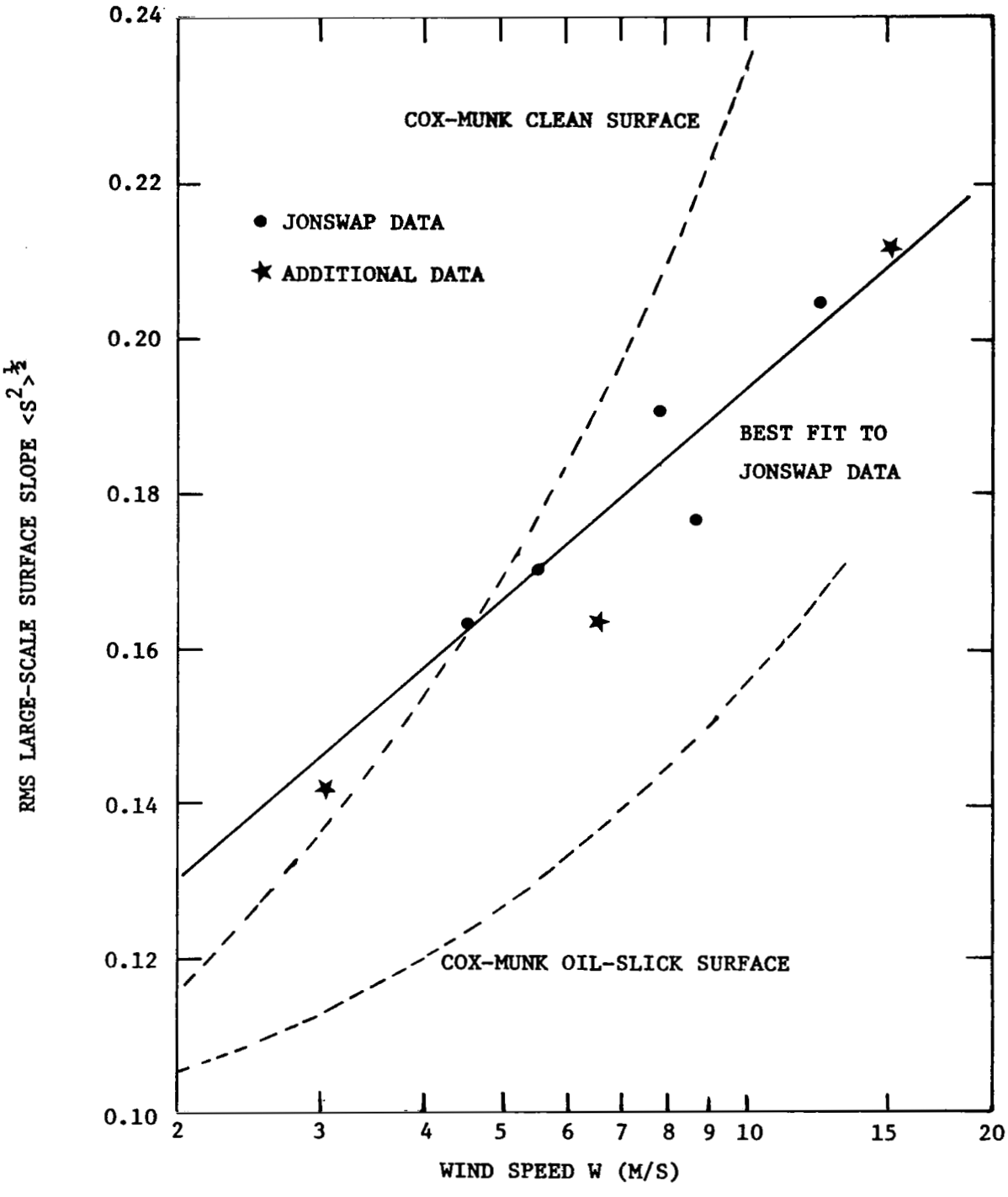

Fig. 2. Semi-log plot of the rms large-scale surface slope versus the wind speed.

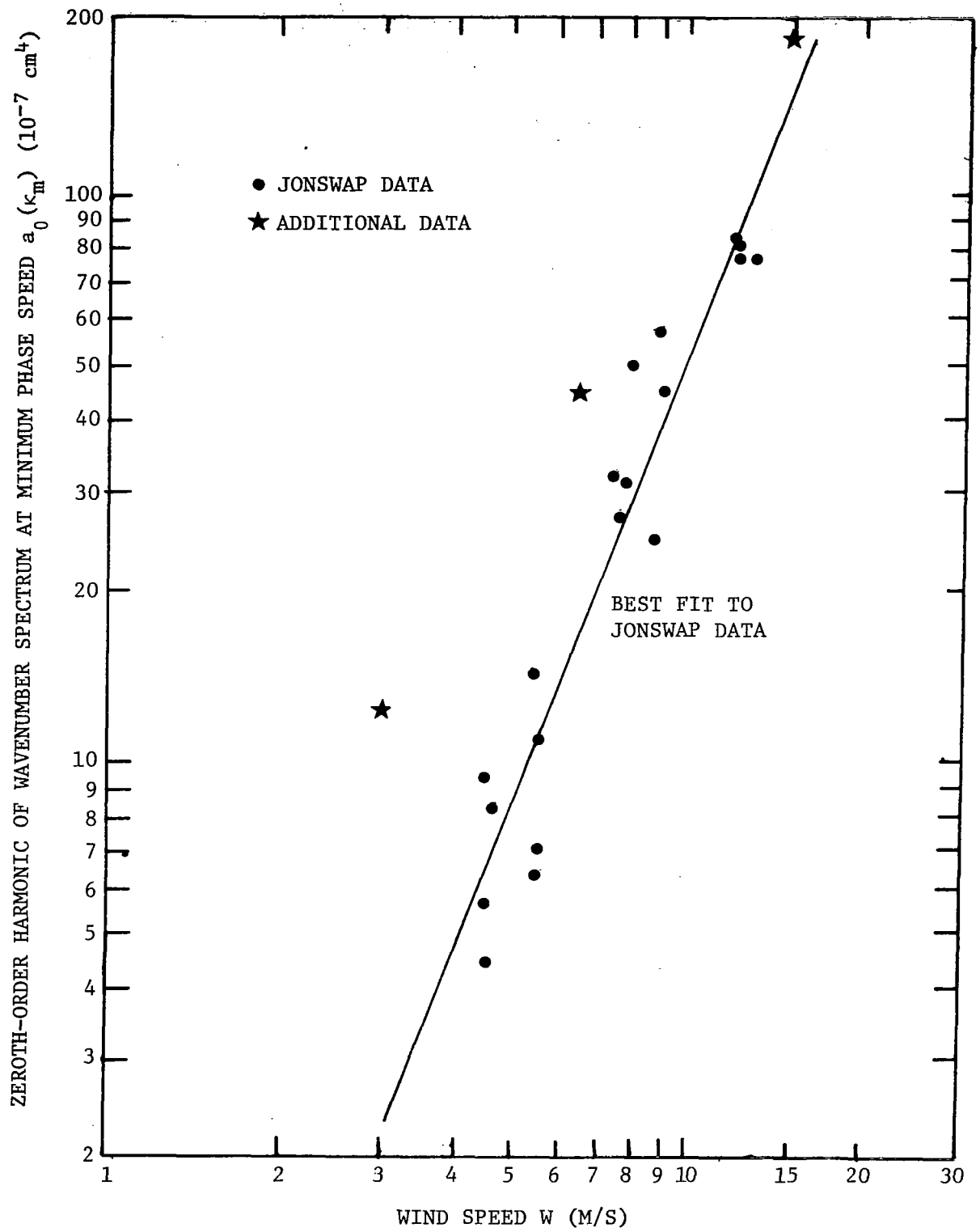

Fig. 3. Log-log plot of the zeroth-order harmonic of the small-scale wavenumber spectrum at the minimum phase speed versus the wind speed.

CONCLUSIONS

The two-scale backscatter model is fitted, in the least-squares sense, to the aircraft scatterometer measurements for vertical polarization taken during JONSWAP '75. The rms variance between the model NRCS and the measurements is, on the average, 0.7 dB. Having determined the model parameters from the best fits, we then compute the NRCS for horizontal polarization. The rms variance between these computations and the horizontal polarization measurements is 2.4 dB. The larger rms variance for horizontal polarization is due in part to the model predicting a greater separation between the two polarizations at the larger nadir angles than is shown by the measurements. Further investigation is required to resolve this discrepancy between the model and the measurements.

The large-scale sea-surface rms slope and the zeroth-order harmonic of the capillary wavenumber spectrum at the minimum phase speed are found from the best fits. Linear, least-squares regressions of these two parameters versus the logarithm of the wind speed yield coefficients of determination equaling 0.84 and 0.91, respectively. Thus the two parameters are highly correlated with the wind speed. Cox and Munk's [1956] expressions for the rms slope of a clean and an oil-slick surface nicely bound our values. Aircraft scatterometer measurements of the Atlantic Ocean and the Gulf of Mexico also agree well with the JONSWAP '75 data with one exception. At the lower wind speeds, the amplitude of the capillary spectrum determined from the measurements of the Gulf of Mexico is larger than that determined from the JONSWAP '75 measurements. The cause of this disagreement has not yet been resolved.

The other parameters have coefficients of determination of the order 0.1 or less, and hence are reasonably independent of the wind speed. The parameters for the non-Gaussian part of the large-scale slope pdf vary about zero and indicate that the pdf is close to Gaussian. The capillary spectrum is highly anisotropic. The mean value of the ratio between its first-order and zeroth-order harmonic is 0.61. Furthermore the power law for the spectrum is found to be -4.9 ± 1.5 which compares favorably with Phillips' [1966] value of -4 for an idealized spectrum. Best fits are obtained by cutting the spectrum off to zero at a wavenumber approximately one half the radiation wavenumber. Finally, the mean value of the power reflectivity for nadir incidence is 0.41 compared to a value of 0.61 for the Fresnel power reflectivity. It thus appears that the small-scale roughness reduces the reflected power by one third.

APPENDIX A

List of Symbols and Comparison of Notations for Part I

Quantity	Symbol	
	This Report	Wentz [1975]
area of mean scattering surface	A	A
differential solid angle in $\vec{k}$ space	$d\vec{k}$	$d\Omega$
differential solid angle in $\vec{n}$ space	$d\vec{n}$	$d\eta^x d\eta^y/\eta^z$
incident local hor. pol. unit vector	$\vec{e}_h(\vec{k}_i,\vec{n})$	$\hat{H}_i$
scattered local hor. pol. unit vector	$\vec{e}_h(\vec{k}_s,\vec{n})$	$\hat{H}_s$
incident local vert. pol. unit vector	$\vec{e}_v(\vec{k}_i,\vec{n})$	$\hat{V}_i$
scattered local vert. pol. unit vector	$\vec{e}_v(\vec{k}_s,\vec{n})$	$\hat{V}_s$
incident polarization unit vector	$\vec{E}_i$	$\hat{P}_i$
scattered polarization unit vector	$\vec{E}_s$	$\hat{P}_s$
small-scale wavenumber spectrum	$F(\vec{\kappa},\vec{n})$	$W(\vec{\kappa})/4$
radiation wavenumber	k	k
incident propagation unit vector	$\vec{k}_i$	$\hat{k}_i$
scattered propagation unit vector	$\vec{k}_s$	$\hat{k}_s$
large-scale surface unit normal	$\vec{n}$	$\hat{\eta}$
specular reflection unit normal	$\vec{n}_r$	$\hat{\eta}_0$
mean large-scale surface unit normal	$\vec{N}$	$\hat{z}$
probability density for $\vec{n}$	$pdf(\vec{n})$	$\eta^z P(\hat{\eta})$
incident power	P_i	none
scattered power	P_s	none

Quantity	Symbol	
	This Report	Wentz[1975]
distance from surface to observer	r	none
reflection scattering function	$S^r(\vec{k}_i,\vec{E}_i;\vec{k}_s,\vec{E}_s;\vec{n}_r)$	none
Bragg scattering function	$S^b(\vec{k}_i,\vec{E}_i;\vec{k}_s,\vec{E}_s;\vec{n})$	$\|T\|^2$
unit step function	$u(\cdots)$	$u(\cdots)$
reflection scattering elements	$\alpha^r_{\mu\nu}$	none
Bragg scattering elements	$\alpha^b_{\mu\nu}$	α_{mn}
two-scale scattering coefficient	$\Gamma(\vec{k}_i,\vec{E}_i;\vec{k}_s,\vec{E}_s;\vec{N})$	$\Gamma(\hat{k}_i,\hat{k}_s)$
subregion scattering coefficient	$\Gamma_\Delta(\vec{k}_i,\vec{E}_i;\vec{k}_s,\vec{E}_s;\vec{n})$	$\Gamma(\hat{k}_i,\hat{k}_s,\hat{\eta})$
large-scale surface subregion	$\Delta\Sigma_\ell$	$\Delta\Sigma_\ell$
permittivity ratio	ε	ε
small-scale height variation	ζ^2	ζ^2
local incidence nadir angle	θ_i	θ_i
local reflection angle	θ_r	θ_i
local scattered nadir angle	θ_s	θ_s
small-scale roughness wavenumber vector	$\vec{\kappa}$	$\vec{\kappa}$
Bragg wavenumber vector	$\vec{\kappa}_b$	$\vec{\kappa}$
radiation wavelength	λ	λ
Fresnel reflection coefficient	$\rho_\mu(\theta_r)$	$\rho_m(\theta_i)$
two-scale NRCS	$\sigma^\circ(\vec{k}_i,\vec{E}_i;\vec{k}_s,\vec{E}_s;\vec{N})$	none
Bragg NRCS	$\sigma^\circ_b(\vec{k}_i,\vec{E}_i;\vec{k}_s,\vec{E}_s;\vec{n})$	none
subregion NRCS	$\sigma^\circ_\Delta(\vec{k}_i,\vec{E}_i;\vec{k}_s,\vec{E}_s;\vec{n})$	none
large-scale surface	Σ_ℓ	Σ_ℓ
local azimuth angle	ϕ	ϕ_s
shadowing function	$\chi(\vec{k}_i,\vec{N})$	$\chi(\hat{k}_i)$

APPENDIX B

Best-Fit Values for the Parameters

Plots of the Computed NRCS and the JONSWAP '75 Measurements

DATA FOR OVERALL FLIGHT

Flight 13, August 29, 1975

Average Wind Speed = 4.5 m/s

Average Wind Direction (out of) = 157° east of North

Large-Scale Parameters:

$\langle S_u^2 \rangle^{\frac{1}{2}} = 0.12$

$\langle S_c^2 \rangle^{\frac{1}{2}} = 0.11$

$c_1 = 0.010$

$c_2 = 0.005$

$c_3 = 0.005$

$c_4 = 0.015$

$c_5 = -0.005$

Small-Scale Anisotropy Ratio:

$a_r = 0.61$

DATA FOR CIRCLES

Flight 13, August 29, 1975

Three circles for θ = 20°, 40°, and 50°

Wind Speed = 4.6 m/s

Small-Scale Parameters:

$a_0(\kappa_m) = 8.27 \times 10^{-7}$ cm^4

$q = 5.8$

$\kappa_c = 2.04$ cm^{-1}

Power Reflectivity at Nadir:

$R = 0.39$

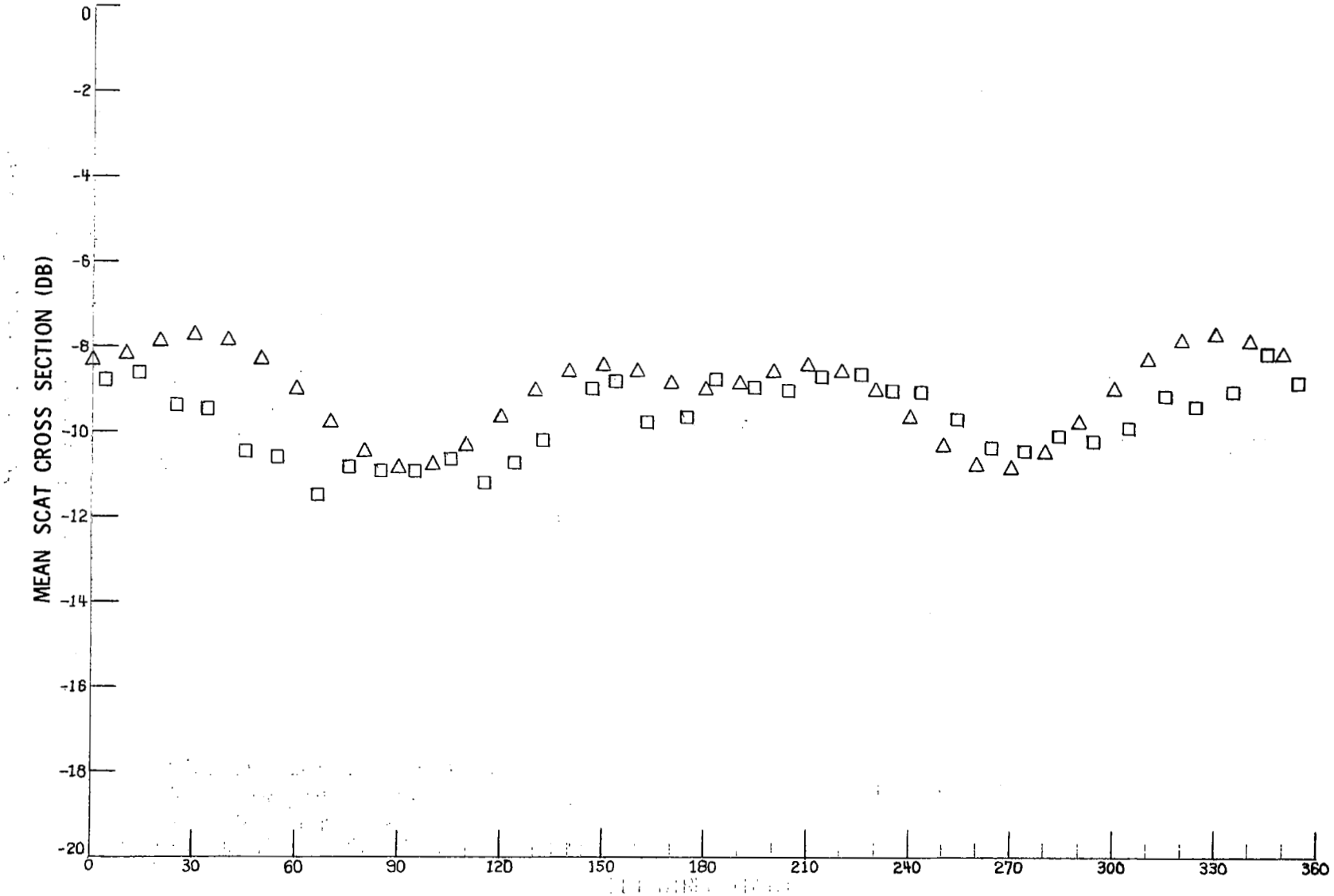
MISSION 318 FLIGHT 13 DATE 8 29 1975
FLT LINE 4 RUN 3 VER POL
DATA CORRECTED TO 20.00° INCIDENCE ANGLE
WIND DIRECTION (OUT OF) 161.0°
□ = CORRECTED RADSCAT DATA
△ = CALCULATED DATA
MEAN SCAT CROSS SECTION (DB)
0
-2
-4
-6
-8
-10
-12
-14
-16
-18
-20
0
30
60
90
120
150
180
210
240
270
300
330
360

MISSION 318 FLIGHT 13 DATE 8 29 1975
FLT LINE 4 RUN 3 HOR POL
DATA CORRECTED TO 20.00° INCIDENCE ANGLE
WIND DIRECTION (OUT OF) 161.0°

□ = CORRECTED RADSCAT DATA
△ = CALCULATED DATA

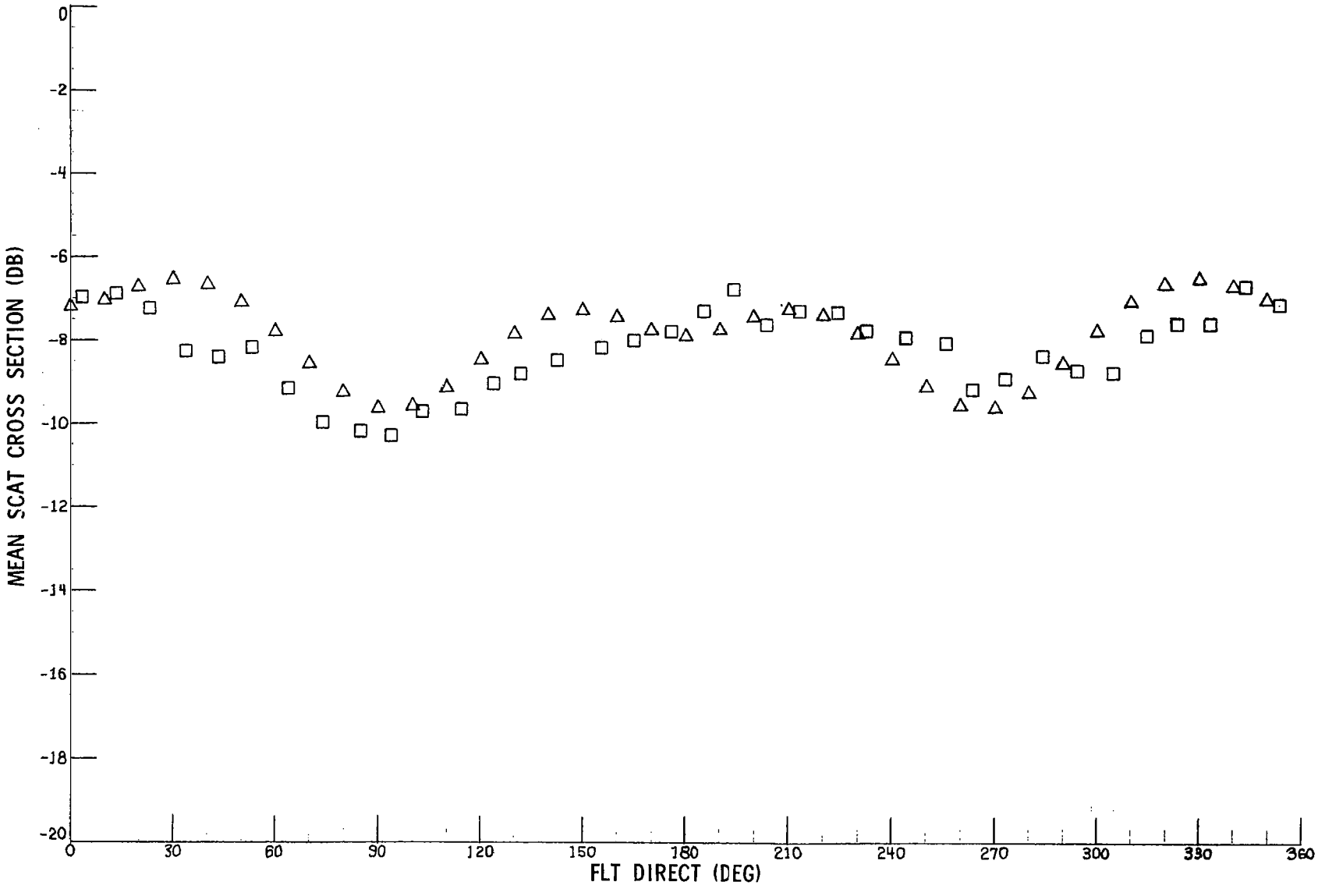

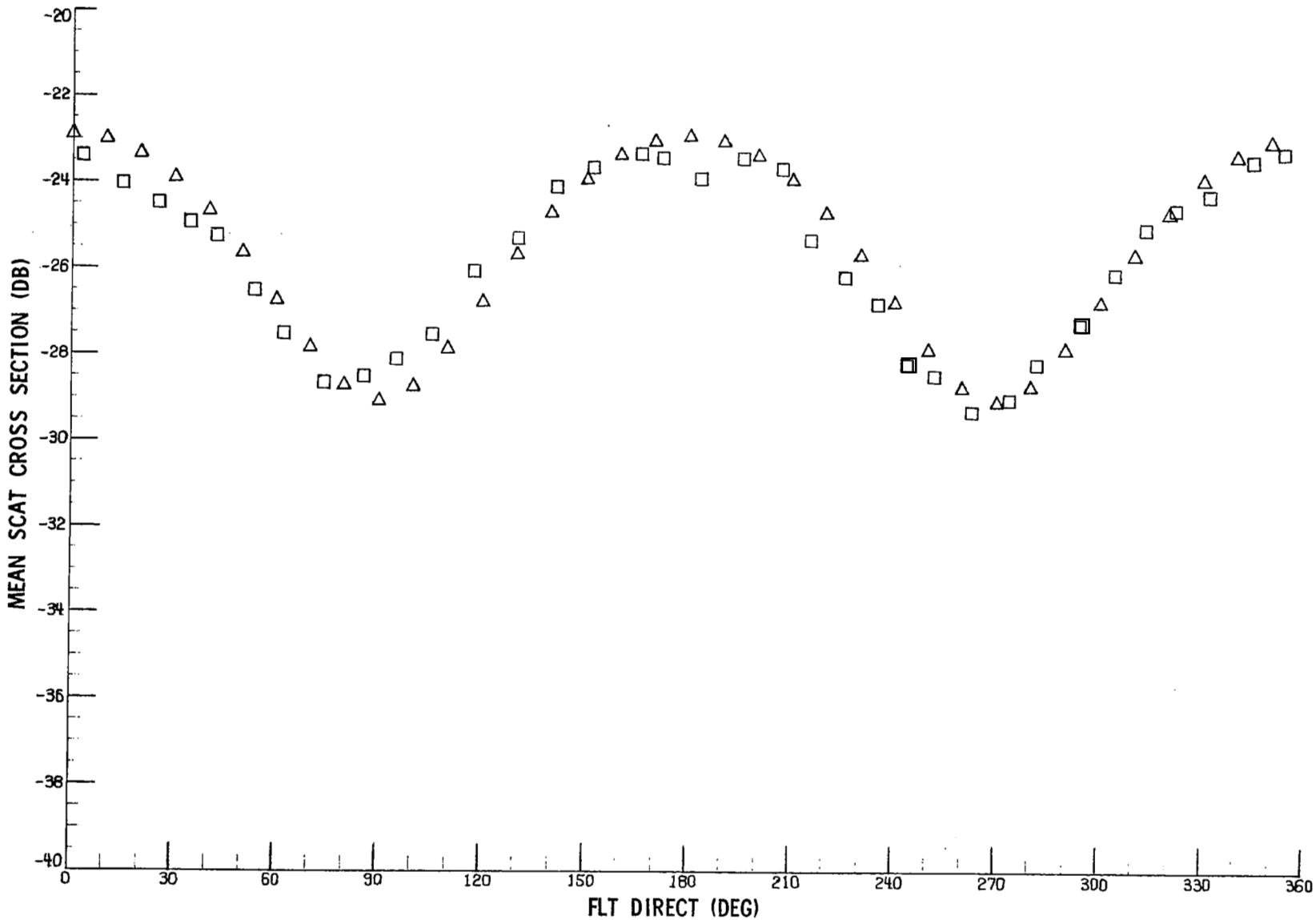
MISSION 318 FLIGHT 13 DATE 8 29 1975
FLT LINE 4 RUN 9 VER POL
DATA CORRECTED TO 40.00° INCIDENCE ANGLE
WIND DIRECTION (OUT OF) 161.0°
□ = CORRECTED RADSCAT DATA
△ = CALCULATED DATA
MEAN SCAT CROSS SECTION (DB)
-20
-22
-24
-26
-28
-30
-32
-34
-36
-38
-40
0
30
60
90
120
150
180
210
240
270
300
330
360
FLT DIRECT (DEG)

MISSION 318 FLIGHT 13 DATE 8 29 1975
FLT LINE 4 RUN 9 HOR POL
DATA CORRECTED TO 40.00° INCIDENCE ANGLE
WIND DIRECTION (OUT OF) 161.0°

□ = CORRECTED RADSCAT DATA
△ = CALCULATED DATA

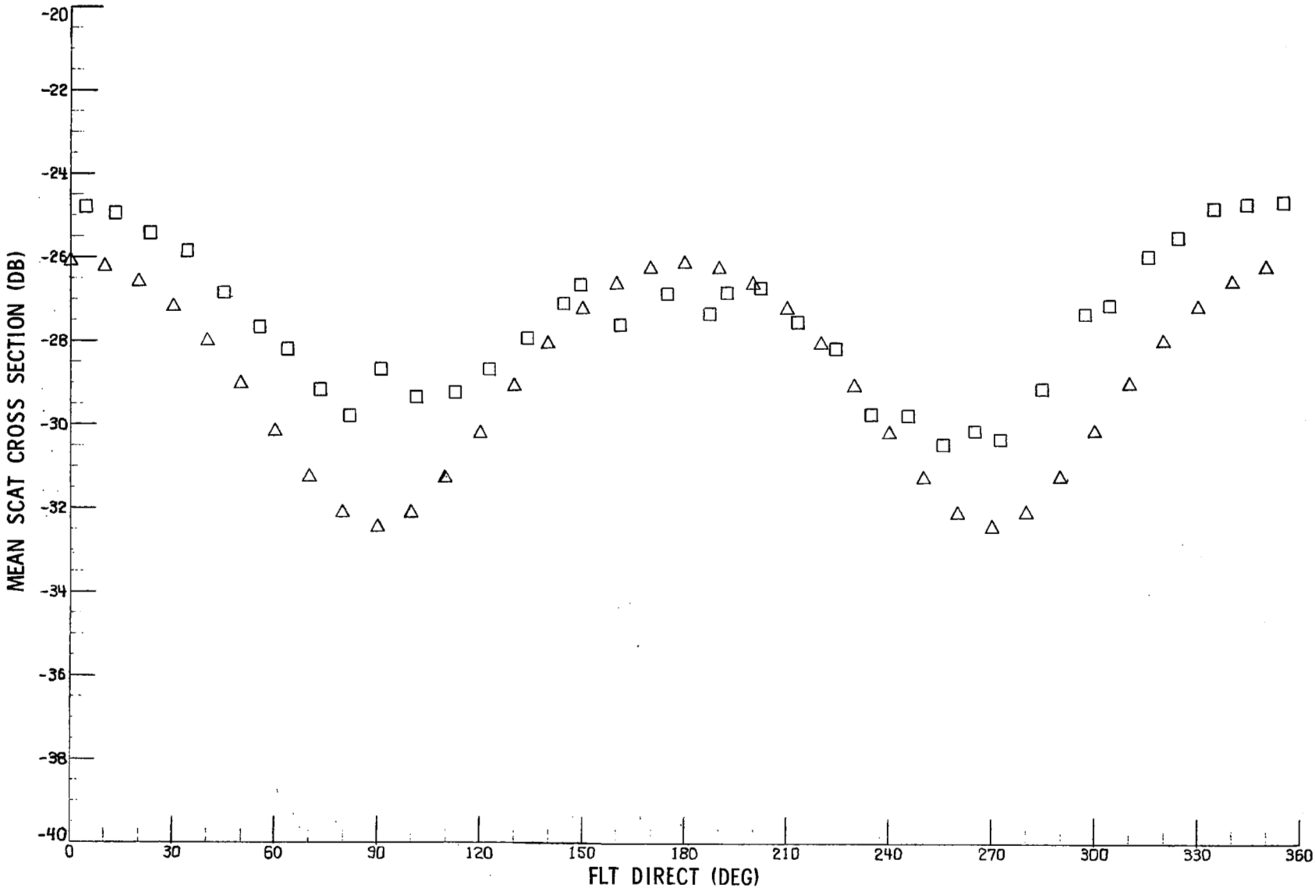

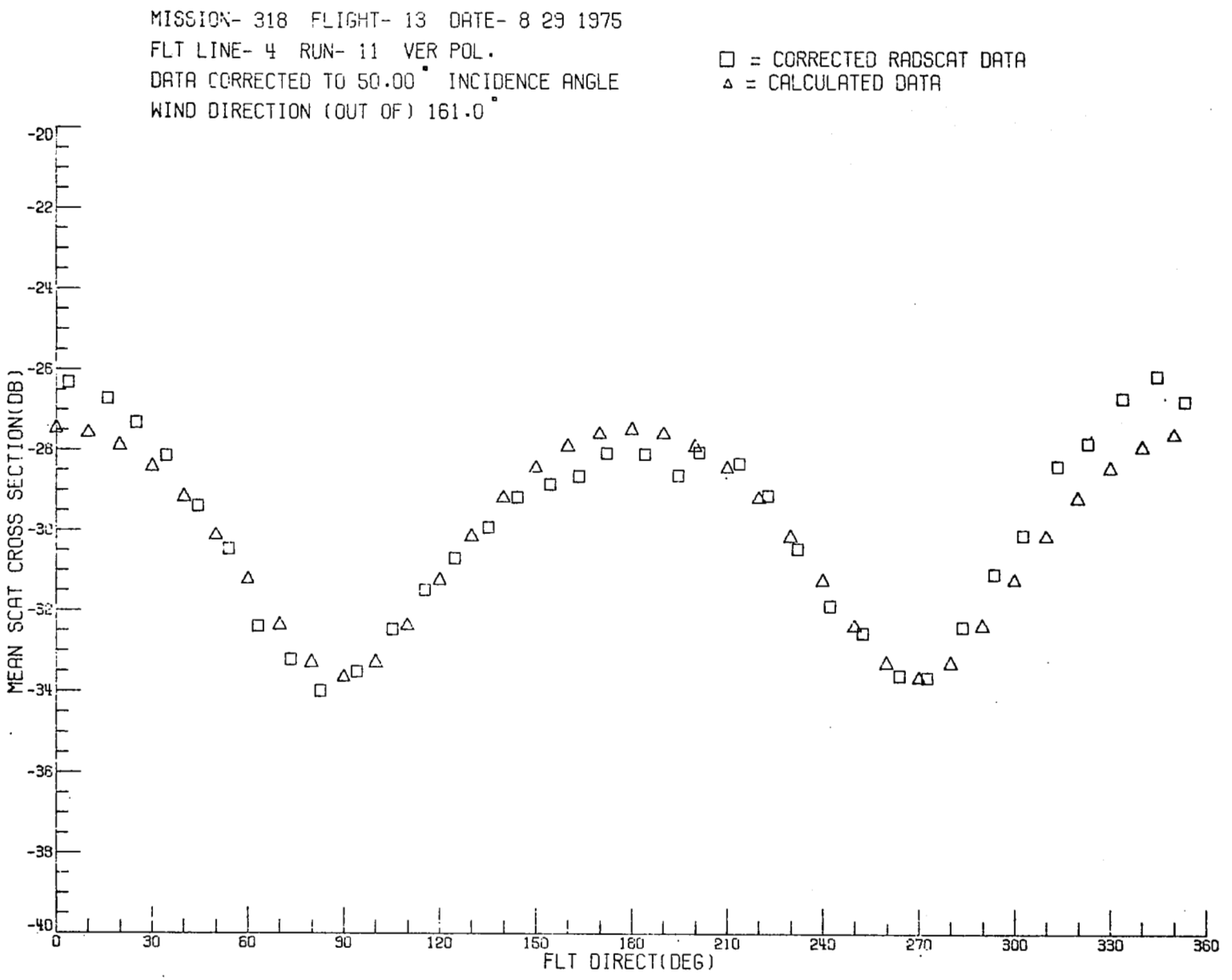
MISSION- 318 FLIGHT- 13 DATE- 8 29 1975
FLT LINE- 4 RUN- 11 VER POL.
DATA CORRECTED TO 50.00° INCIDENCE ANGLE
WIND DIRECTION (OUT OF) 161.0°
□ = CORRECTED RADSCAT DATA
△ = CALCULATED DATA
MEAN SCAT CROSS SECTION(DB)
-20
-22
-24
-26
-28
-30
-32
-34
-36
-38
-40
0
30
60
90
120
150
180
210
240
270
300
330
360
FLT DIRECT(DEG)

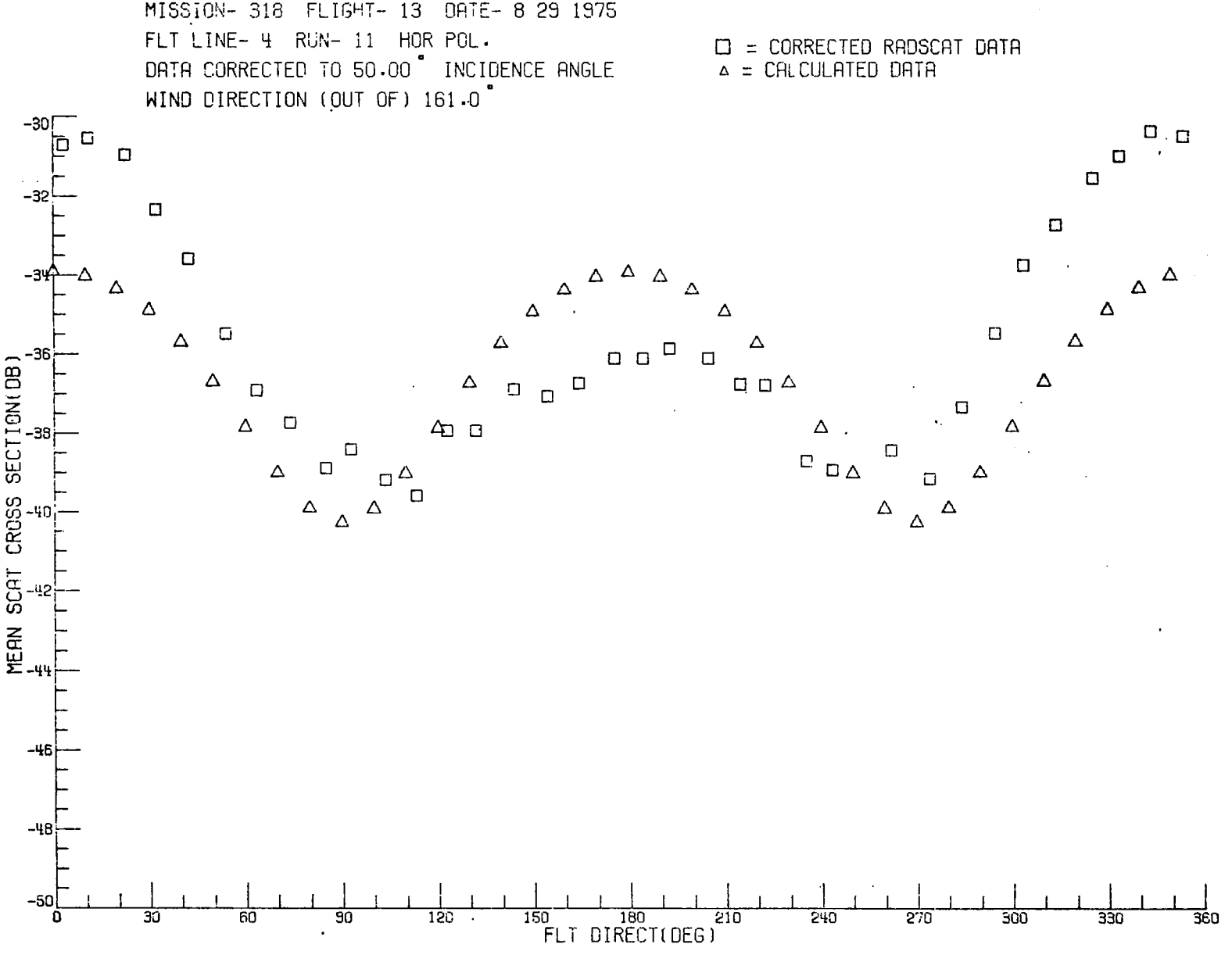
MISSION- 318 FLIGHT- 13 DATE- 8 29 1975
FLT LINE- 4 RUN- 11 HOR POL.
DATA CORRECTED TO 50.00° INCIDENCE ANGLE
WIND DIRECTION (OUT OF) 161.0°
□ = CORRECTED RADSCAT DATA
△ = CALCULATED DATA
MEAN SCAT CROSS SECTION(DB)
-30
-32
-34
-36
-38
-40
-42
-44
-46
-48
-50
0
30
60
90
120
150
180
210
240
270
300
330
360
FLT DIRECT(DEG)

DATA FOR A LINE

Flight 13, August 29, 1975

Line 3, Run 1, Crosswind

Wind Speed = 4.5 m/s

Azimuth viewing angle relative to upwind = 238°

Small-Scale Parameters:

$a_0(\kappa_m) = 8.66\times10^{-8}$ cm^4

$q = 6.3$

$\kappa_c = 0.85$ cm^{-1}

Power Reflectivity at Nadir:

$R = 0.31$

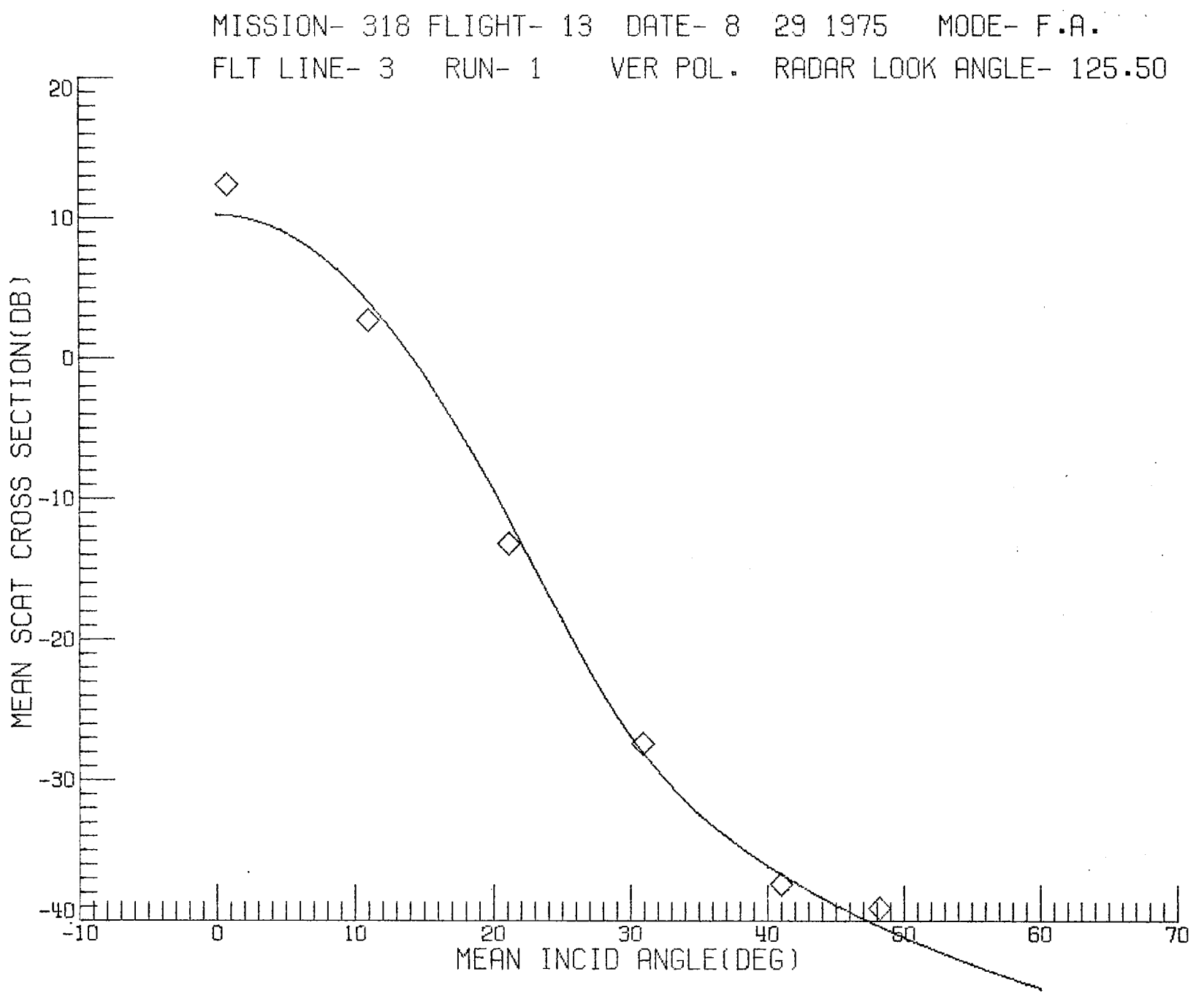
MISSION- 318 FLIGHT- 13 DATE- 8 29 1975 MODE- F.A.
FLT LINE- 3 RUN- 1 VER POL. RADAR LOOK ANGLE- 125.50
MEAN SCAT CROSS SECTION(DB)
20
10
0
-10
-20
-30
-40
-10
0
10
20
30
40
50
60
70
MEAN INCID ANGLE(DEG)

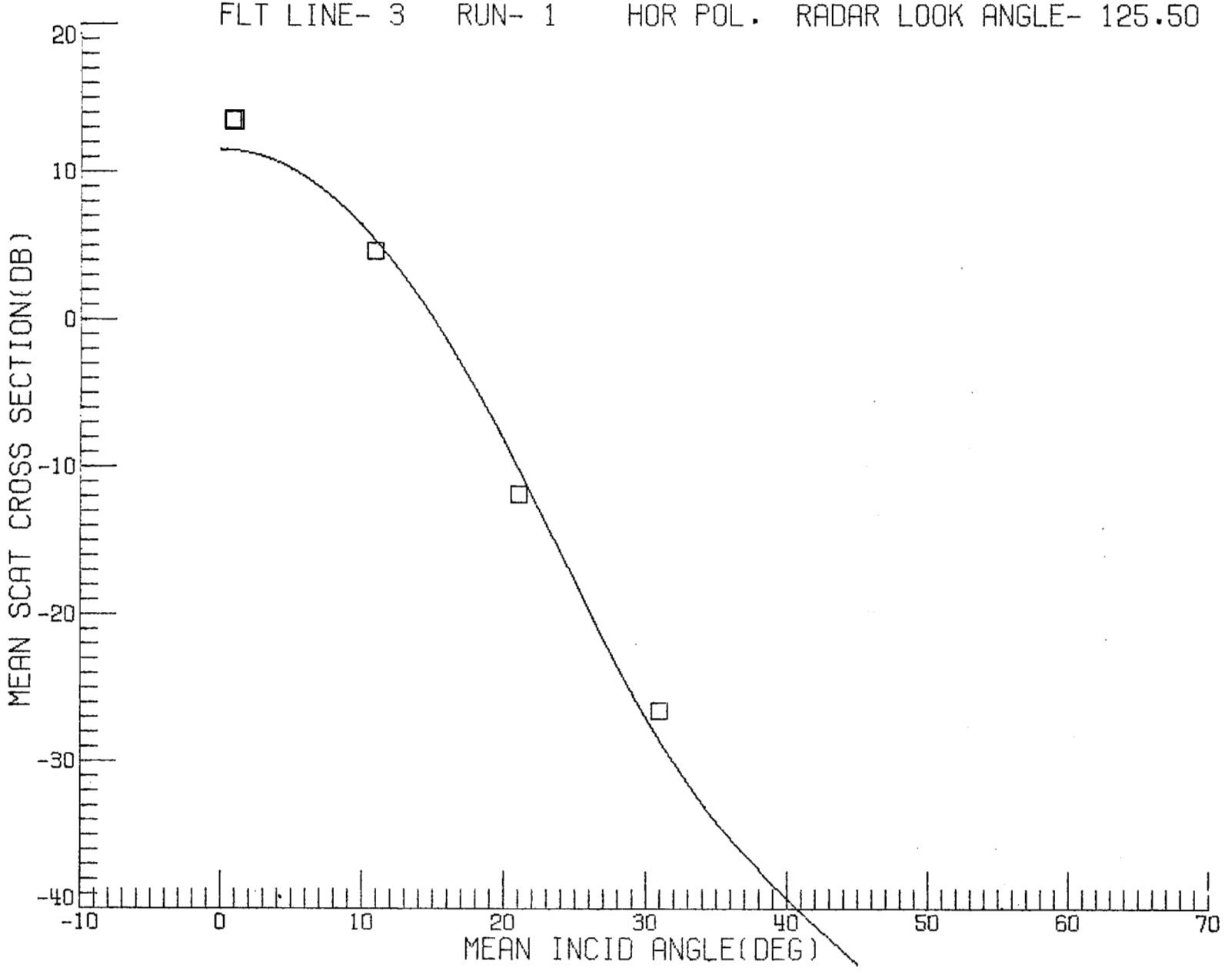
MISSION- 318 FLIGHT- 13 DATE- 8 29 1975 MODE- F.A.
FLT LINE- 3 RUN- 1 HOR POL. RADAR LOOK ANGLE- 125.50
MEAN SCAT CROSS SECTION(DB)
20
10
0
-10
-20
-30
-40
-10
0
10
20
30
40
50
60
70
MEAN INCID ANGLE(DEG)

DATA FOR A LINE

Flight 13, August 29, 1975

Line 3, Run 2, Crosswind

Wind Speed = 4.5 m/s

Azimuth viewing angle relative to upwind = 58°

Small-Scale Parameters:

$a_0(\kappa_m) = 4.48 \times 10^{-7}$ cm^4

$q = 8.3$

$\kappa_c = 2.60$ cm^{-1}

Power Reflectivity at Nadir:

$R = 0.33$

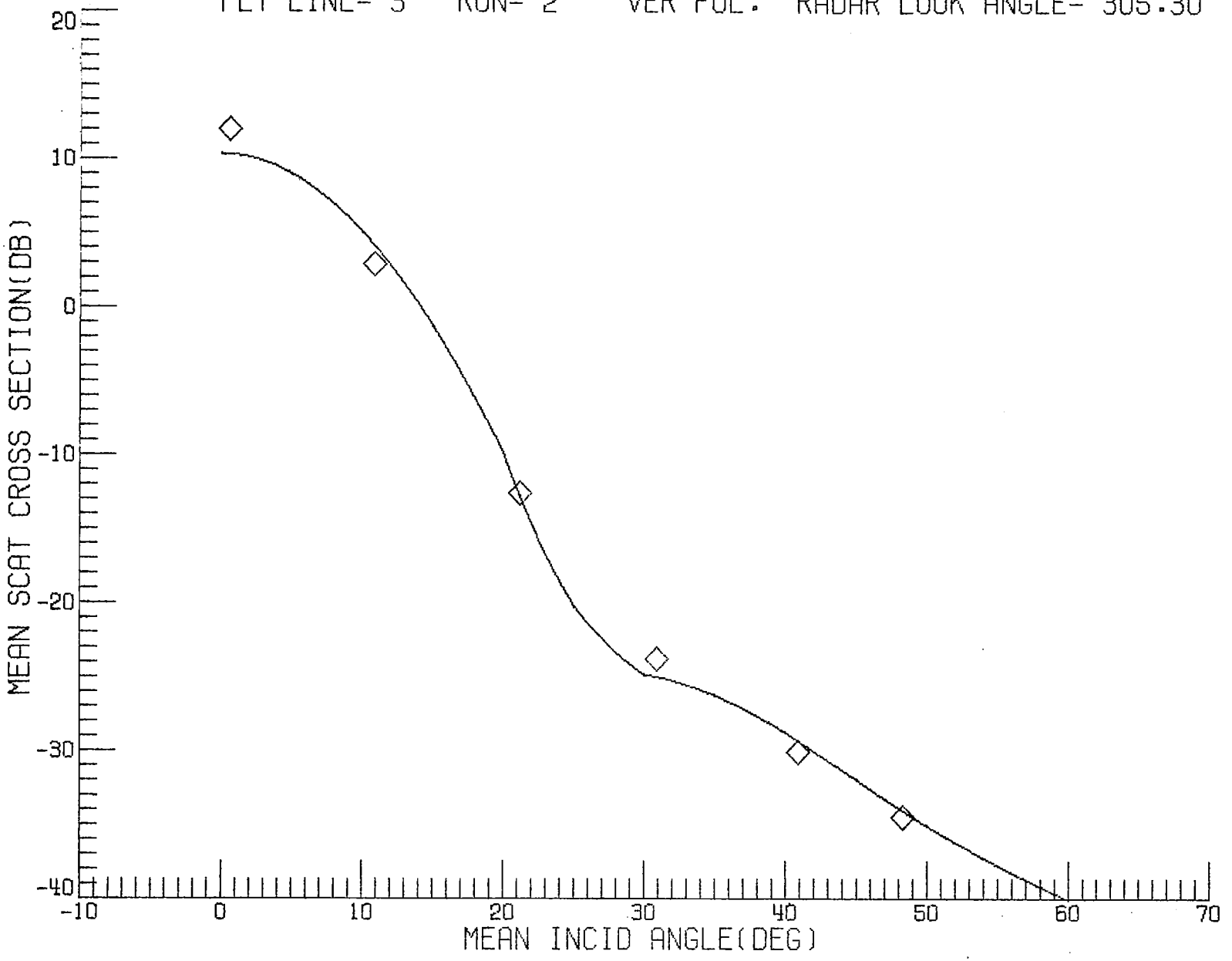
MISSION- 318 FLIGHT- 13 DATE- 8 29 1975 MODE- F.A.
FLT LINE- 3 RUN- 2 VER POL. RADAR LOOK ANGLE- 305.30
MEAN SCAT CROSS SECTION(DB)
20
10
0
-10
-20
-30
-40
-10
0
10
20
30
40
50
60
70
MEAN INCID ANGLE(DEG)

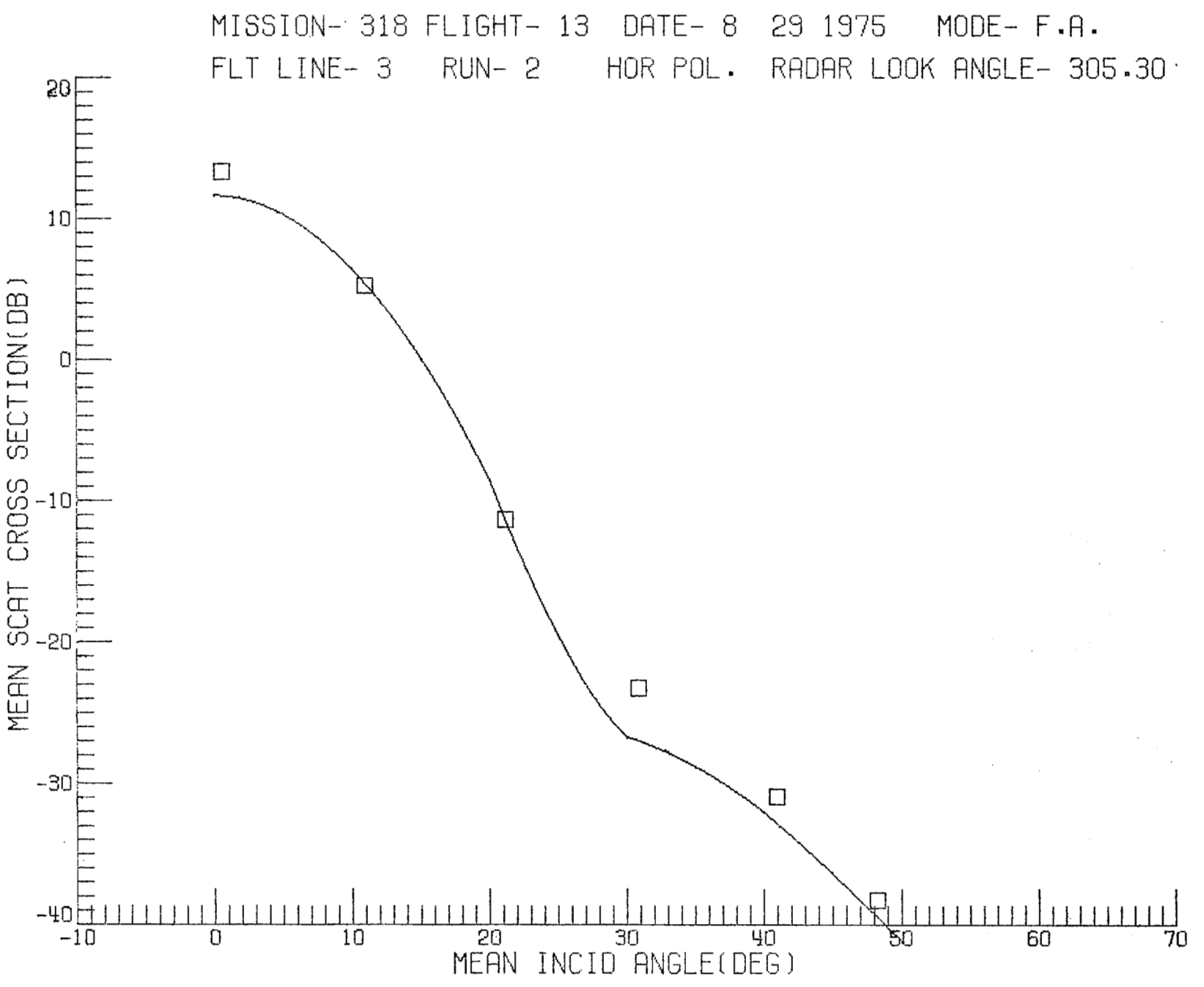
MISSION- 318 FLIGHT- 13 DATE- 8 29 1975 MODE- F.A.
FLT LINE- 3 RUN- 2 HOR POL. RADAR LOOK ANGLE- 305.30
MEAN SCAT CROSS SECTION(DB)
20
10
0
-10
-20
-30
-40
-10
0
10
20
30
40
50
60
70
MEAN INCID ANGLE(DEG)

DATA FOR A LINE

Flight 13, August 29, 1975

Line 6, Run 1, Upwind

Wind Speed = 4.5 m/s

Azimuth viewing angle relative to upwind = 16°

Small-Scale Parameters:

$a_0(\kappa_m) = 5.63 \times 10^{-7}$ cm^4

$q = 6.8$

$\kappa_c = 2.30$ cm^{-1}

Power Reflectivity at Nadir:

$R = 0.47$

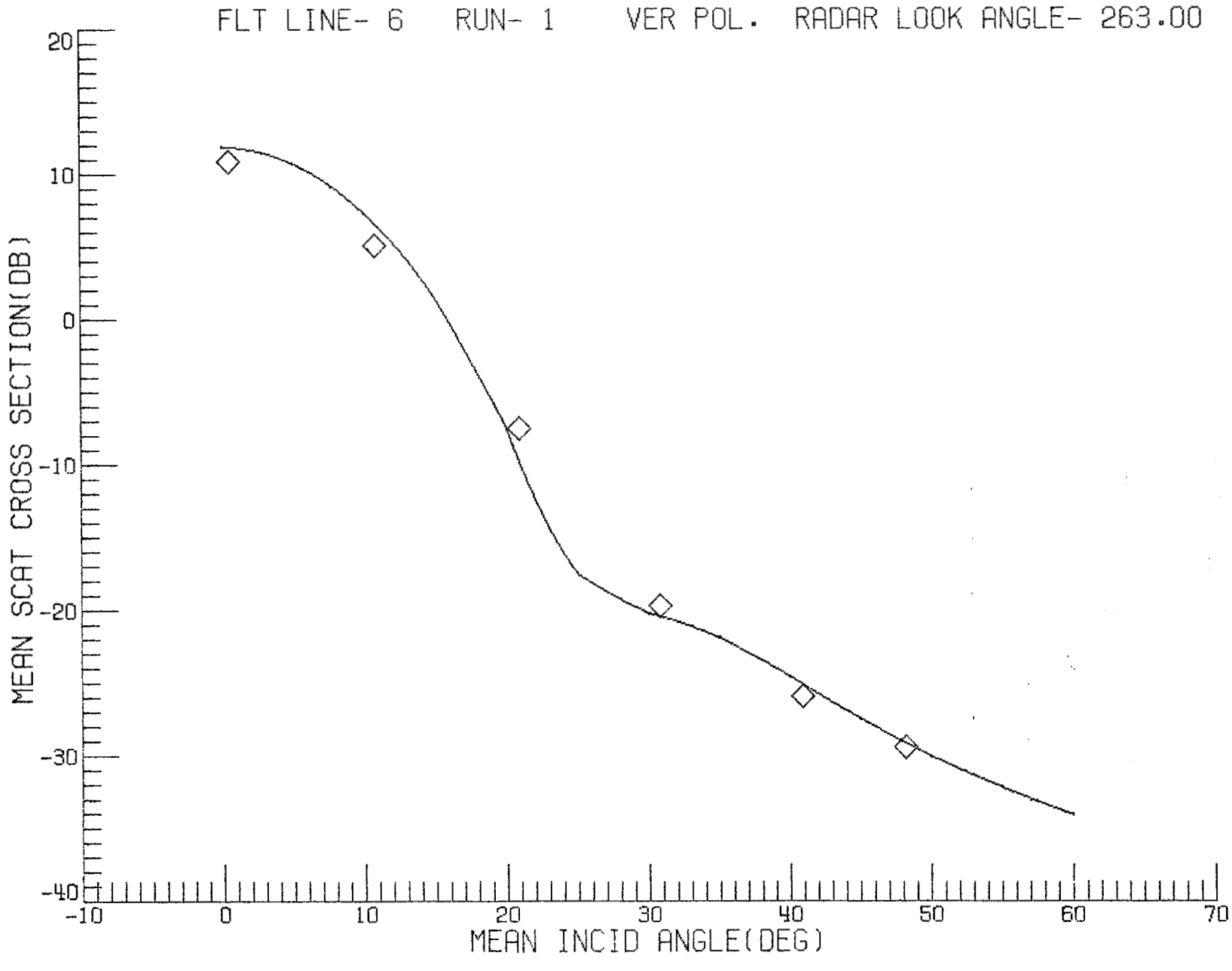
MISSION- 318 FLIGHT- 13 DATE- 8 29 1975 MODE- F.A.
FLT LINE- 6 RUN- 1 VER POL. RADAR LOOK ANGLE- 263.00
MEAN SCAT CROSS SECTION(DB)
20
10
0
-10
-20
-30
-40
-10
0
10
20
30
40
50
60
70
MEAN INCID ANGLE(DEG)

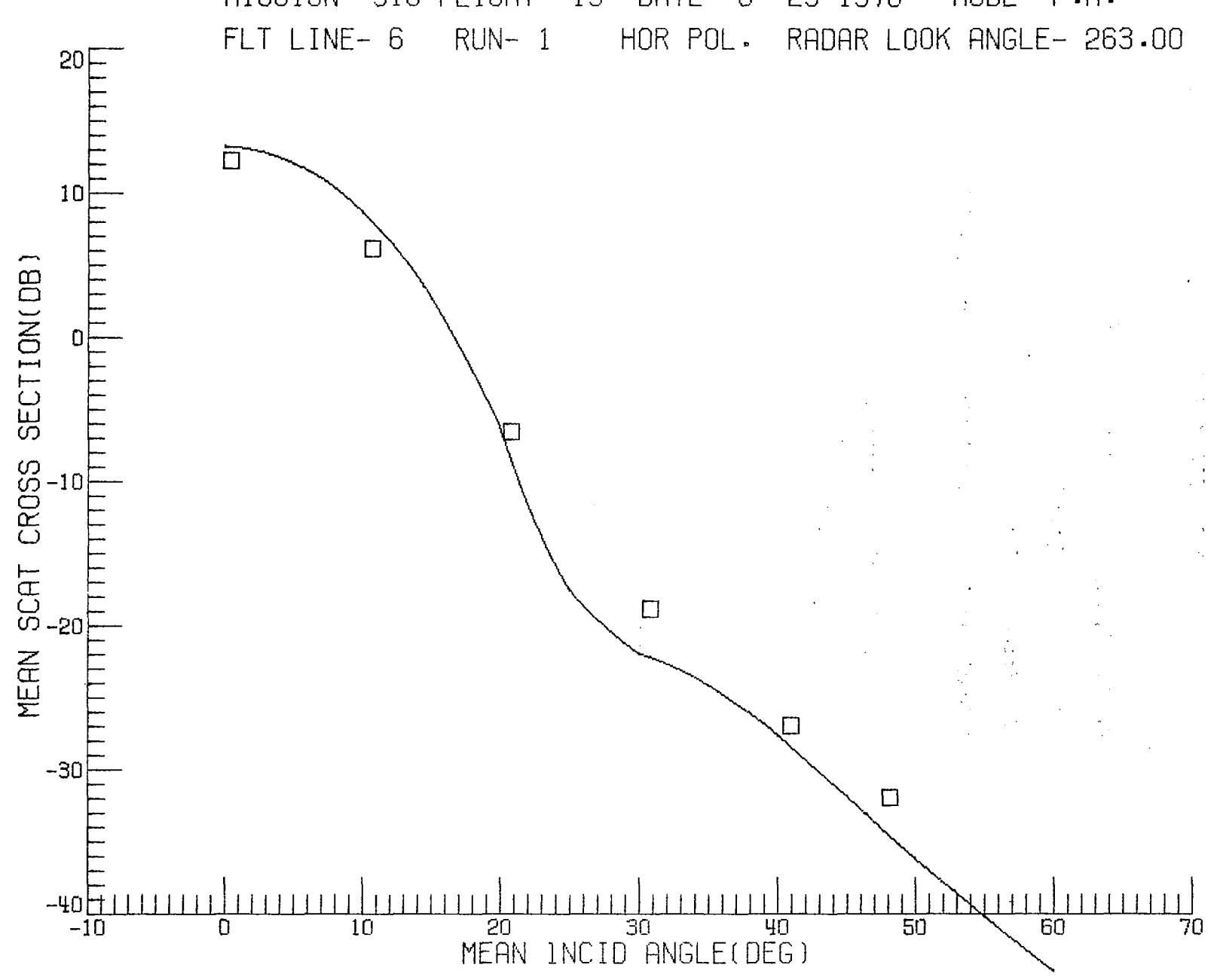
MISSION- 318 FLIGHT- 13 DATE- 8 29 1975 MODE- F.A.
FLT LINE- 6 RUN- 1 HOR POL. RADAR LOOK ANGLE- 263.00
MEAN SCAT CROSS SECTION(DB)
20
10
0
-10
-20
-30
-40
-10
0
10
20
30
40
50
60
70
MEAN INCID ANGLE(DEG)

DATA FOR A LINE

Flight 13, August 29, 1975

Line 2, Run 2, Upwind

Wind Speed = 4.5 m/s

Azimuth viewing angle relative to upwind = 331°

Small-Scale Parameters:

$a_0(\kappa_m) = 9.36 \times 10^{-7}$ cm^4

$q = 6.7$

$\kappa_c = 2.40$ cm^{-1}

Power Reflectivity at Nadir:

$R = 0.31$

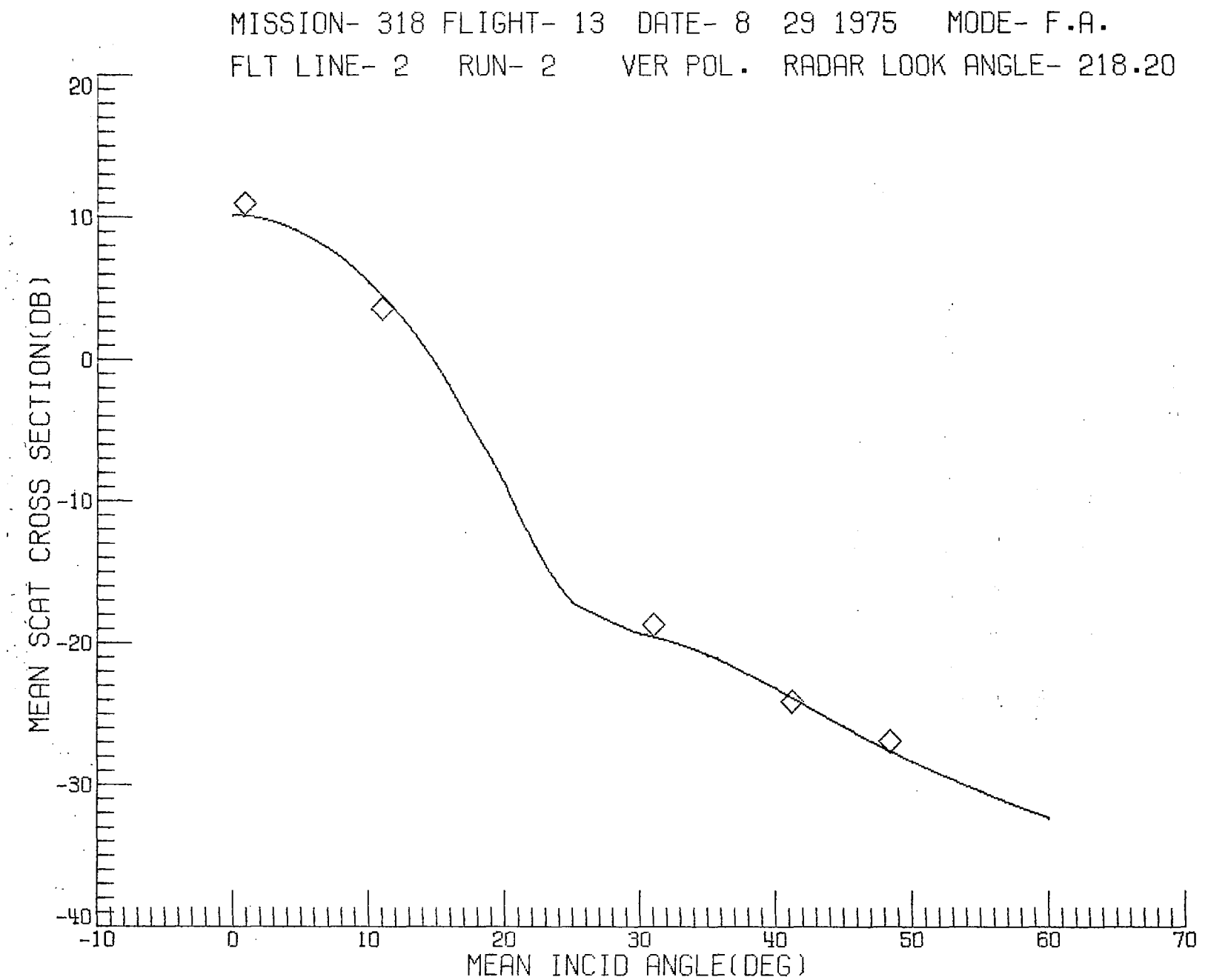
MISSION- 318 FLIGHT- 13 DATE- 8 29 1975 MODE- F.A.
FLT LINE- 2 RUN- 2 VER POL. RADAR LOOK ANGLE- 218.20
MEAN SCAT CROSS SECTION(DB)
20
10
0
-10
-20
-30
-40
-10
0
10
20
30
40
50
60
70
MEAN INCID ANGLE(DEG)

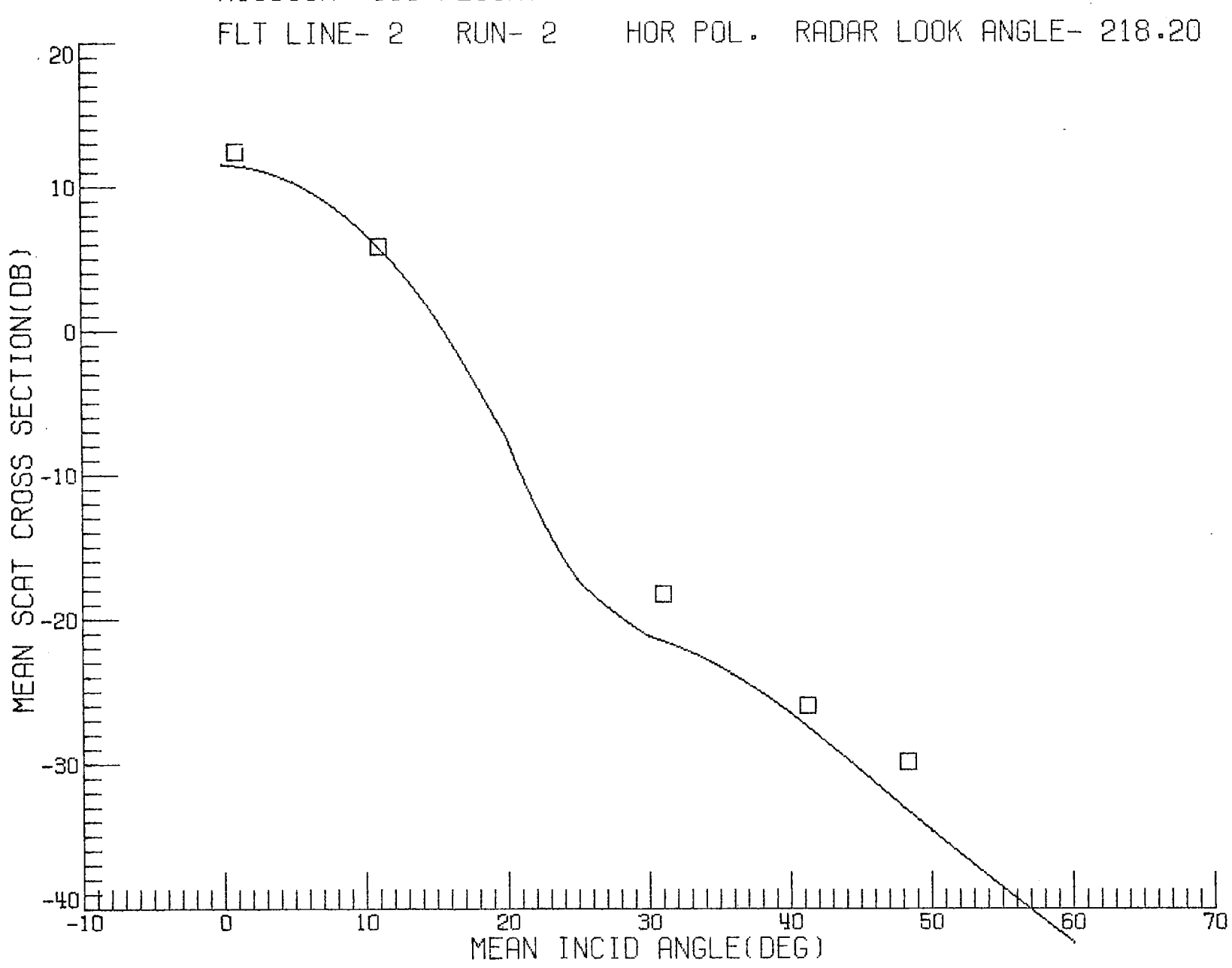
MISSION- 318 FLIGHT- 13 DATE- 8 29 1975 MODE- F.A.
FLT LINE- 2 RUN- 2 HOR POL. RADAR LOOK ANGLE- 218.20
MEAN SCAT CROSS SECTION(DB)
20
10
0
-10
-20
-30
-40
-10
0
10
20
30
40
50
60
70
MEAN INCID ANGLE(DEG)

DATA FOR OVERALL FLIGHT

Flight 14, September 2, 1975

Average Wind Speed = 5.5 m/s

Average Wind Direction (out of) = 49° east of North

Large-Scale Parameters:

$\langle S_u^2 \rangle^{\frac{1}{2}} = 0.12$

$\langle S_c^2 \rangle^{\frac{1}{2}} = 0.12$

$c_1 = 0.01$

$c_2 = 0.00$

$c_3 = 0.01$

$c_4 = 0.05$

$c_5 = 0.02$

Small-Scale Anisotropy Ratio:

$a_r = 0.52$

DATA FOR CIRCLES

Flight 14, September 2, 1975

Three circles for θ = 20°, 40° and 65°

Wind Speed = 5.5 m/s

Small-Scale Parameters:

$a_0(\kappa_m) = 1.09 \times 10^{-6}$ cm^4

$q = 4.6$

$\kappa_c = 1.21$ cm^{-1}

Power Reflectivity at Nadir:

$R = 0.36$

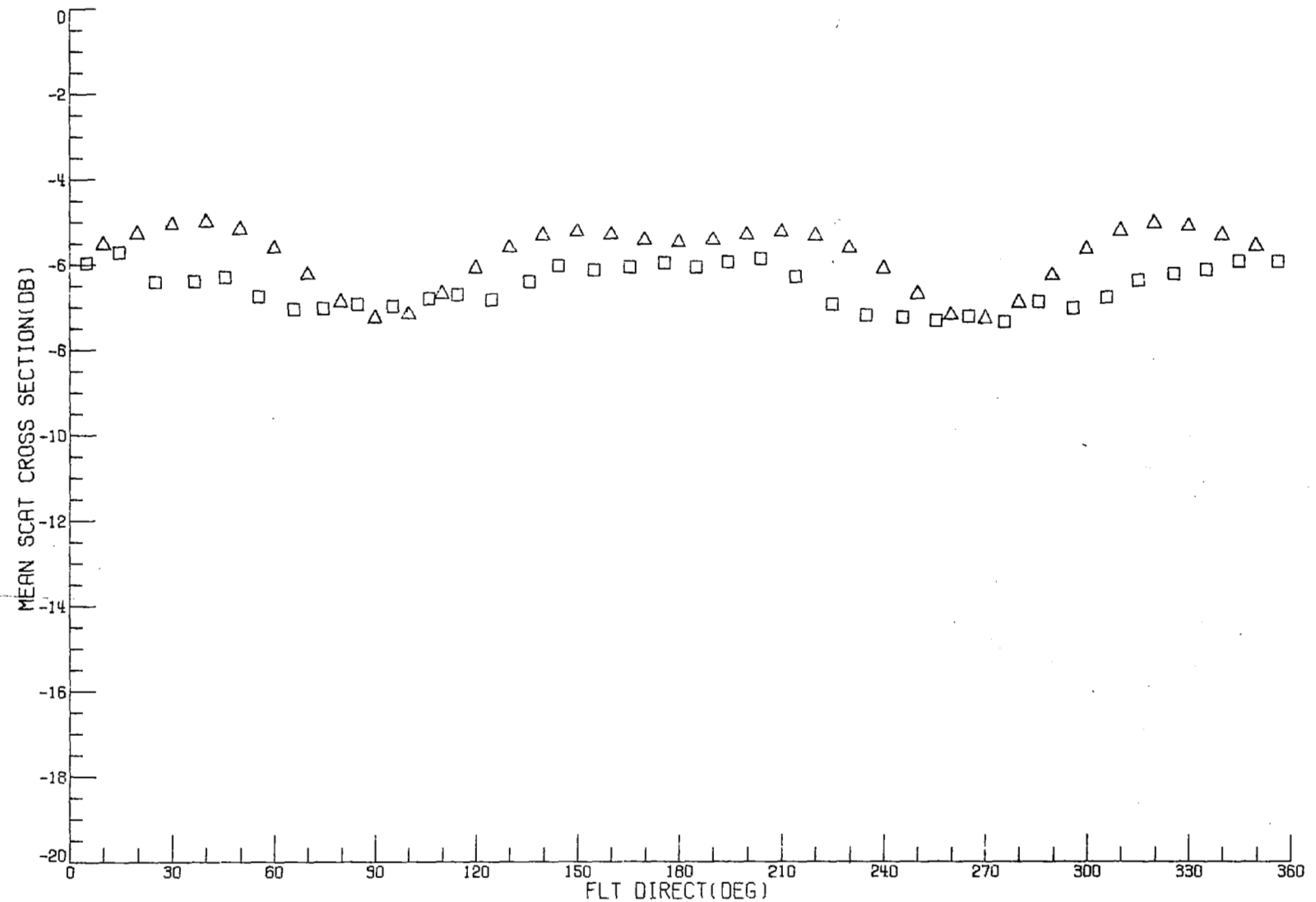
MISSION- 318 FLIGHT- 14 DATE- 9 2 1975
FLT LINE- 4 RUN- 1 VER POL.
DATA CORRECTED TO 20.00° INCIDENCE ANGLE
□ = CORRECTED RADSCAT DATA
△ = CALCULATED DATA
MEAN SCAT CROSS SECTION(DB)
0
-2
-4
-6
-8
-10
-12
-14
-16
-18
-20
0
30
60
90
120
150
180
210
240
270
300
330
360
FLT DIRECT(DEG)

MISSION- 318 FLIGHT- 14 DATE- 9 2 1975
FLT LINE- 4 RUN- 1 HOR POL.
DATA CORRECTED TO 20.00° INCIDENCE ANGLE

□ = CORRECTED RADSCAT DATA
△ = CALCULATED DATA

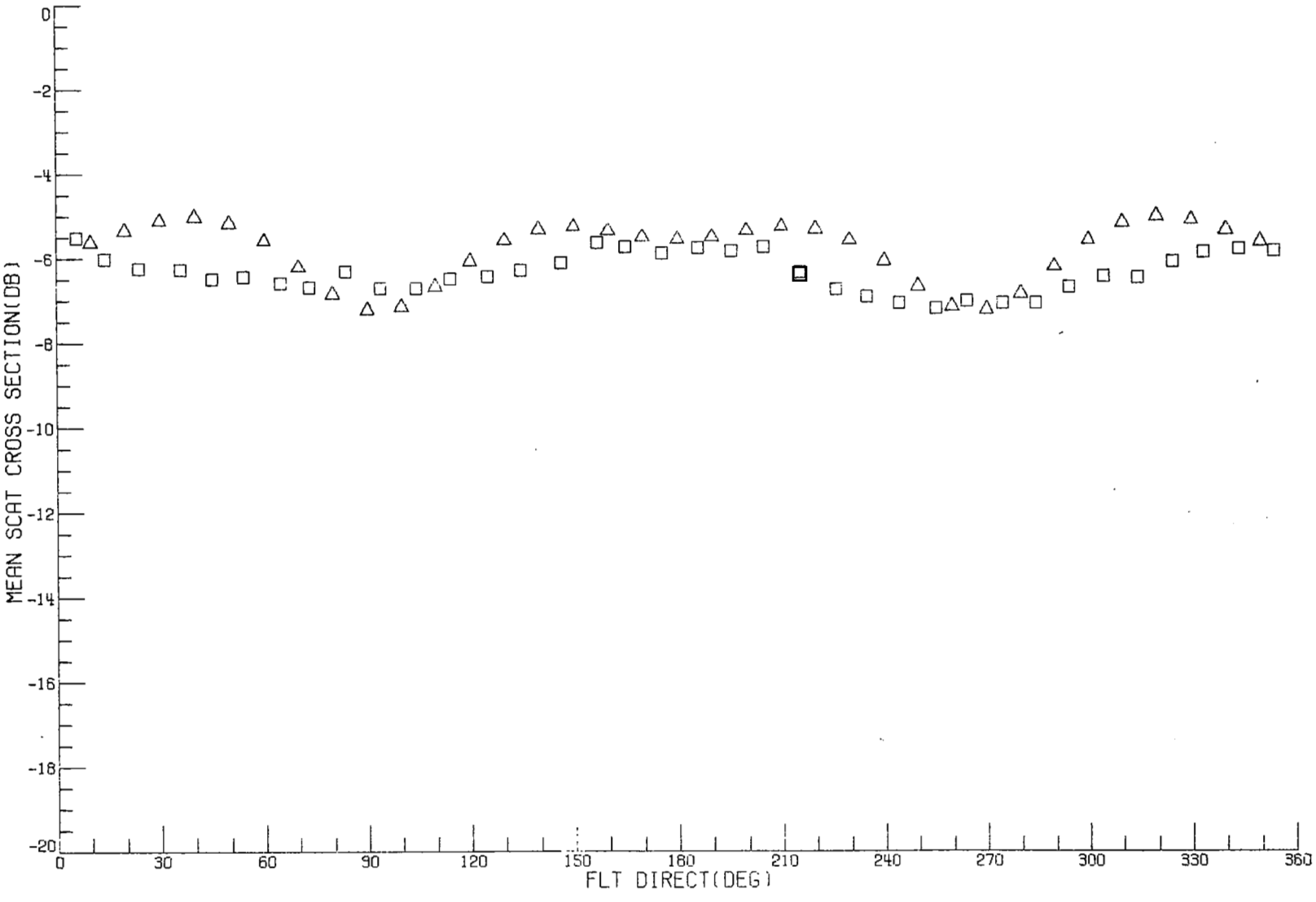

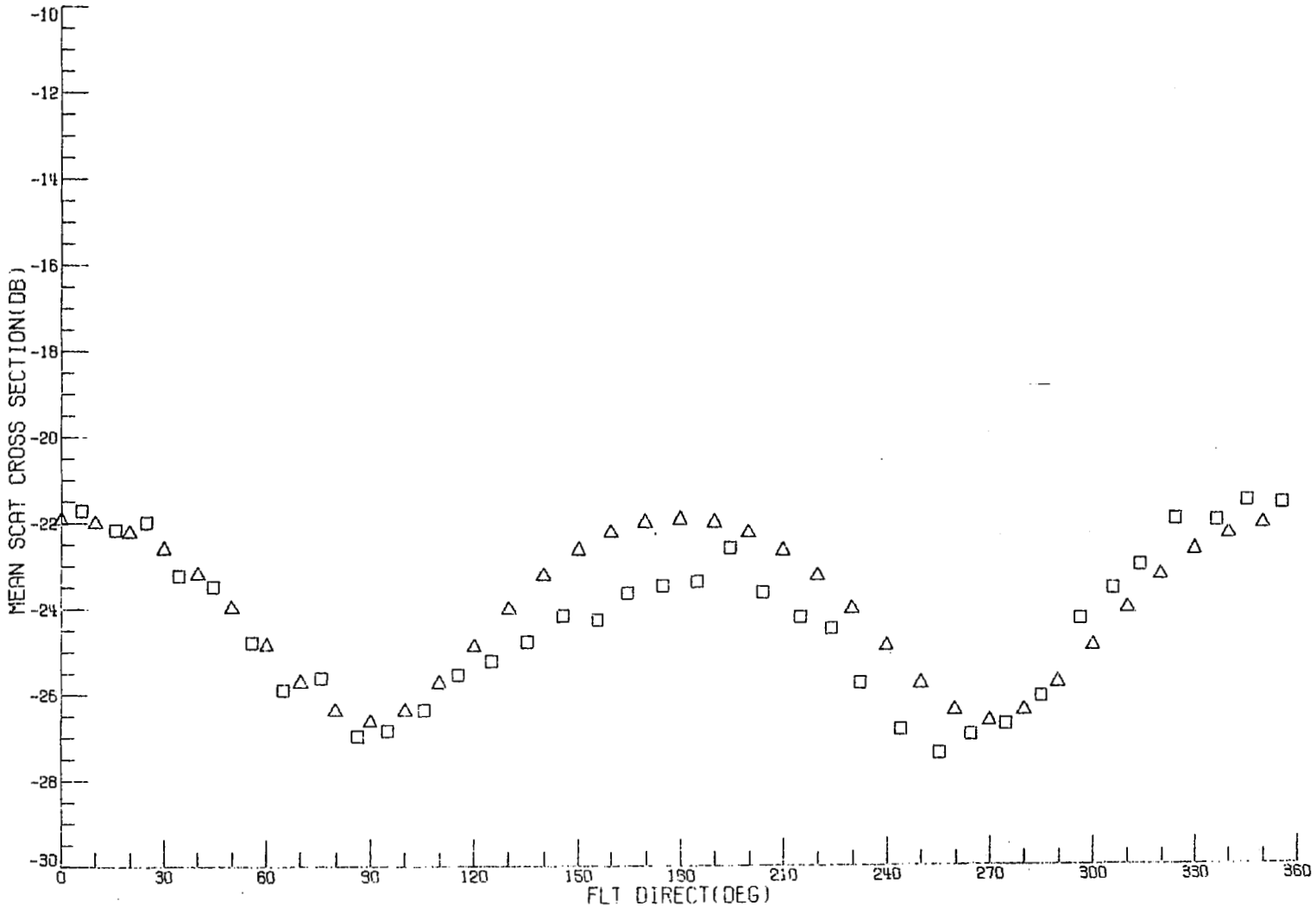
MISSION- 318 FLIGHT- 14 DATE- 9 2 1975
FLT LINE- 4 RUN- 7 VER POL.
DATA CORRECTED TO 40.00° INCIDENCE ANGLE
WIND DIRECTION (OUT OF) 50.0°
= CORRECTED RADSCAT DATA
= CALCULATED DATA
MEAN SCAT CROSS SECTION(DB)
-10
-12
-14
-16
-18
-20
-22
-24
-26
-28
-30
0
30
60
90
120
150
180
210
240
270
300
330
360
FLT DIRECT(DEG)

MISSION- 318 FLIGHT- 14 DATE- 9 2 1975
FLT LINE- 4 · RUN- 7 HOR POL.
DATA CORRECTED TO 40.00° INCIDENCE ANGLE
WIND DIRECTION (OUT OF) 50.0°

□ = CORRECTED RADSCAT DATA
△ = CALCULATED DATA

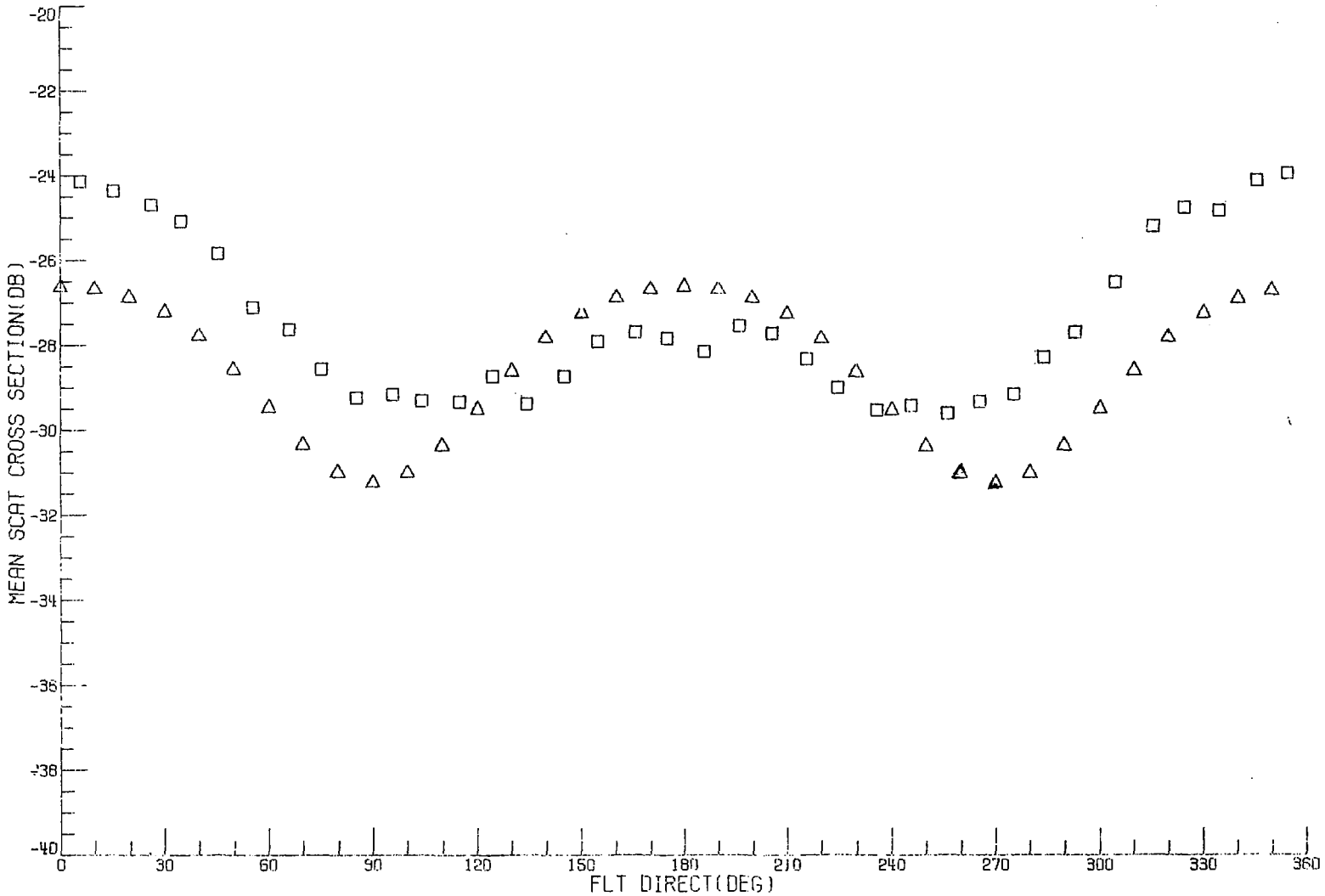

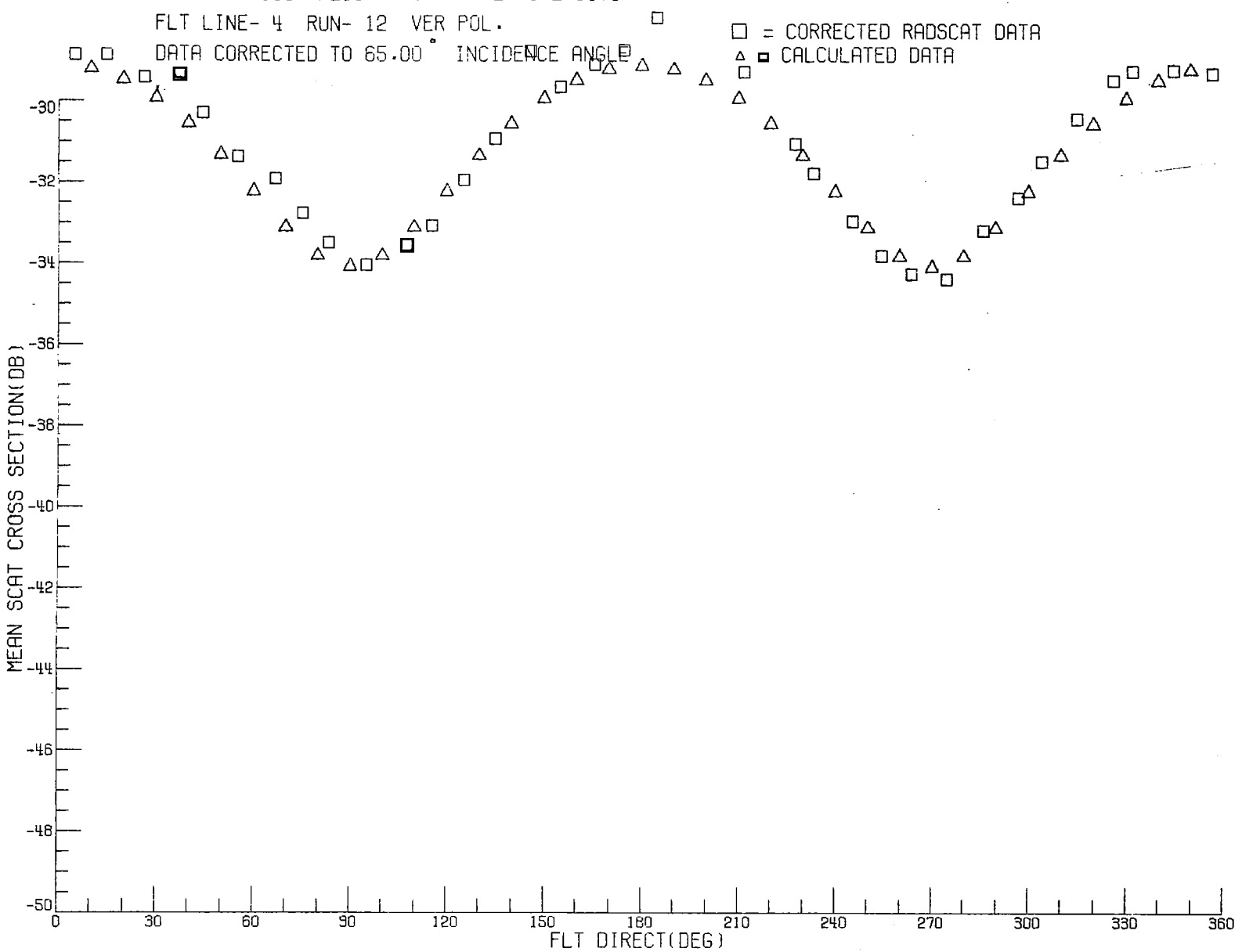
MISSION- 318 FLIGHT- 14 DATE- 9 2 1975
FLT LINE- 4 RUN- 12 VER POL.
DATA CORRECTED TO 65.00° INCIDENCE ANGLE
□ = CORRECTED RADSCAT DATA
△ ■ CALCULATED DATA
MEAN SCAT CROSS SECTION(DB)
-30
-32
-34
-36
-38
-40
-42
-44
-46
-48
-50
0
30
60
90
120
150
180
210
240
270
300
330
360
FLT DIRECT(DEG)

MISSION- 318 FLIGHT- 14 DATE- 9 2 1975
FLT LINE- 4 RUN- 12 HOR POL.
DATA CORRECTED TO 65.00° INCIDENCE ANGLE

□ = CORRECTED RADSCAT DATA
△ = CALCULATED DATA

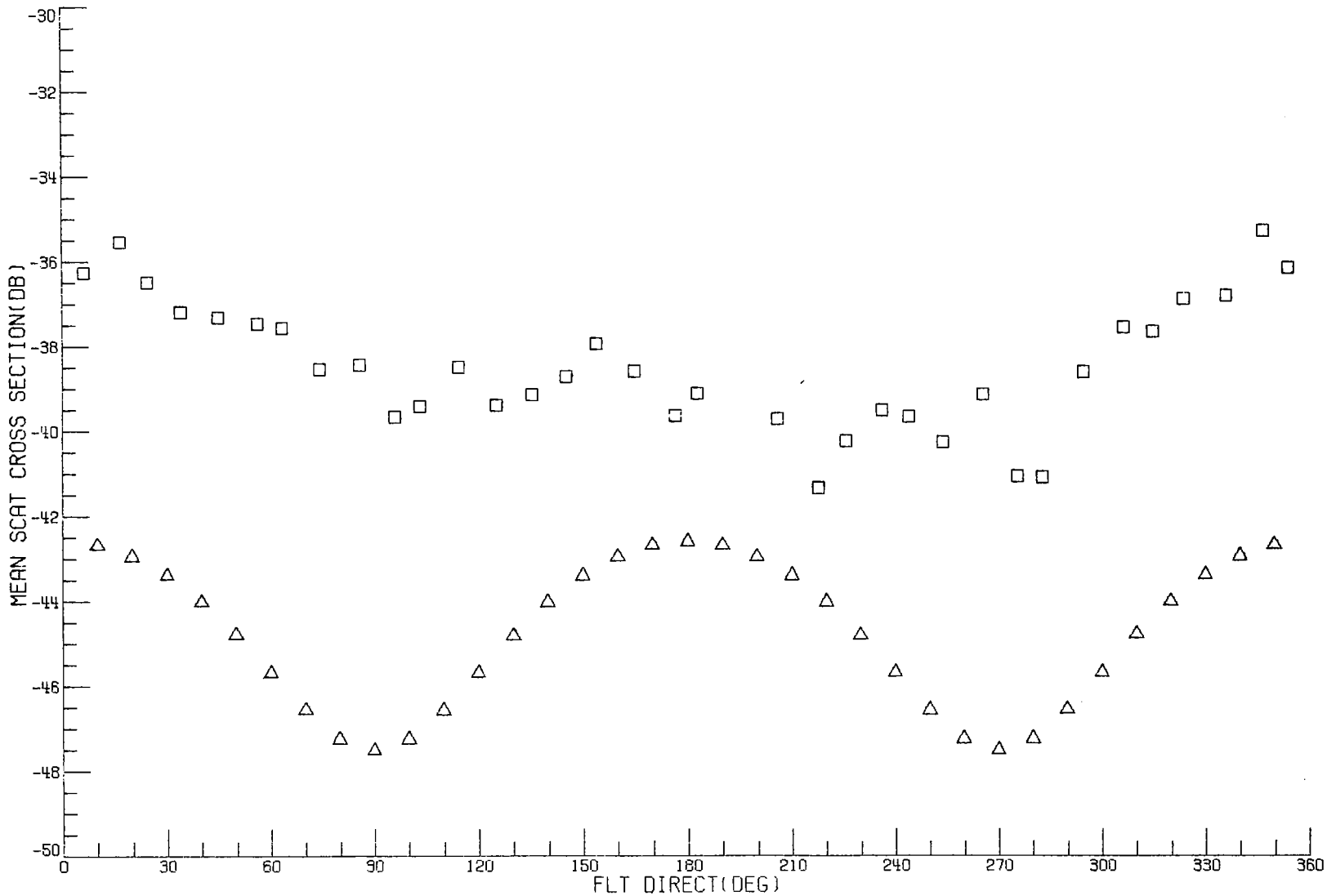

DATA FOR A LINE

Flight 14, September 2, 1975

Line 3, Run 2, Downwind

Wind Speed = 5.5 m/s

Azimuth viewing angle relative to upwind = 172°

Small-Scale Parameters:

$a_0(\kappa_m) = 1.43 \times 10^{-6}$ cm^4

$q = 2.7$

$\kappa_c = 1.07$ cm^{-1}

Power Reflectivity at Nadir:

$R = 0.49$

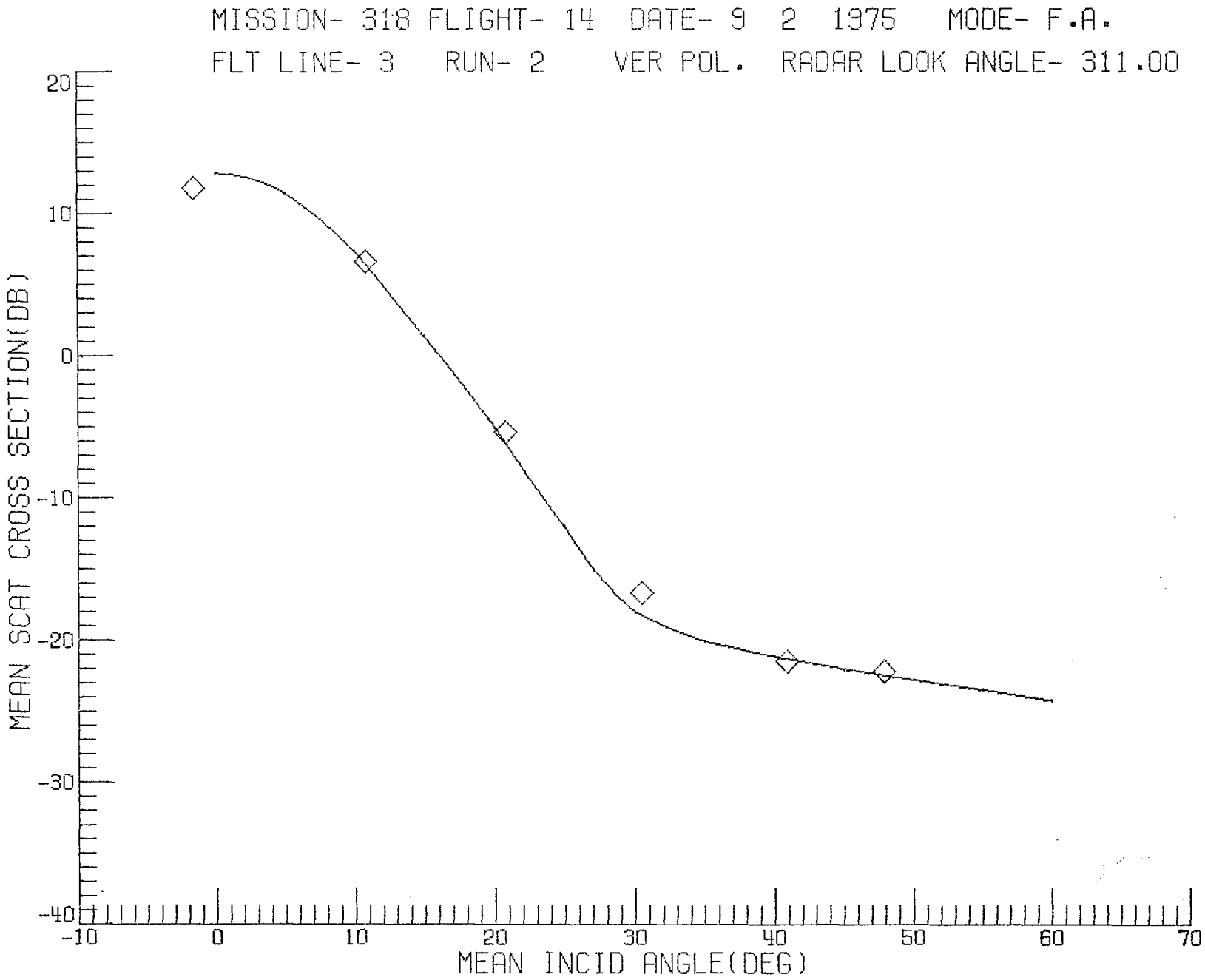
MISSION- 318 FLIGHT- 14 DATE- 9 2 1975 MODE- F.A.
FLT LINE- 3 RUN- 2 VER POL. RADAR LOOK ANGLE- 311.00
MEAN SCAT CROSS SECTION(DB)
20
10
0
-10
-20
-30
-40
-10
0
10
20
30
40
50
60
70
MEAN INCID ANGLE(DEG)

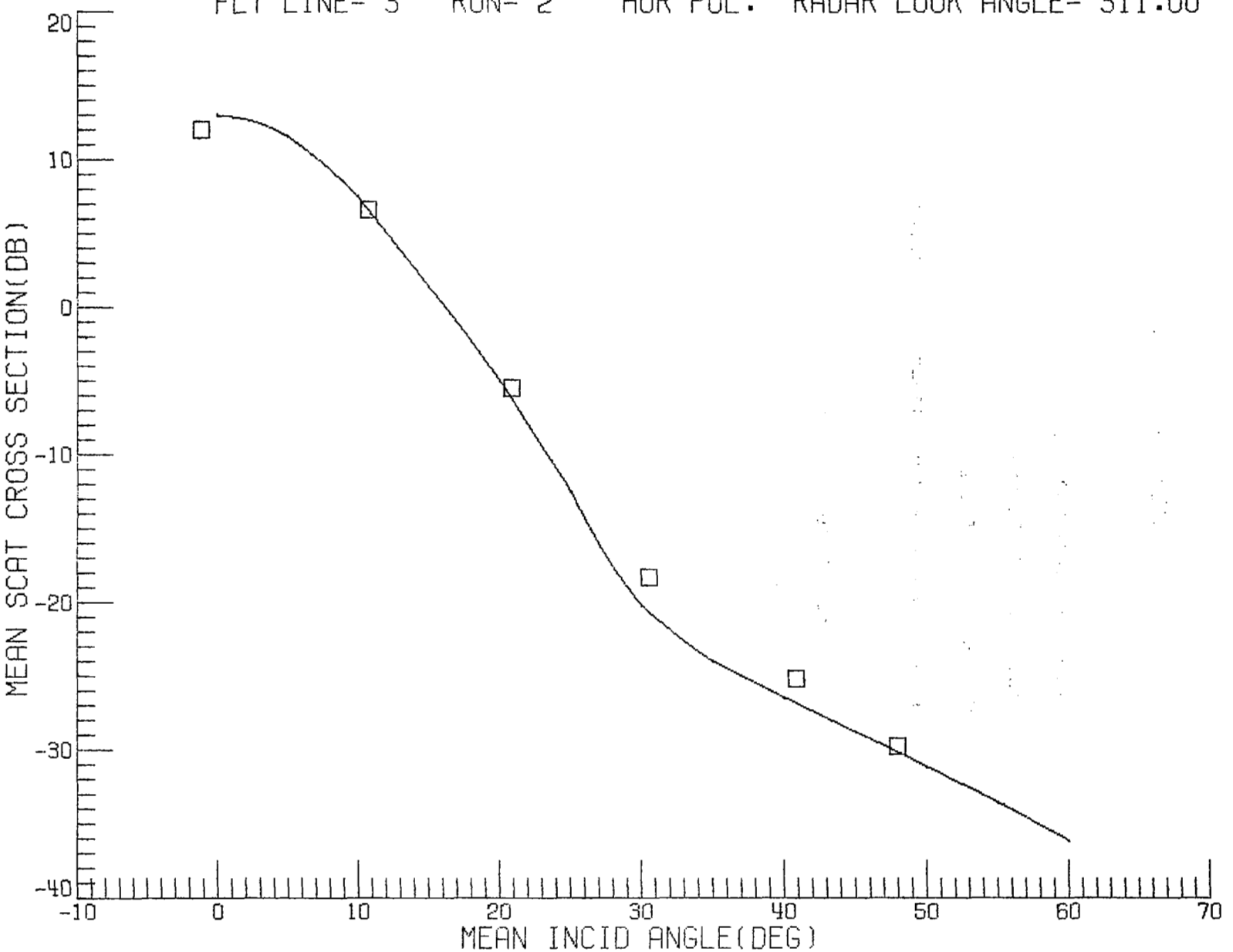
MISSION- 318 FLIGHT- 14 DATE- 9 2 1975 MODE- F.A.
FLT LINE- 3 RUN- 2 HOR POL. RADAR LOOK ANGLE- 311.00
MEAN SCAT CROSS SECTION(DB)
20
10
0
-10
-20
-30
-40
-10
0
10
20
30
40
50
60
70
MEAN INCID ANGLE(DEG)

DATA FOR A LINE

Flight 14, September 2, 1975

Line 3, Run 1, Upwind

Wind Speed = 5.5 m/s

Azimuth viewing angle relative to upwind = 352°

Small-Scale Parameters:

$a_0(\kappa_m) = 6.38\times10^{-7}$ cm^4

$q = 5.2$

$\kappa_c = 1.50$ cm^{-1}

Power Reflectivity at Nadir:

$R = 0.41$

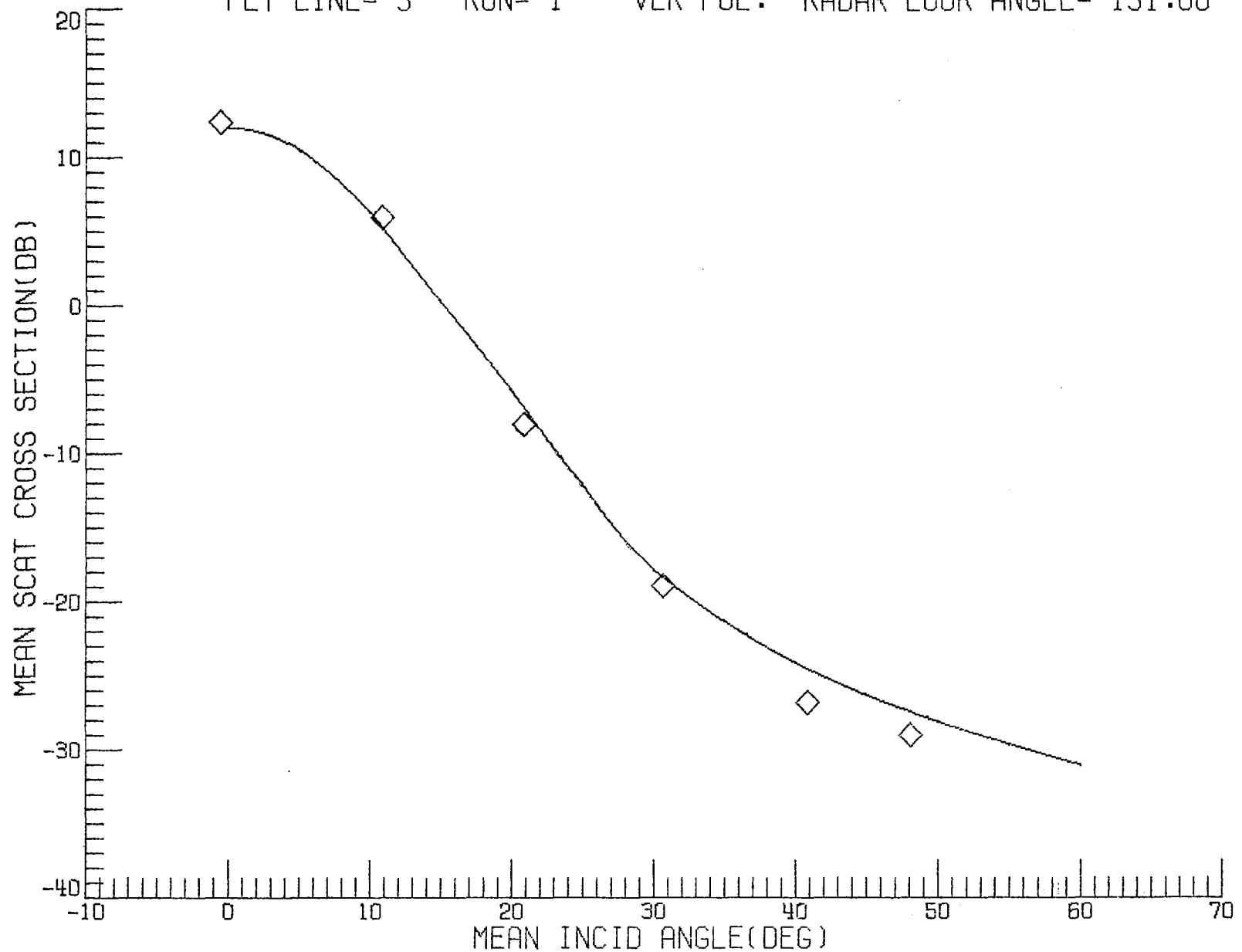
MISSION- 318 FLIGHT- 14 DATE- 9 2 1975 MODE- F.A.
FLT LINE- 3 RUN- 1 VER POL. RADAR LOOK ANGLE- 131.00
MEAN SCAT CROSS SECTION(DB)
20
10
0
-10
-20
-30
-40
-10
0
10
20
30
40
50
60
70
MEAN INCID ANGLE(DEG)

MISSION- 318 FLIGHT- 14 DATE- 9 2 1975 MODE- F.A.
FLT LINE- 3 RUN- 1 HOR POL. RADAR LOOK ANGLE- 131.00

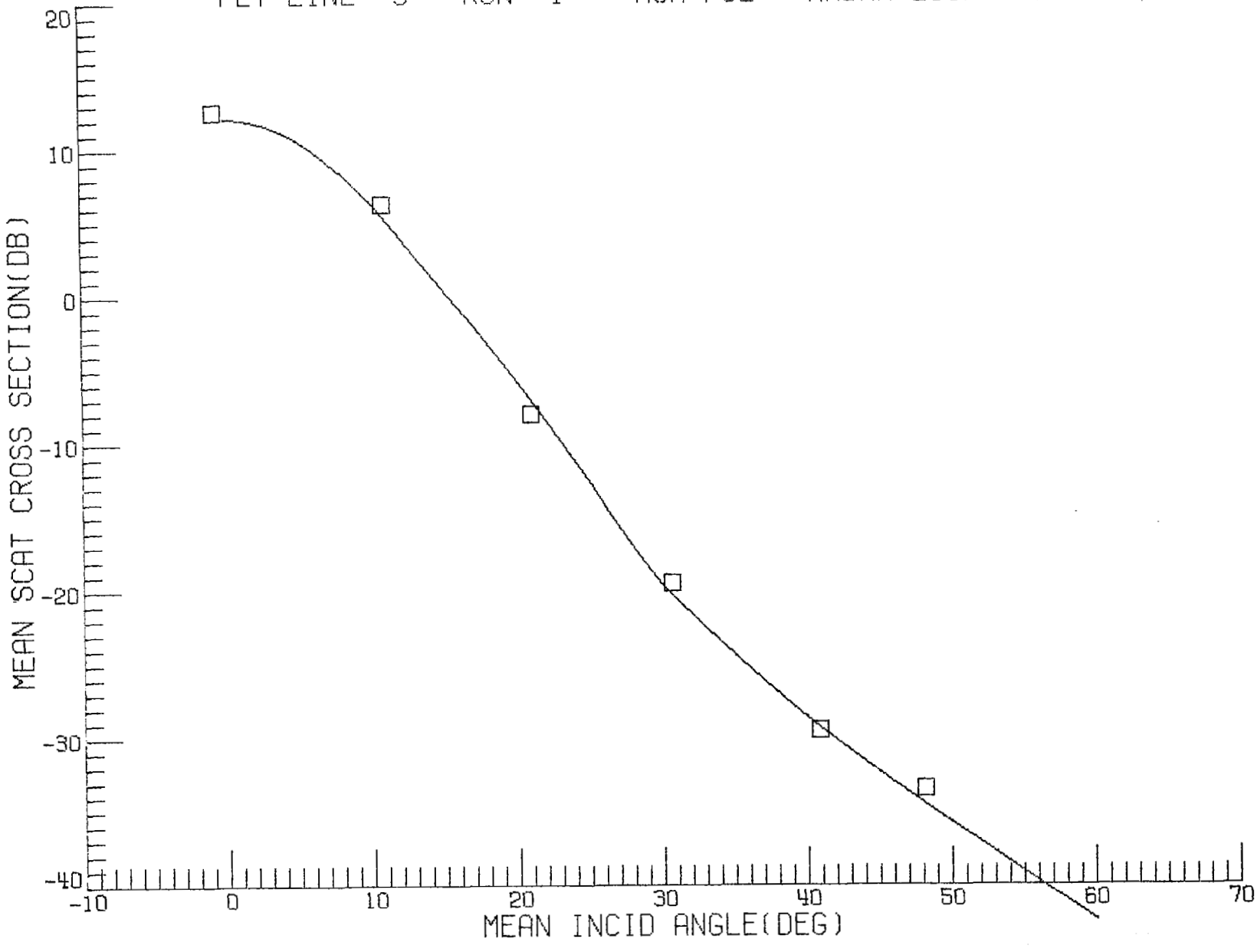

DATA FOR A LINE

Flight 14, September 2, 1975

Line 2, Run 3, Crosswind

Wind Speed = 5.5 m/s

Azimuth viewing angle relative to upwind = 262°

Small-Scale Parameters:

$a_0(\kappa_m) = 6.99 \times 10^{-7}$ cm^4

$q = 4.1$

$\kappa_c = 1.06$ cm^{-1}

Power Reflectivity at Nadir:

$R = 0.40$

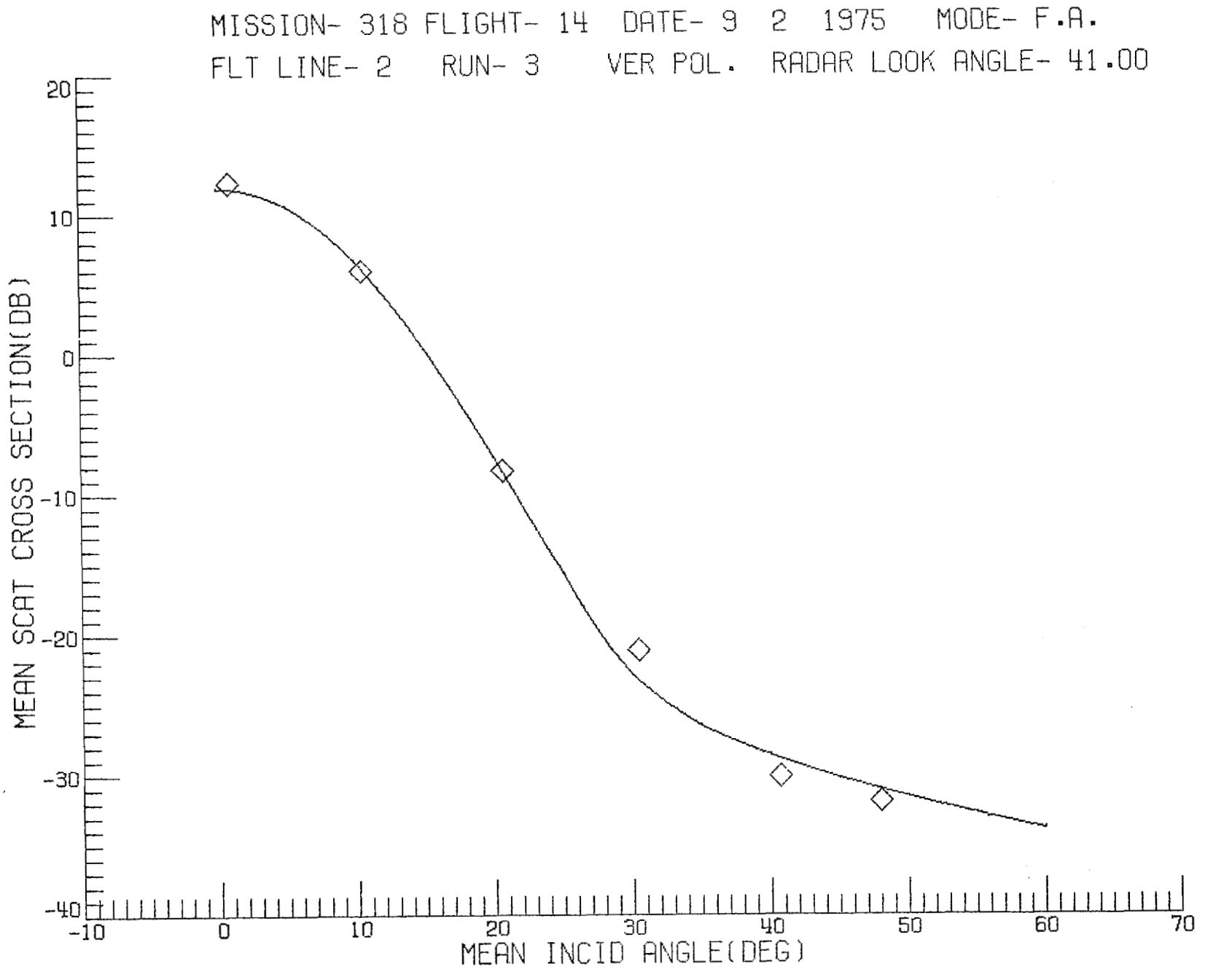
MISSION- 318 FLIGHT- 14 DATE- 9 2 1975 MODE- F.A.
FLT LINE- 2 RUN- 3 VER POL. RADAR LOOK ANGLE- 41.00
MEAN SCAT CROSS SECTION(DB)
20
10
0
-10
-20
-30
-40
-10
0
10
20
30
40
50
60
70
MEAN INCID ANGLE(DEG)

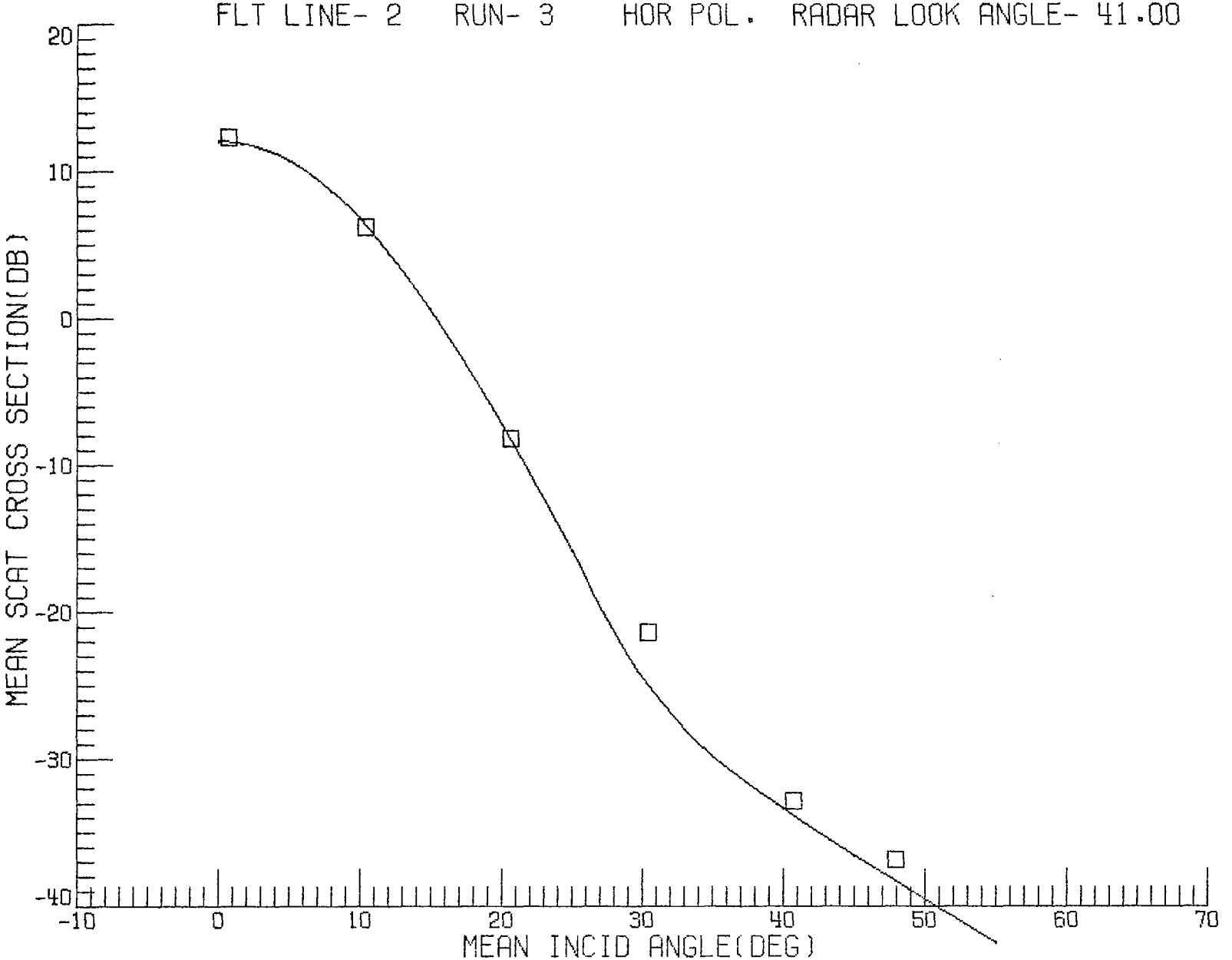
MISSION- 318 FLIGHT- 14 DATE- 9 2 1975 MODE- F.A.
FLT LINE- 2 RUN- 3 HOR POL. RADAR LOOK ANGLE- 41.00
MEAN SCAT CROSS SECTION(DB)
20
10
0
-10
-20
-30
-40
-10
0
10
20
30
40
50
60
70
MEAN INCID ANGLE(DEG)

DATA FOR OVERALL FLIGHT

Flight 16, September 8, 1975

Average Wind Speed = 8.6 m/s

Average Wind Direction (out of) = 204° east of North

Large-Scale Parameters:

$\langle S_u^2 \rangle^{\frac{1}{2}} = 0.13$

$\langle S_c^2 \rangle^{\frac{1}{2}} = 0.12$

$c_1 = -0.035$

$c_2 = -0.005$

$c_3 = 0.025$

$c_4 = 0.095$

$c_5 = 0.035$

Small-Scale Anisotropy Ratio:

$a_r = 0.72$

DATA FOR CIRCLES

Flight 16, September 8, 1975

Three circles for θ = 20°, 40°, and 65°

Wind Speed = 8.7 m/s

Small-Scale Parameters:

$a_0(\kappa_m) \doteq 2.46 \times 10^{-6}$ cm^4

$q = 3.4$

$\kappa_c = 1.93$ cm^{-1}

Power Reflectivity at Nadir:

$R = 0.41$

MISSION- 318 FLIGHT- 16 DATE- 9 8 1975
FLT LINE- 4 RUN- 4 VER POL.
DATA CORRECTED TO 20.00° INCIDENCE ANGLE

□ = CORRECTED RADSCAT DATA
△ □ CALCULATED DATA

squares should be moved 20° to the right

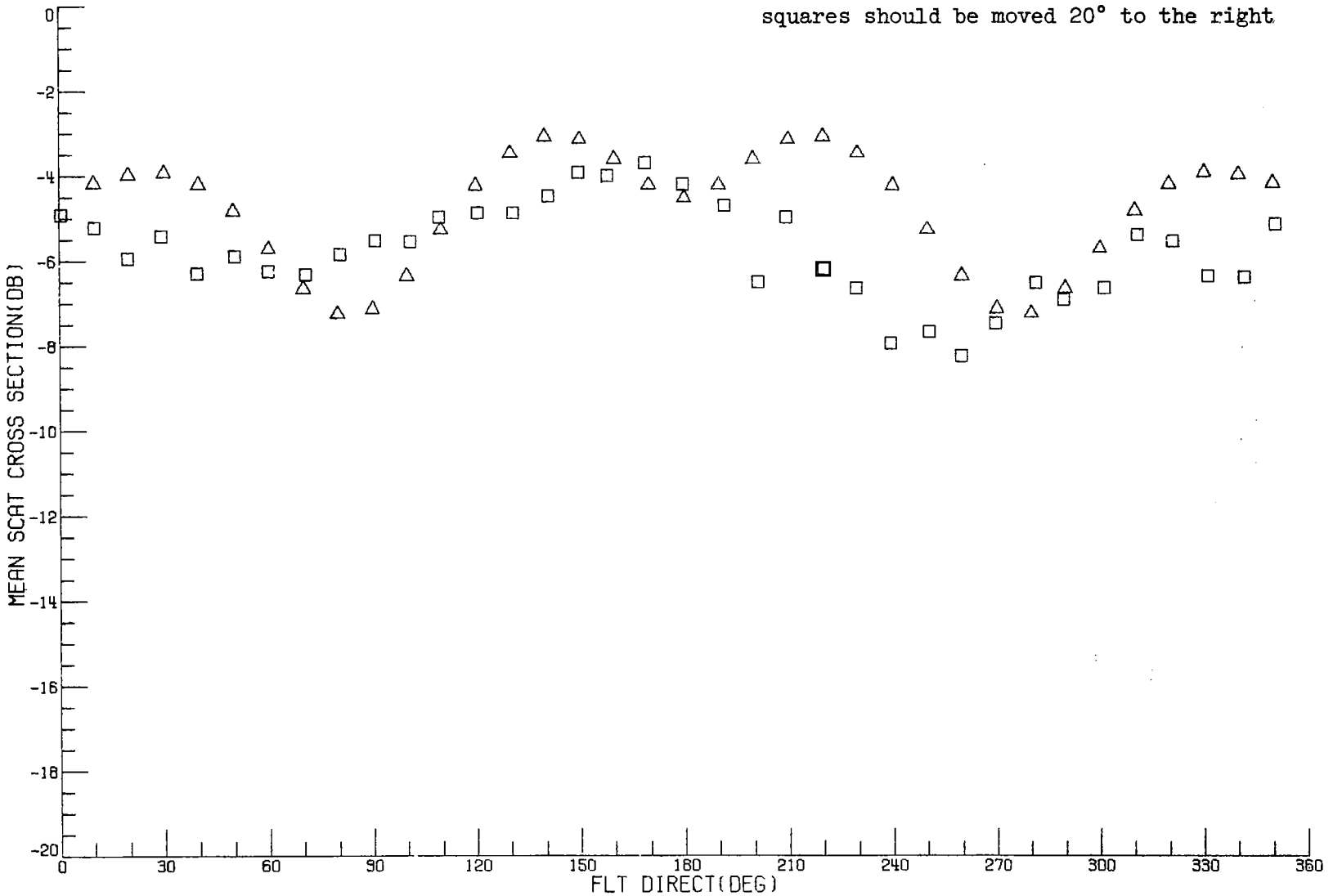

MISSION- 318 FLIGHT- 16 DATE- 9 8 1975
FLT LINE- 4 RUN- 4 HOR POL.
DATA CORRECTED TO 20.00° INCIDENCE ANGLE

□ = CORRECTED RADSCAT DATA
△ = CALCULATED DATA
squares should be moved 20° to the right

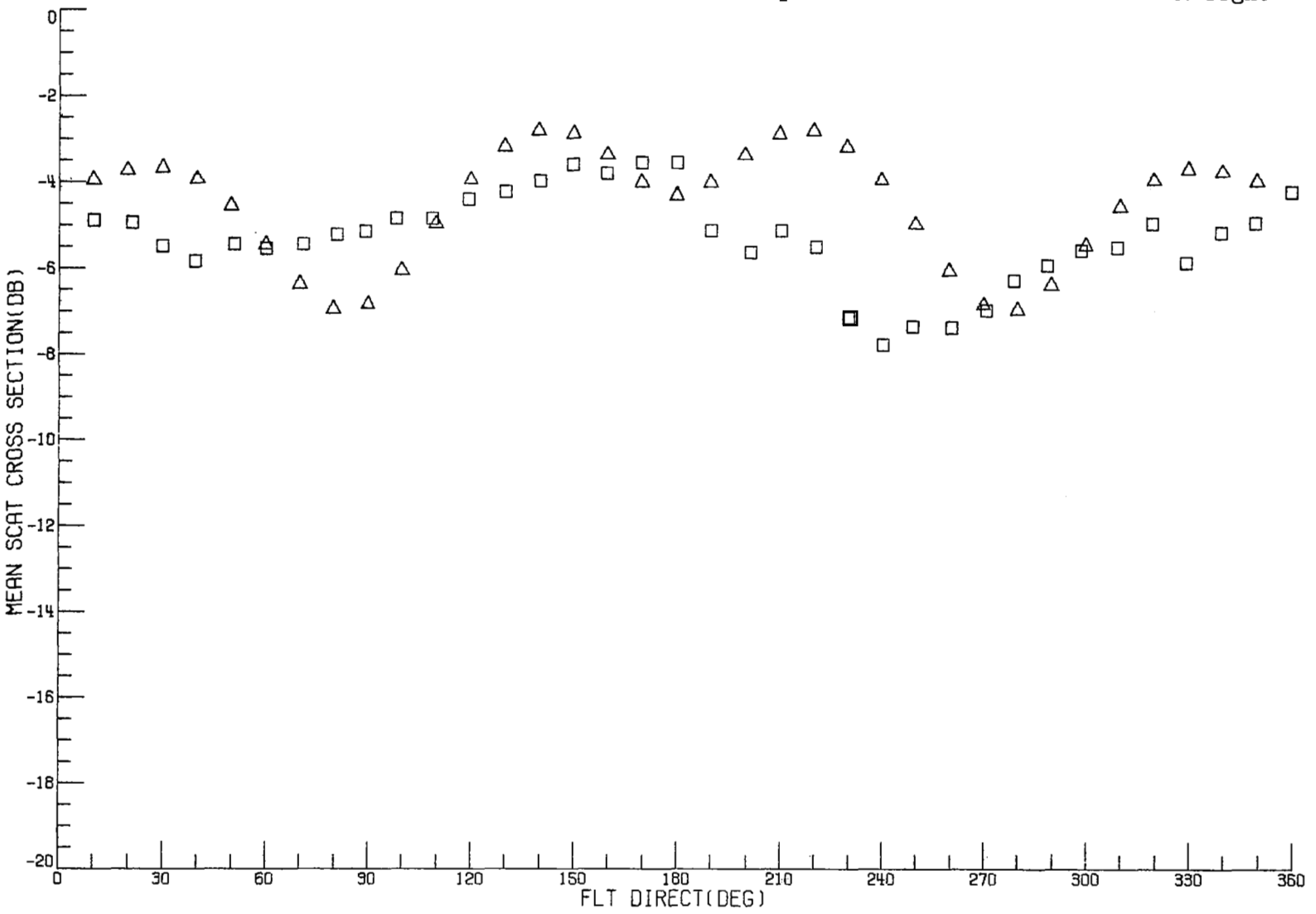

MISSION- 318 FLIGHT- 16 DATE- 9 8 1975
FLT LINE- 4 RUN- 9 VER POL.
DATA CORRECTED TO 40.00° INCIDENCE ANGLE

□ = CORRECTED RADSCAT DATA
△ = CALCULATED DATA
squares should be moved 20° to the right

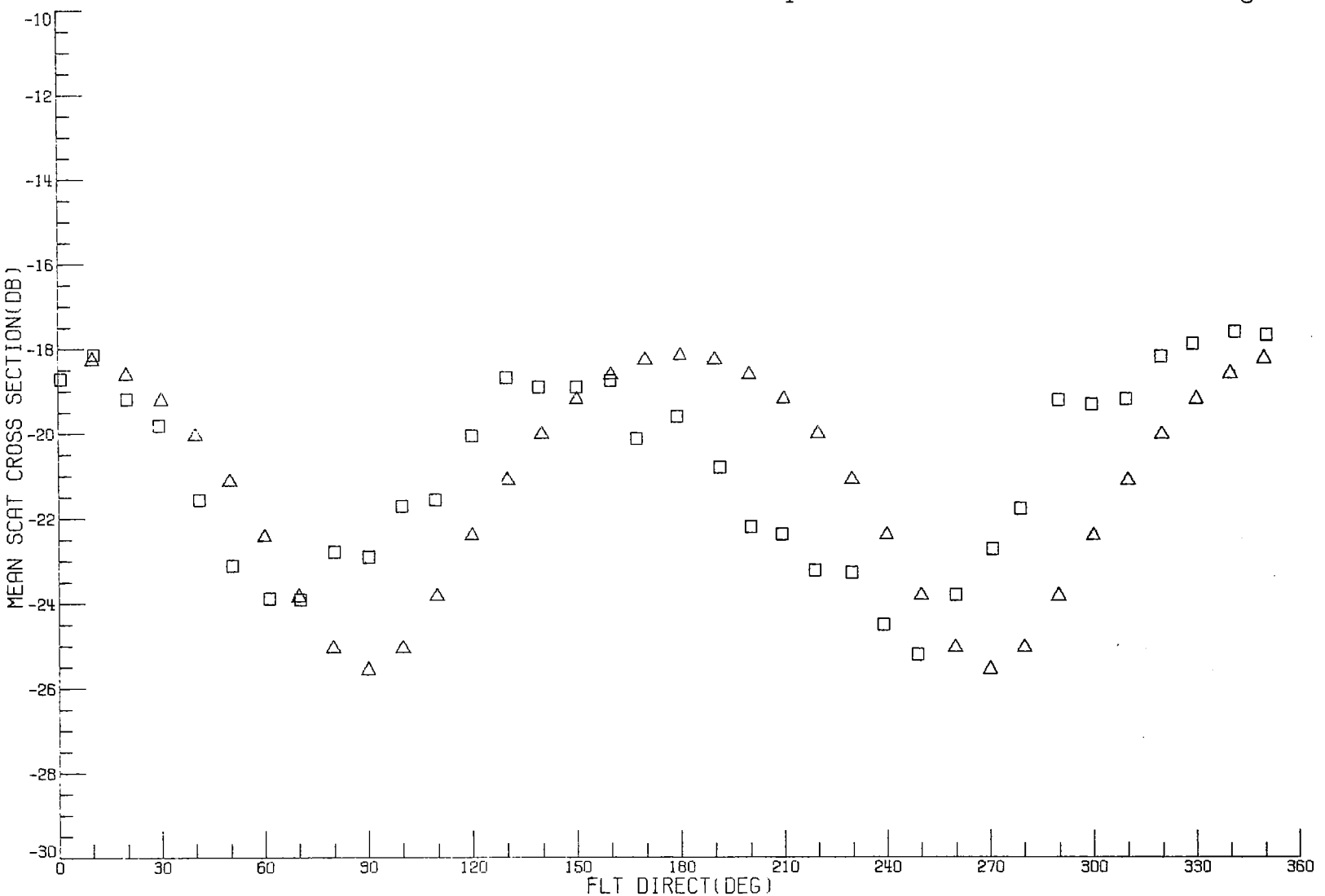

MISSION- 318 FLIGHT- 16 DATE- 9 8 1975
FLT LINE- 4 RUN- 9 HOR POL.
DATA CORRECTED TO 40.00° INCIDENCE ANGLE

□ = CORRECTED RADSCAT DATA
△ = CALCULATED DATA

squares should be moved 20° to the right

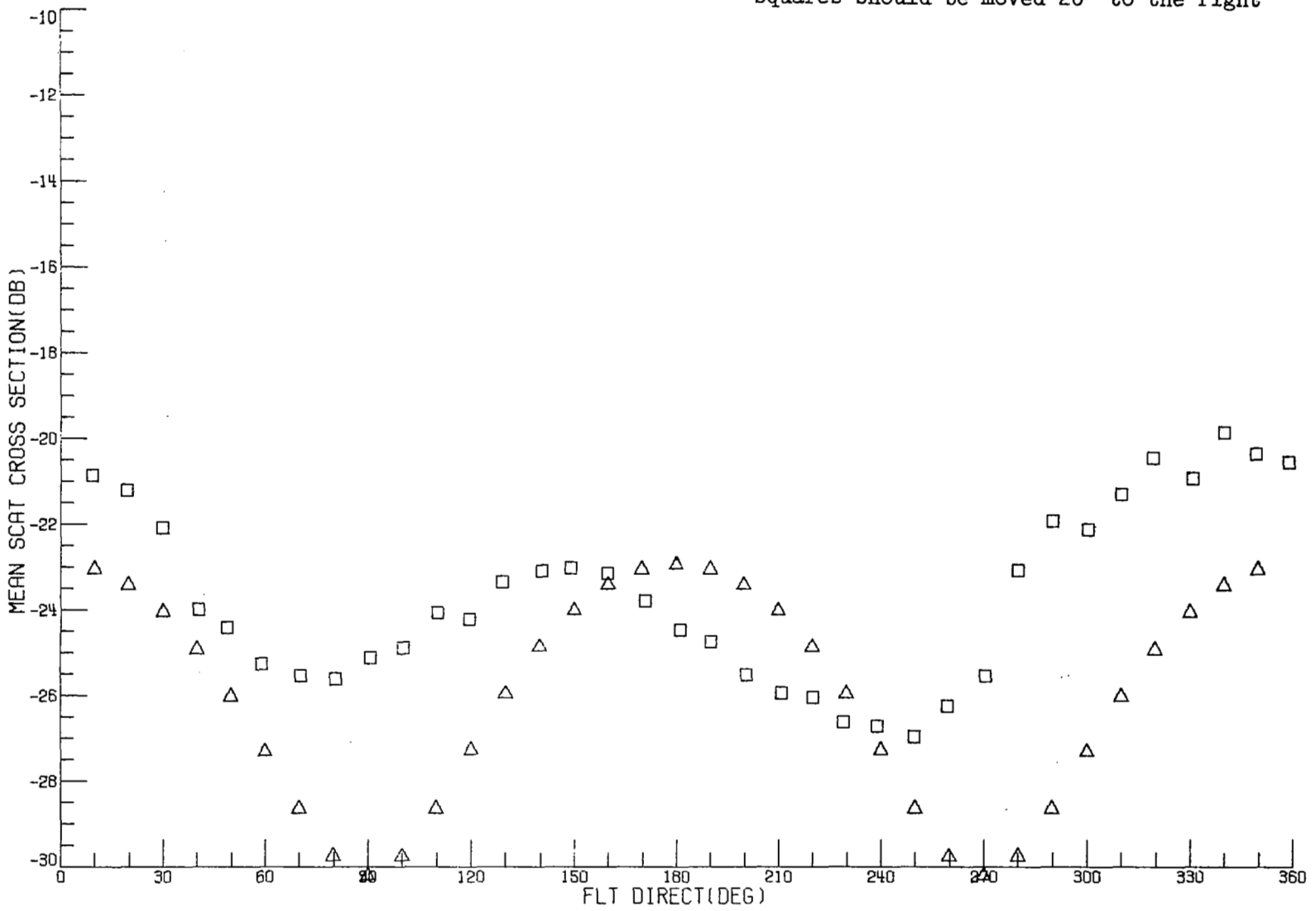

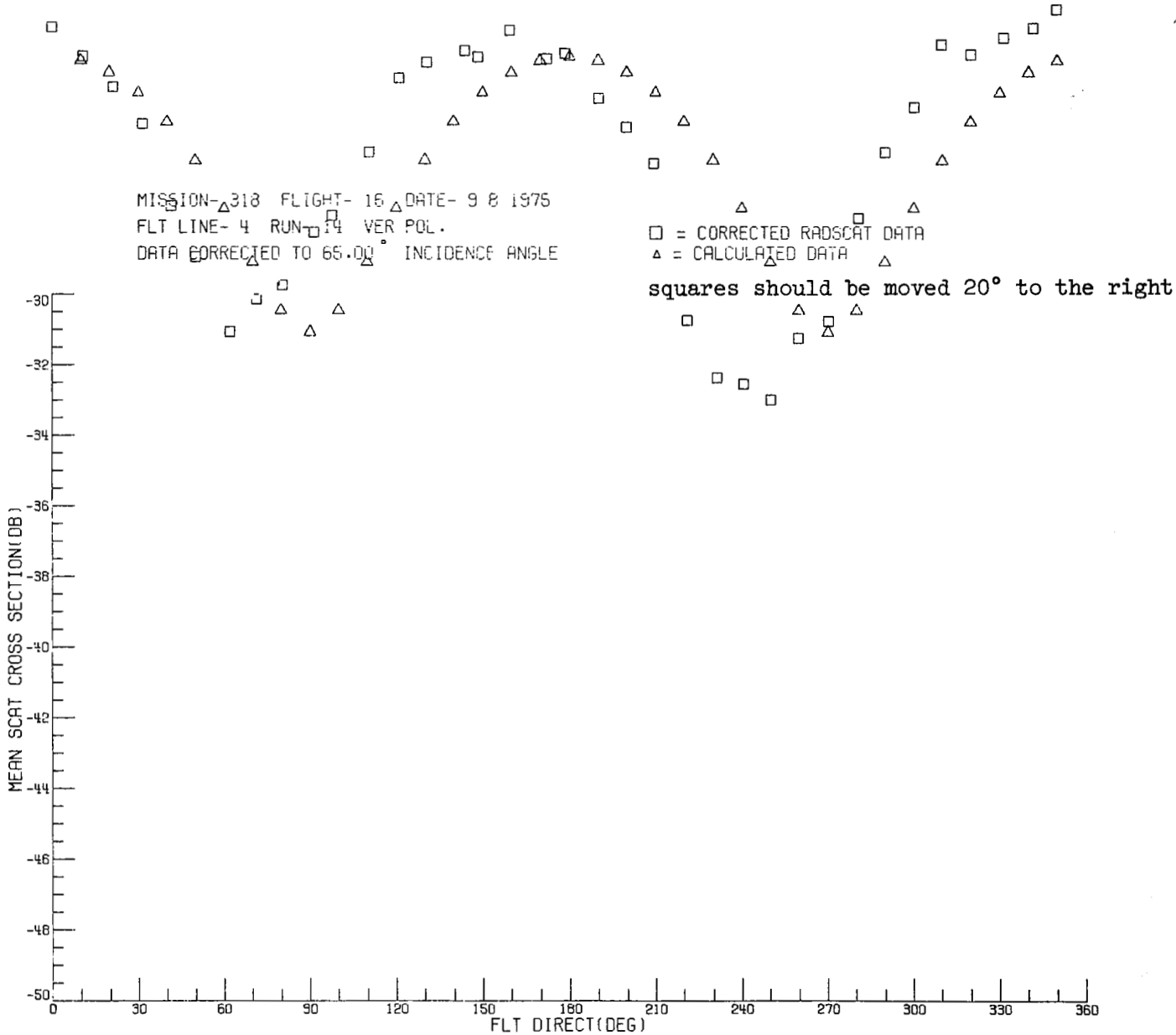
MISSION-318 FLIGHT- 16 DATE- 9 8 1975
FLT LINE- 4 RUN- 14 VER POL.
DATA CORRECTED TO 65.00° INCIDENCE ANGLE
□ = CORRECTED RADSCAT DATA
△ = CALCULATED DATA
squares should be moved 20° to the right
MEAN SCAT CROSS SECTION(DB)
-30
-32
-34
-36
-38
-40
-42
-44
-46
-48
-50
0
30
60
90
120
150
180
210
240
270
300
330
360
FLT DIRECT(DEG)

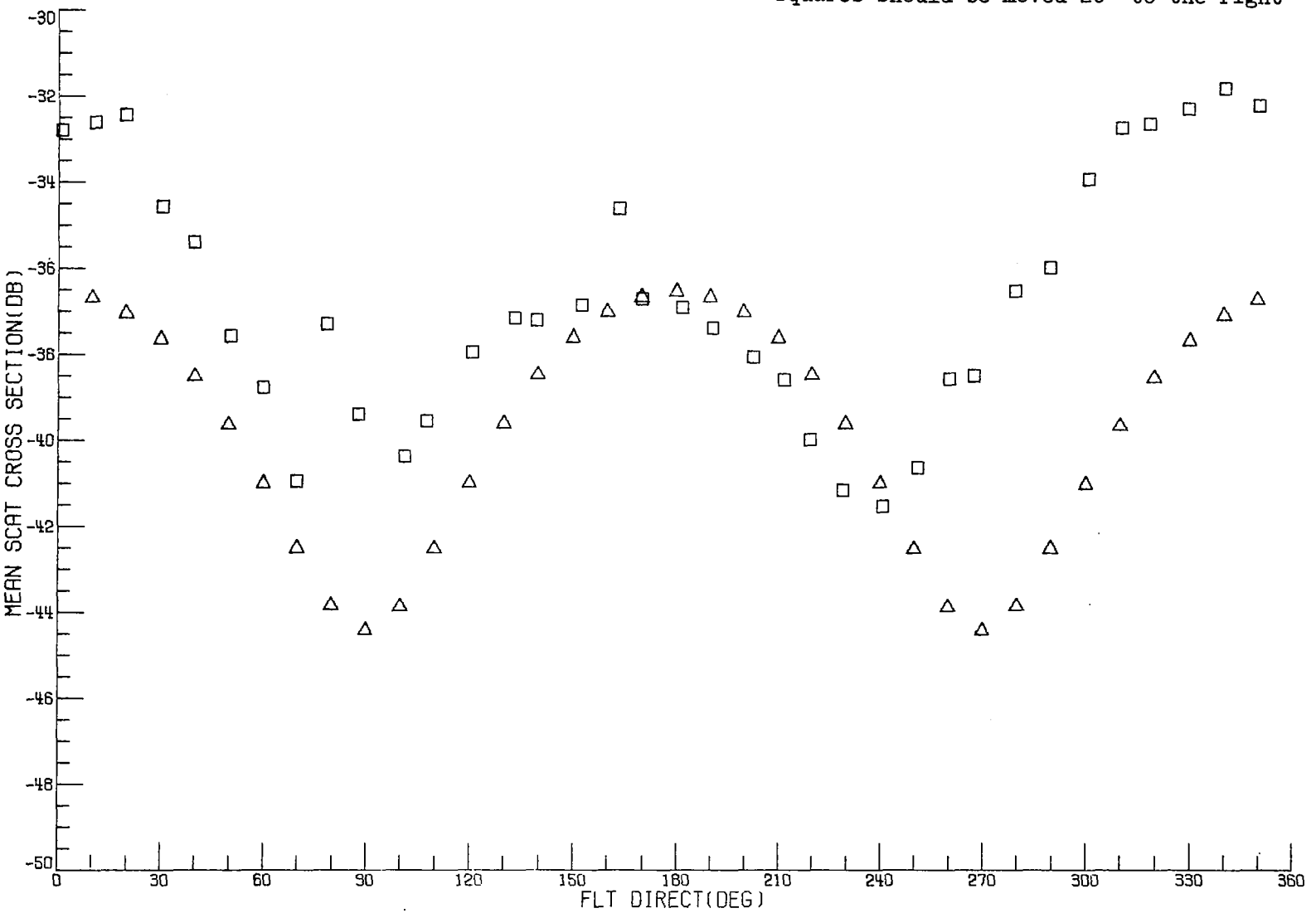
MISSION- 318 FLIGHT- 16 DATE- 9 8 1975
FLT LINE- 4 RUN- 14 HOR POL.
DATA CORRECTED TO 65.00° INCIDENCE ANGLE
□ = CORRECTED RADSCAT DATA
△ = CALCULATED DATA
squares should be moved 20° to the right
MEAN SCAT CROSS SECTION(DB)
-30
-32
-34
-36
-38
-40
-42
-44
-46
-48
-50
0
30
60
90
120
150
180
210
240
270
300
330
360
FLT DIRECT(DEG)

DATA FOR A LINE

Flight 16, September 8, 1975

Line 2, Run 5, Crosswind

Wind Speed = 7.7 m/s

Azimuth viewing angle relative to upwind = 90°

Small-Scale Parameters:

$a_0(\kappa_m) = 2.65 \times 10^{-6}$ cm^4

$q = 5.7$

$\kappa_c = 1.90$ cm^{-1}

Power Reflectivity at Nadir:

$R = 0.45$

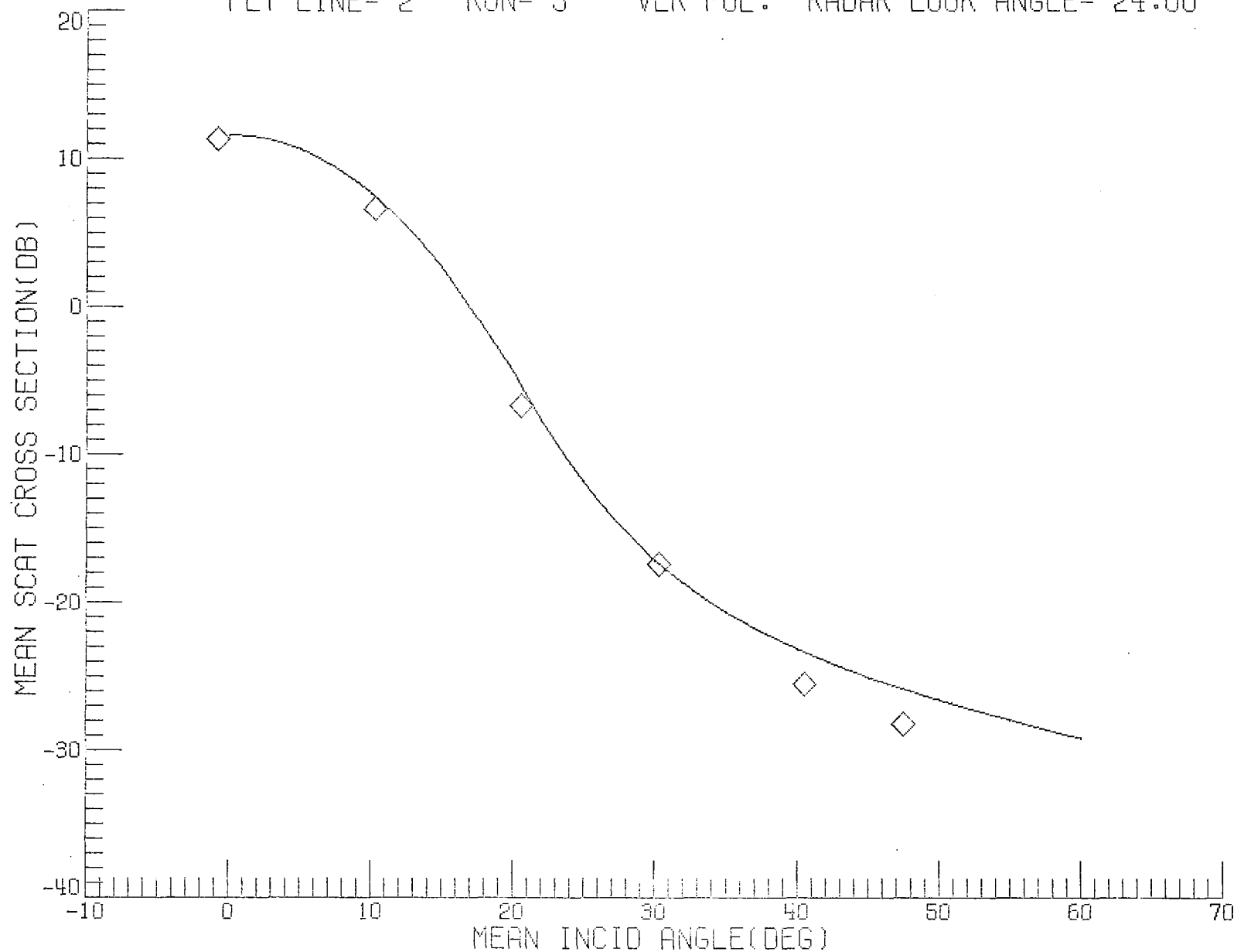
MISSION- 318 FLIGHT- 16 DATE- 9 8 1975 MODE- F.A.
FLT LINE- 2 RUN- 5 VER POL. RADAR LOOK ANGLE- 24.00
MEAN SCAT CROSS SECTION(DB)
20
10
0
-10
-20
-30
-40
-10
0
10
20
30
40
50
60
70
MEAN INCID ANGLE(DEG)

MISSION- 318 FLIGHT- 16 DATE- 9 8 1975 MODE- F.A.
FLT LINE- 2 RUN- 5 HOR POL. RADAR LOOK ANGLE- 24.00

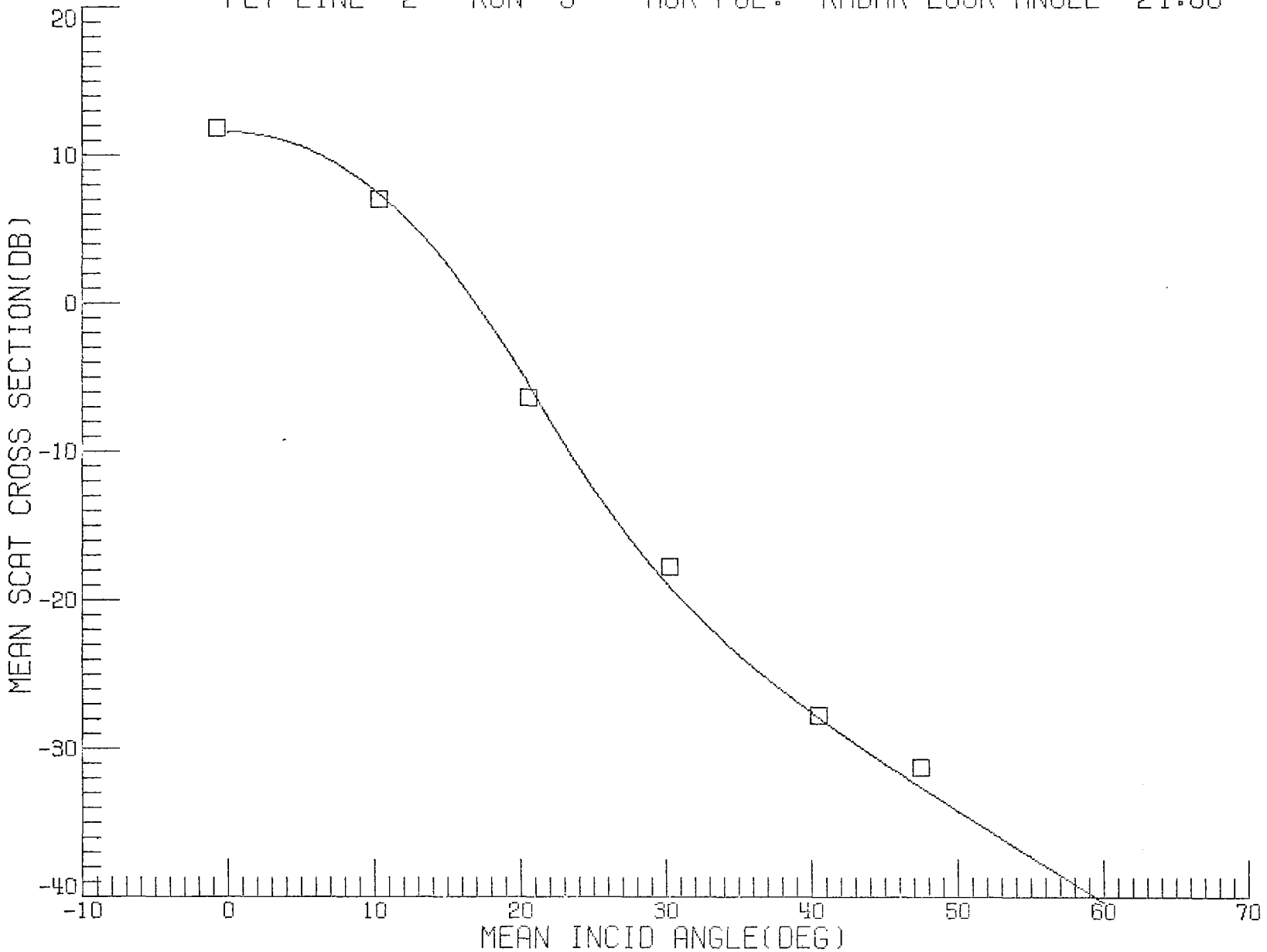

DATA FOR A LINE

Flight 16, September 8, 1975

Line 3, Run 2, Upwind

Wind Speed = 8.9 m/s

Azimuth viewing angle relative to upwind = 358°

Small-Scale Parameters:

$a_0(\kappa_m) = 5.82 \times 10^{-6}$ cm^4

$q = 3.6$

$\kappa_c = 1.60$ cm^{-1}

Power Reflectivity at Nadir:

$R = 0.40$

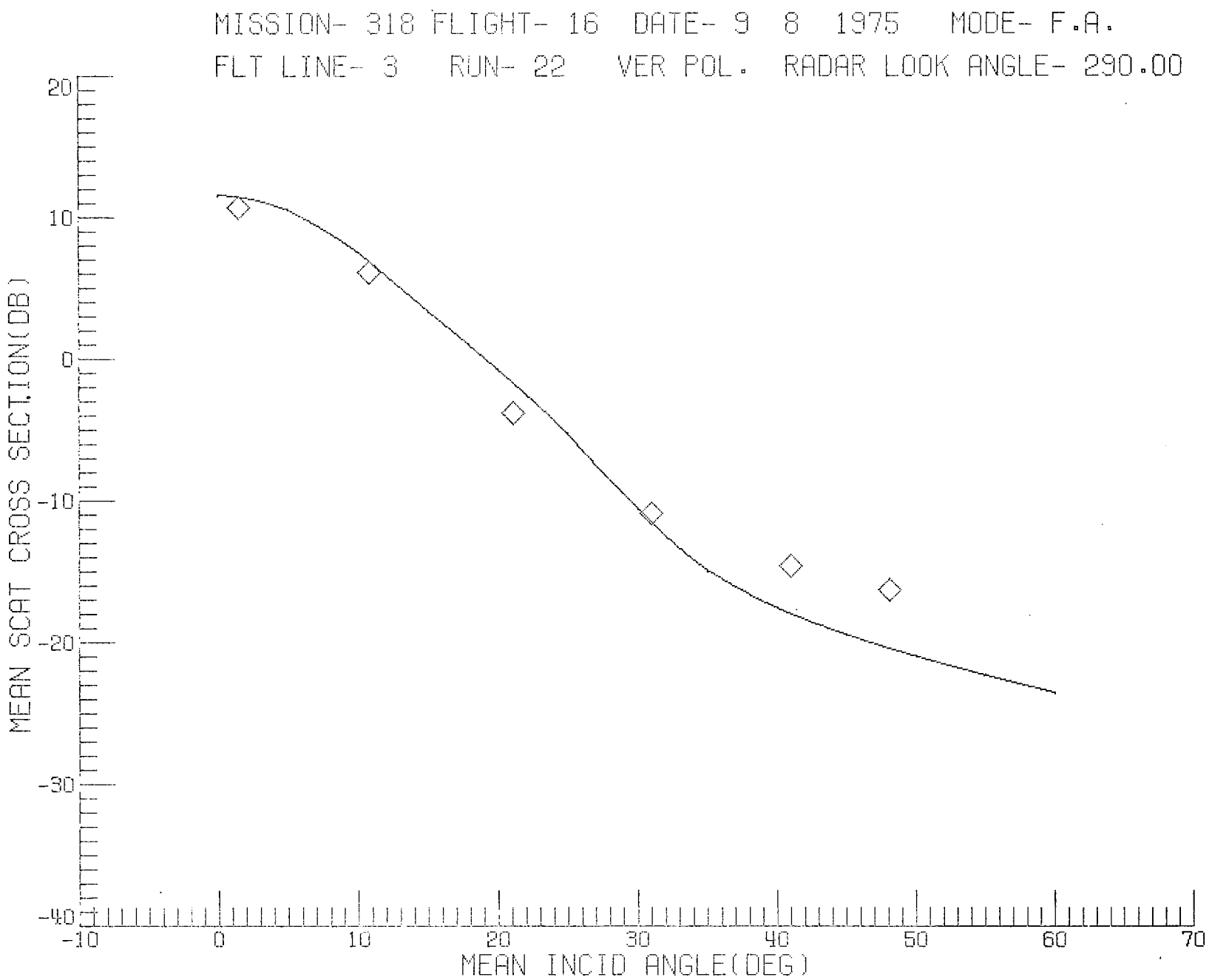
MISSION- 318 FLIGHT- 16 DATE- 9 8 1975 MODE- F.A.
FLT LINE- 3 RUN- 22 VER POL. RADAR LOOK ANGLE- 290.00
MEAN SCAT CROSS SECTION(DB)
20
10
0
-10
-20
-30
-40
-10
0
10
20
30
40
50
60
70
MEAN INCID ANGLE(DEG)

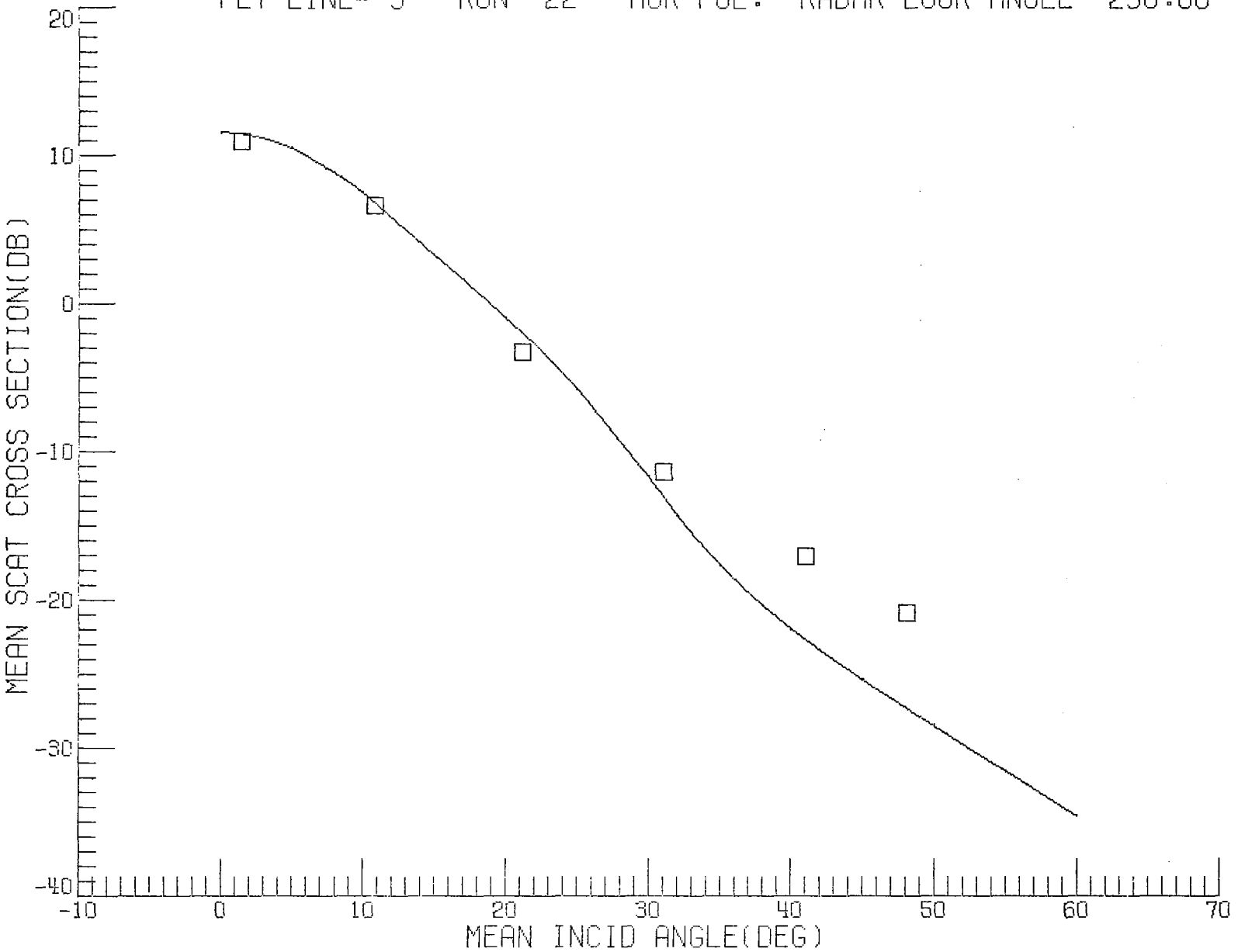
MISSION- 318 FLIGHT- 16 DATE- 9 8 1975 MODE- F.A.
FLT LINE- 3 RUN- 22 HOR POL. RADAR LOOK ANGLE- 290.00
MEAN SCAT CROSS SECTION(DB)
20
10
0
-10
-20
-30
-40
-10
0
10
20
30
40
50
60
70
MEAN INCID ANGLE(DEG)

DATA FOR A LINE

Flight 16, September 8, 1975

Line 3, Run 3, Downwind

Wind Speed = 9.1 m/s

Azimuth viewing angle relative to upwind = 188°

Small-Scale Parameters:

$a_0(\kappa_m) = 4.43 \times 10^{-6}$ cm^4

$q = 4.1$

$\kappa_c = 2.30$ cm^{-1}

Power Reflectivity at Nadir:

$R = 0.46$

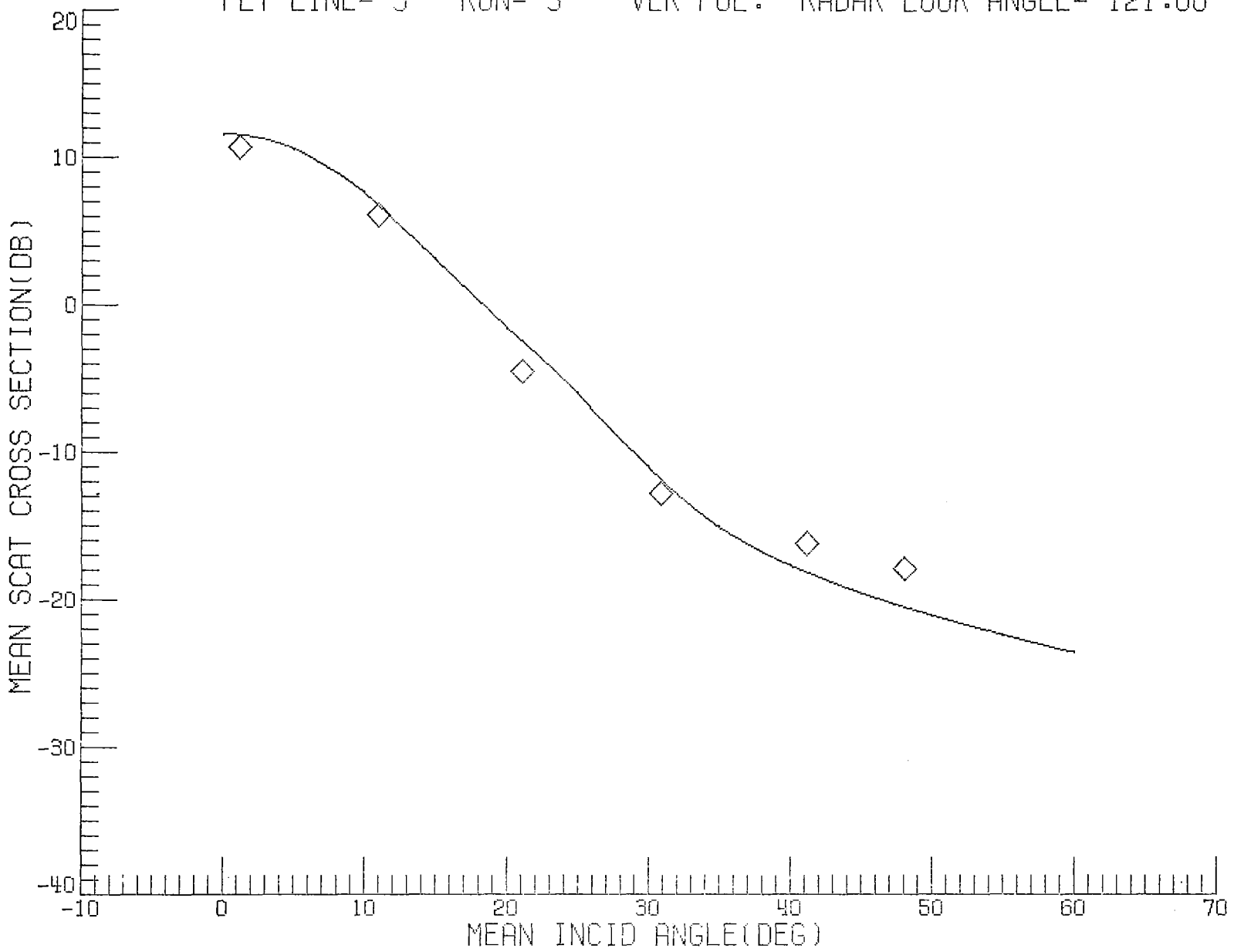
MISSION- 318 FLIGHT- 16 DATE- 9 8 1975 MODE- F.A.
FLT LINE- 3 RUN- 3 VER POL. RADAR LOOK ANGLE- 121.00
MEAN SCAT CROSS SECTION(DB)
20
10
0
-10
-20
-30
-40
-10
0
10
20
30
40
50
60
70
MEAN INCID ANGLE(DEG)

MISSION- 318 FLIGHT- 16 DATE- 9 8 1975 MODE- F.A.
FLT LINE- 3 RUN- 3 HOR POL. RADAR LOOK ANGLE- 121.00

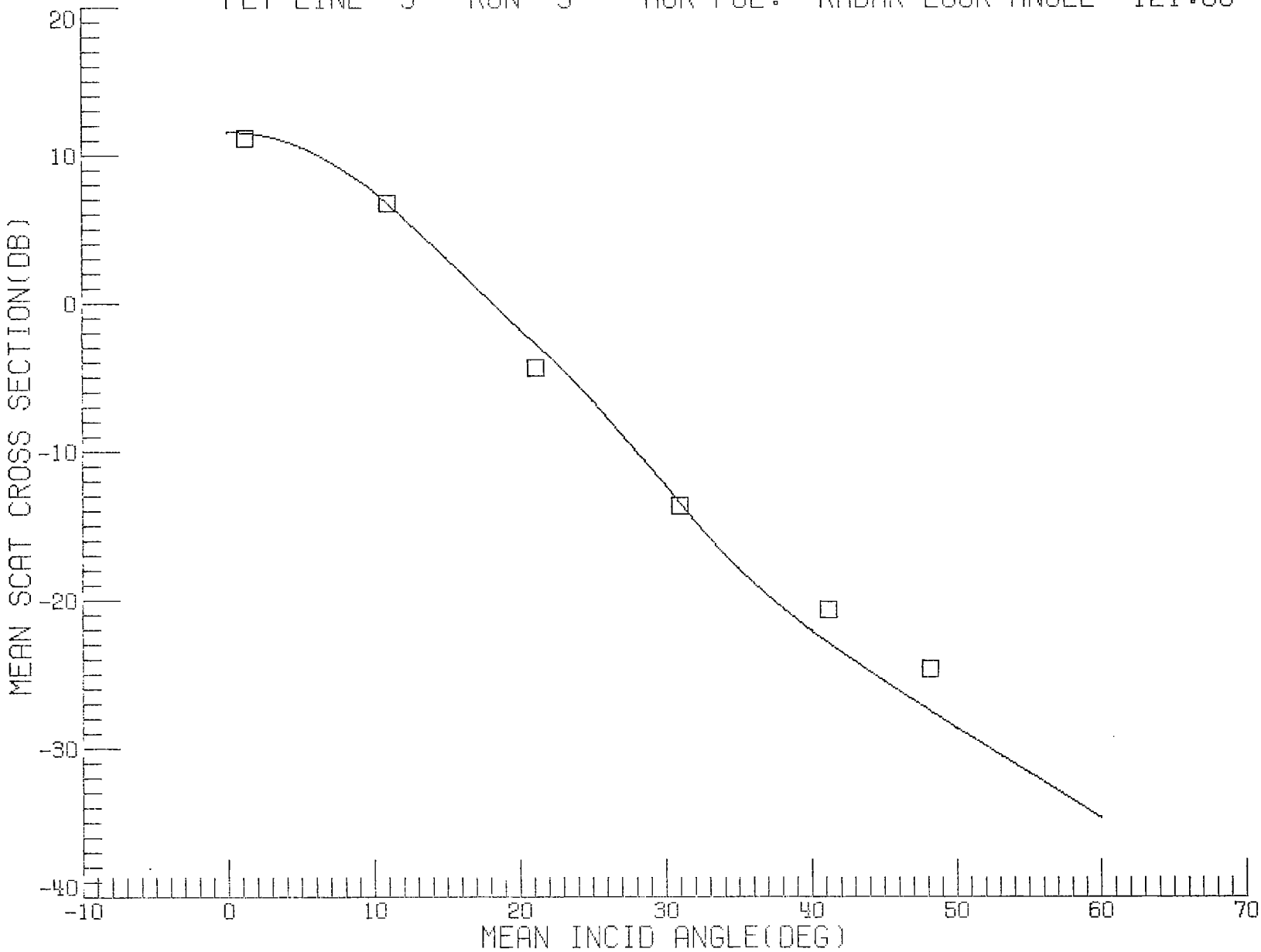

DATA FOR OVERALL FLIGHT

Flight 17, September 9, 1975

Average Wind Speed = 12.3 m/s

Average Wind Direction (out of) = 211° east of North

Large-Scale Parameters:

$\langle S_u^2 \rangle^{\frac{1}{2}} = 0.15$

$\langle S_c^2 \rangle^{\frac{1}{2}} = 0.14$

$c_1 = 0.02$

$c_2 = 0.005$

$c_3 = -0.01$

$c_4 = 0.02$

$c_5 = 0.005$

Small-Scale Anisotropy Ratio:

$a_r = 0.55$

DATA FOR CIRCLES

Flight 17, September 9, 1975

Three circles for θ = 20°, 40°, and 65°

Wind Speed = 12.8 m/s

Small-Scale Parameters:

$a_0(\kappa_m) = 7.60 \times 10^{-6}$ cm^4

$q = 3.7$

$\kappa_c = 2.03$ cm^{-1}

Power Reflectivity at Nadir:

$R = 0.41$

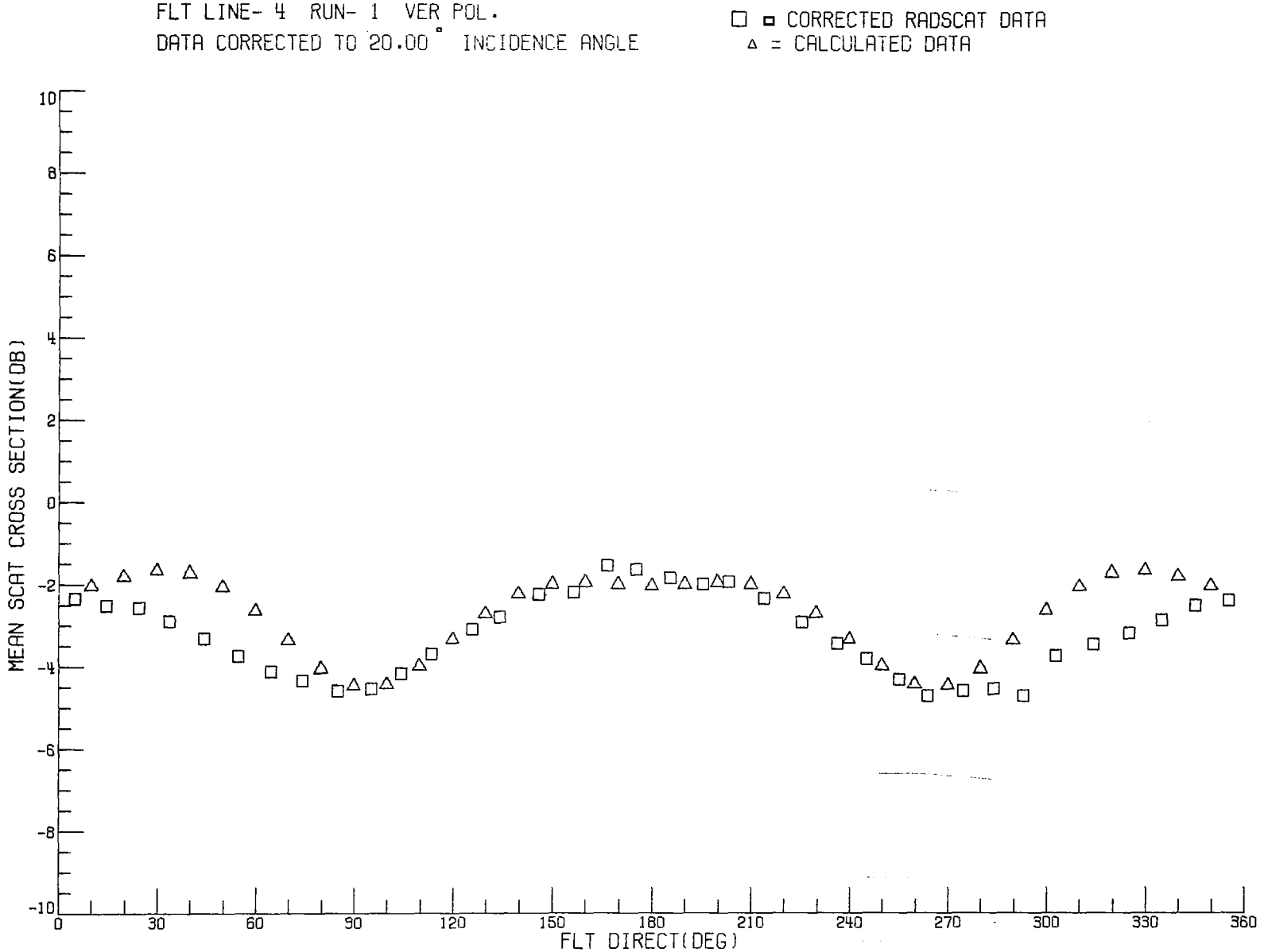
MISSION- 318 FLIGHT- 17 DATE- 9 9 1975
FLT LINE- 4 RUN- 1 VER POL.
DATA CORRECTED TO 20.00° INCIDENCE ANGLE
□ ▫ CORRECTED RADSCAT DATA
△ = CALCULATED DATA
MEAN SCAT CROSS SECTION(DB)
10
8
6
4
2
0
-2
-4
-6
-8
-10
0
30
60
90
120
150
180
210
240
270
300
330
360
FLT DIRECT(DEG)

MISSION- 318 FLIGHT- 17 DATE- 9 9 1975
FLT LINE- 4 RUN- 1 HOR POL.
DATA CORRECTED TO 20.00° INCIDENCE ANGLE

□ = CORRECTED RADSCAT DATA
△ = CALCULATED DATA

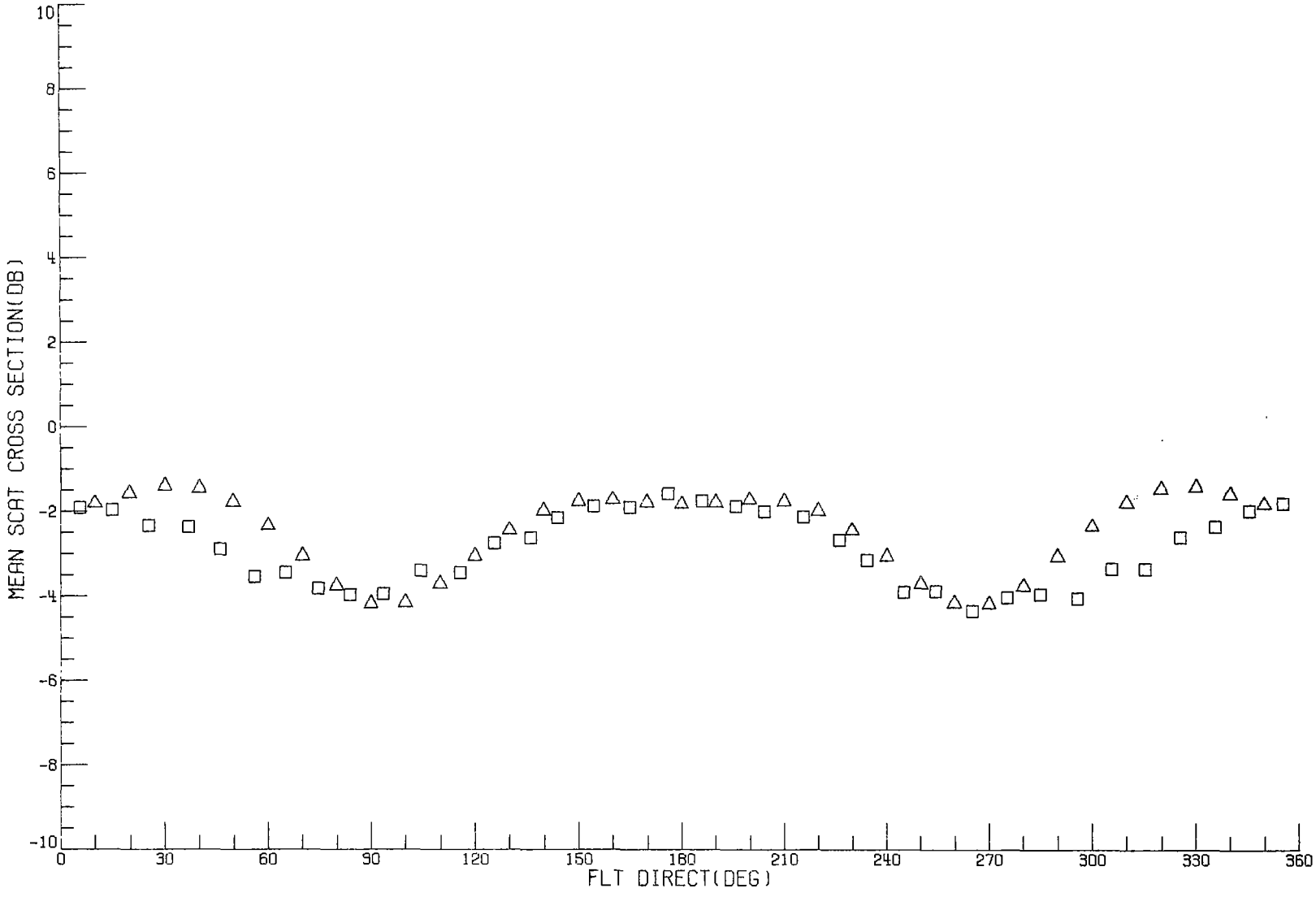

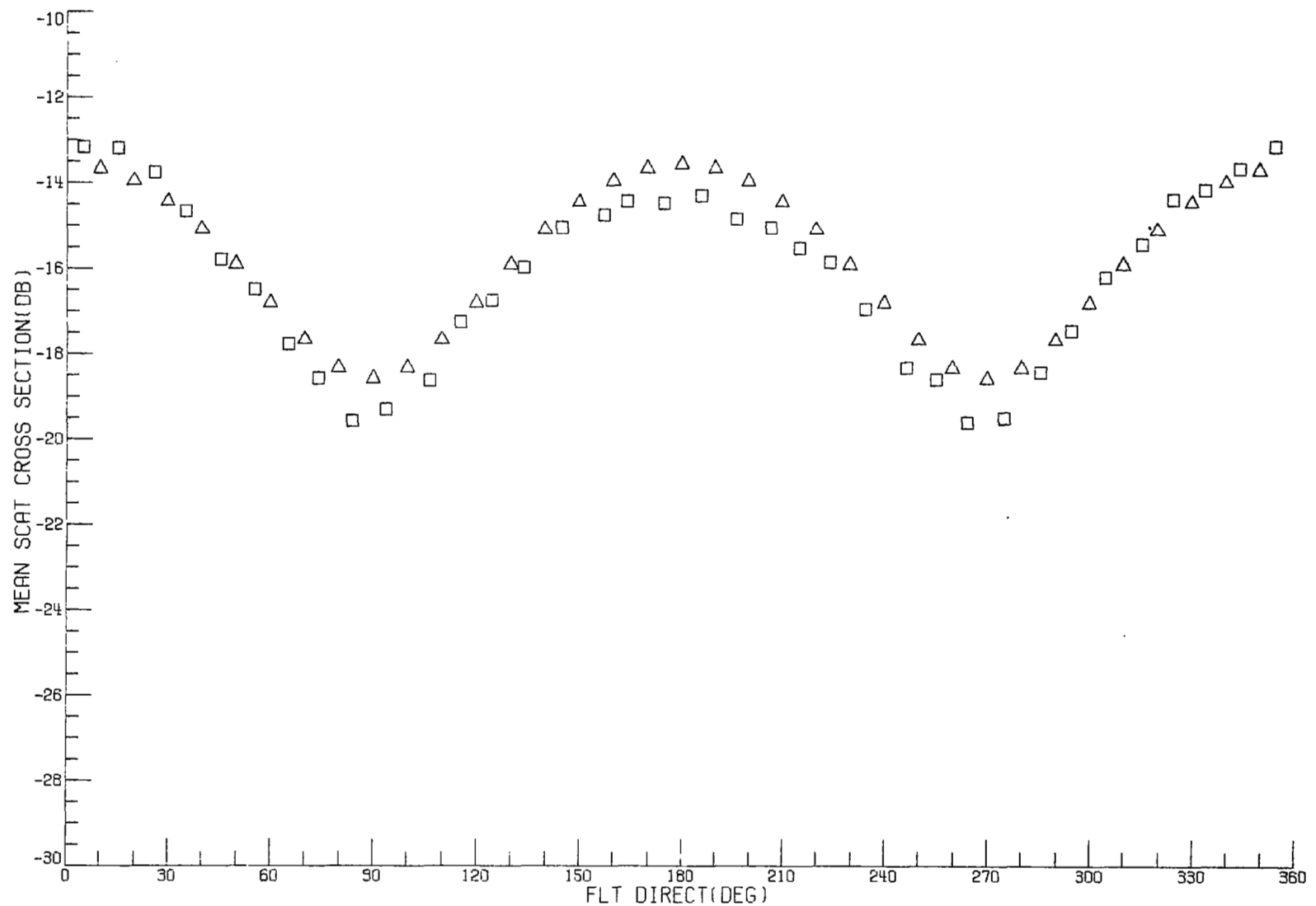
MISSION- 318 FLIGHT- 17 DATE- 9 9 1975
FLT LINE- 4 RUN- 8 VER POL.
DATA CORRECTED TO 40.00° INCIDENCE ANGLE
□ = CORRECTED RADSCAT DATA
△ = CALCULATED DATA
MEAN SCAT CROSS SECTION(DB)
-10
-12
-14
-16
-18
-20
-22
-24
-26
-28
-30
0
30
60
90
120
150
180
210
240
270
300
330
360
FLT DIRECT(DEG)

MISSION- 318 FLIGHT- 17 DATE- 9 9 1975
FLT LINE- 4 RUN- 8 HOR POL.
DATA CORRECTED TO 40.00° INCIDENCE ANGLE

□ = CORRECTED RADSCAT DATA
△ = CALCULATED DATA

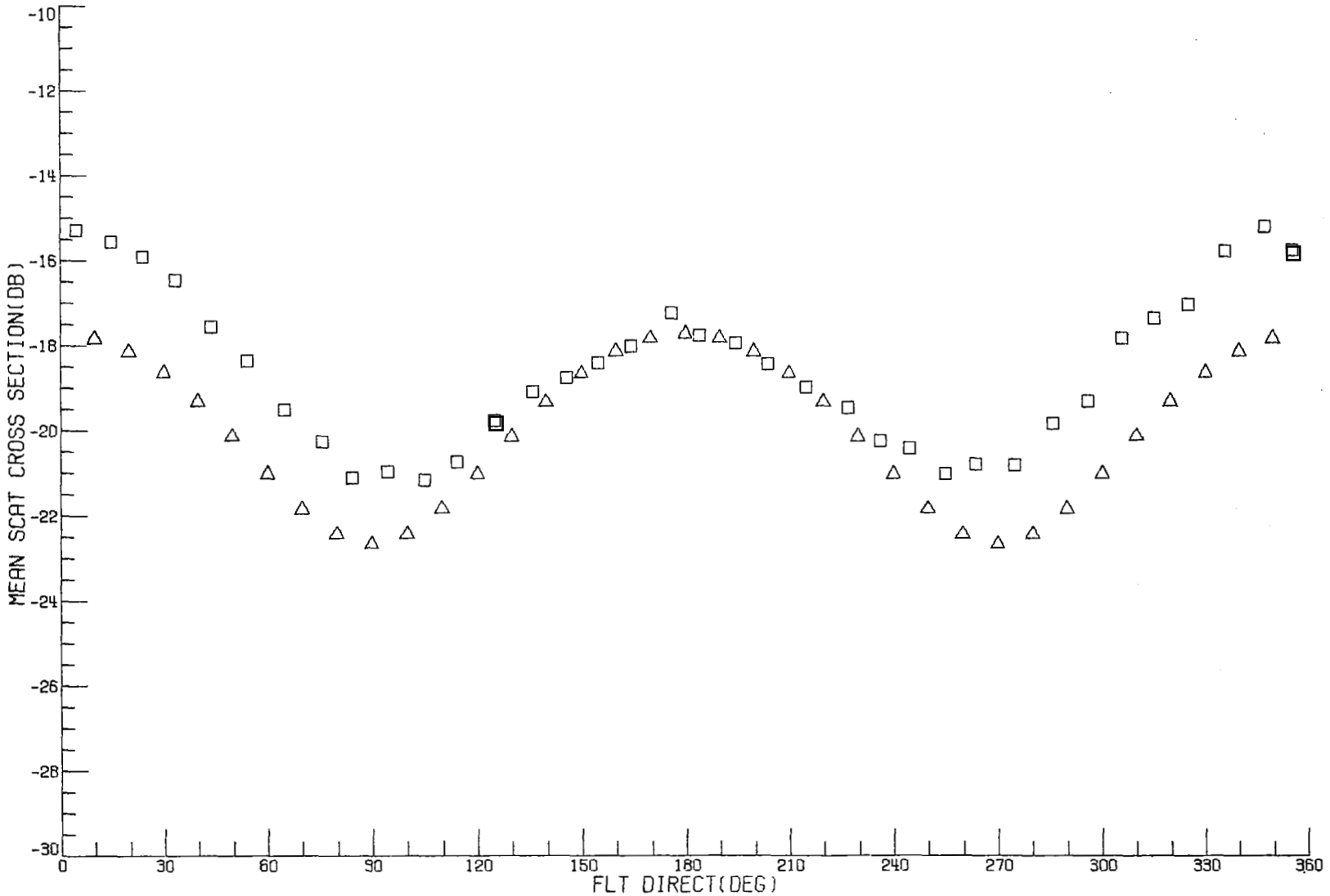

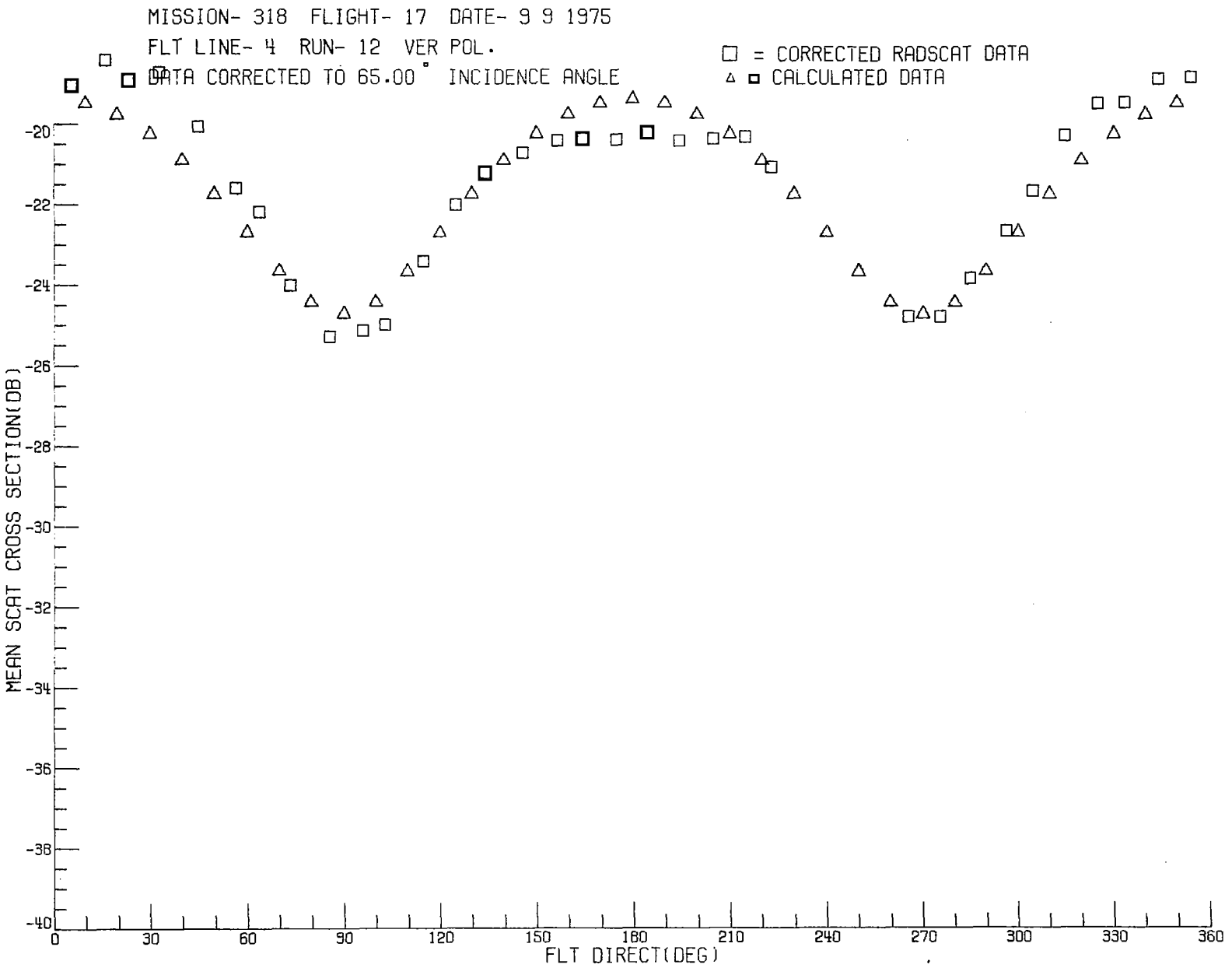
MISSION- 318 FLIGHT- 17 DATE- 9 9 1975
FLT LINE- 4 RUN- 12 VER POL.
DATA CORRECTED TO 65.00° INCIDENCE ANGLE
□ = CORRECTED RADSCAT DATA
△ □ CALCULATED DATA
MEAN SCAT CROSS SECTION(DB)
-20
-22
-24
-26
-28
-30
-32
-34
-36
-38
-40
0
30
60
90
120
150
180
210
240
270
300
330
360
FLT DIRECT(DEG)

MISSION- 318 FLIGHT- 17 DATE- 9 9 1975
FLT LINE- 4 RUN- 12 HOR POL.
DATA CORRECTED TO 65.00° INCIDENCE ANGLE

□ = CORRECTED RADSCAT DATA
△ ■ CALCULATED DATA

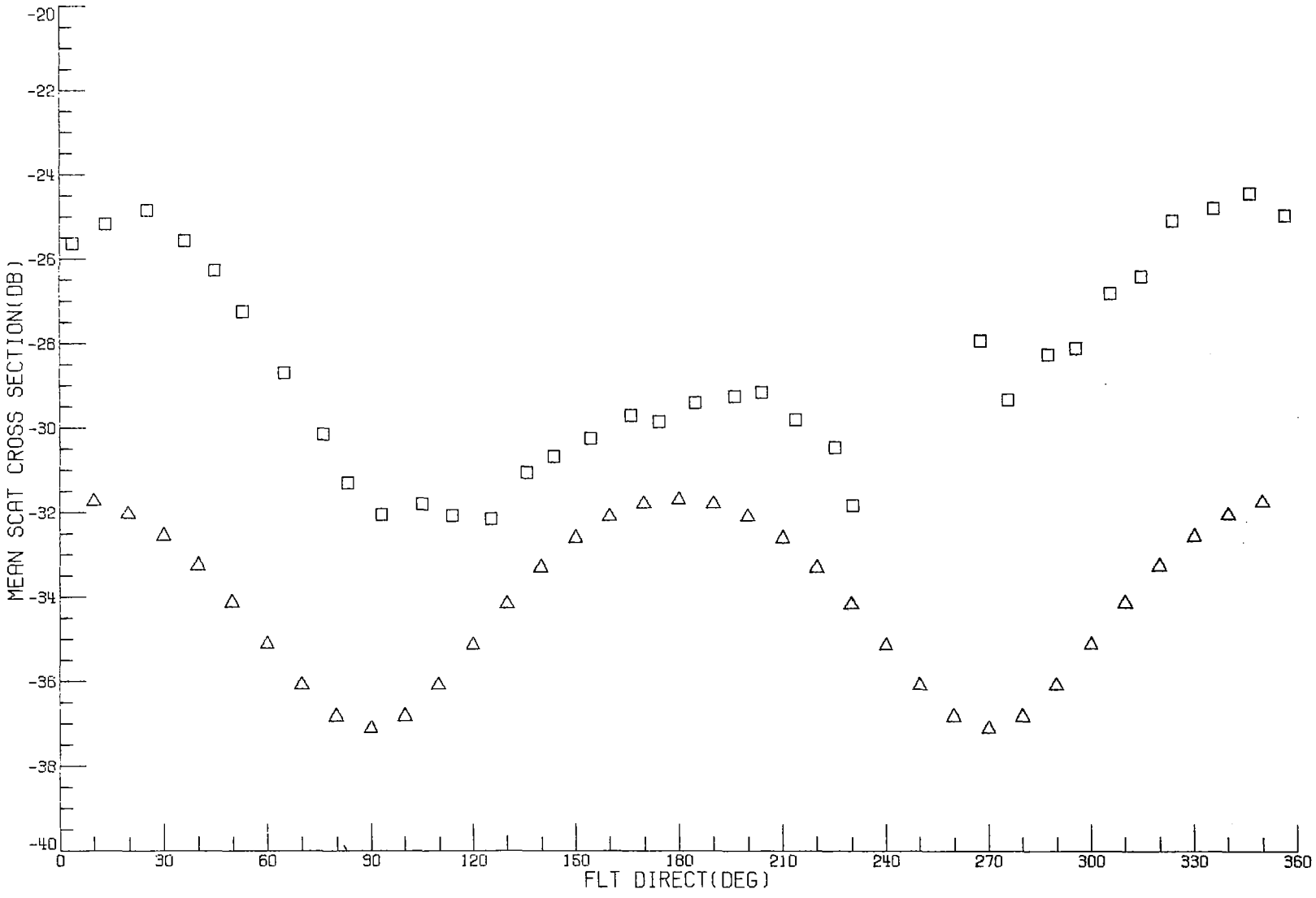

DATA FOR A LINE

Flight 17, September 9, 1975

Line 2, Run 2, Crosswind

Wind Speed = 12.0 m/s

Azimuth viewing angle relative to upwind = 269°

Small-Scale Parameters:

$a_0(\kappa_m) = 8.35 \times 10^{-6}$ cm^4

$q = 5.2$

$\kappa_c = 2.30$ cm^{-1}

Power Reflectivity at Nadir:

$R = 0.46$

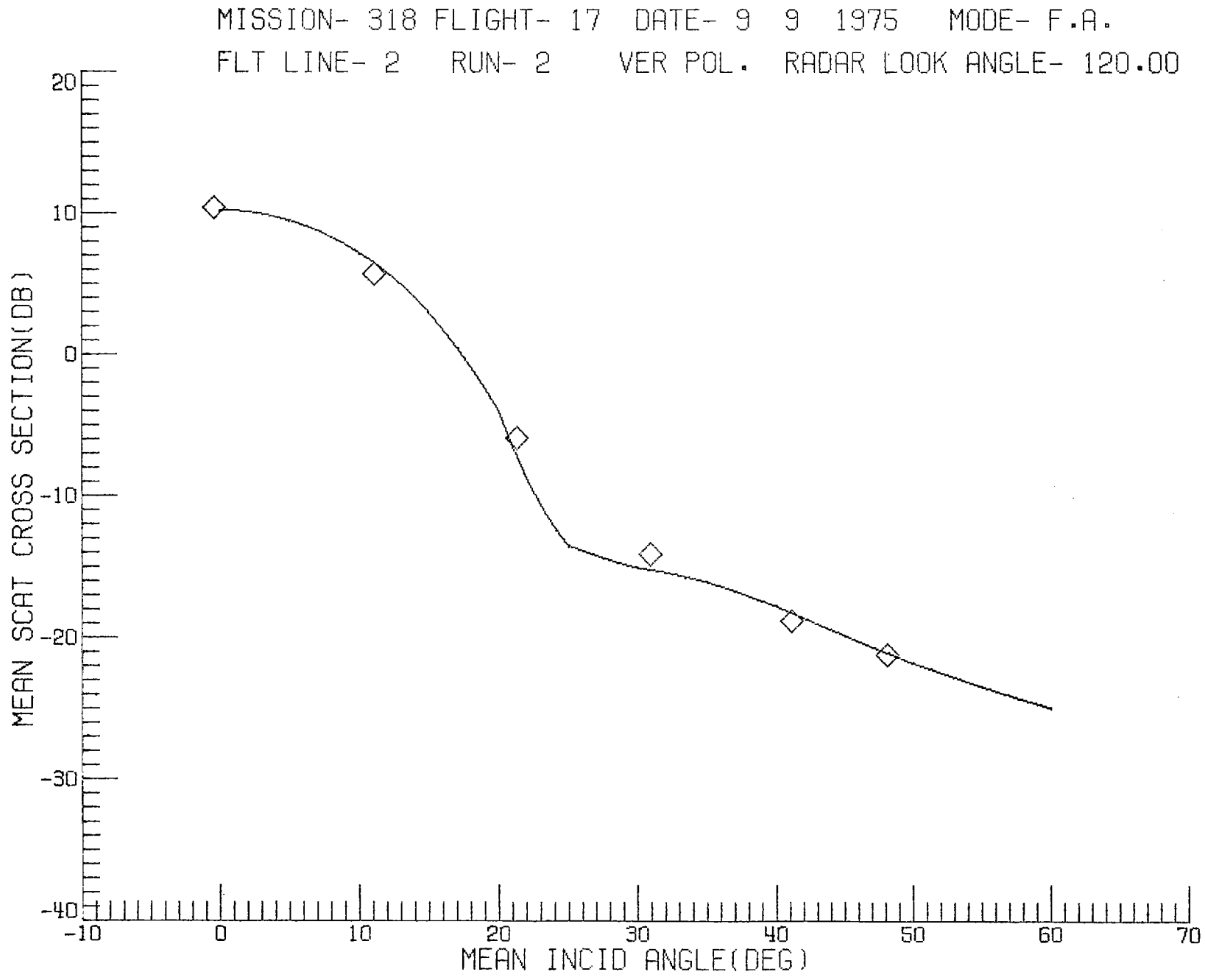
MISSION- 318 FLIGHT- 17 DATE- 9 9 1975 MODE- F.A.
FLT LINE- 2 RUN- 2 VER POL. RADAR LOOK ANGLE- 120.00
MEAN SCAT CROSS SECTION(DB)
20
10
0
-10
-20
-30
-40
-10
0
10
20
30
40
50
60
70
MEAN INCID ANGLE(DEG)

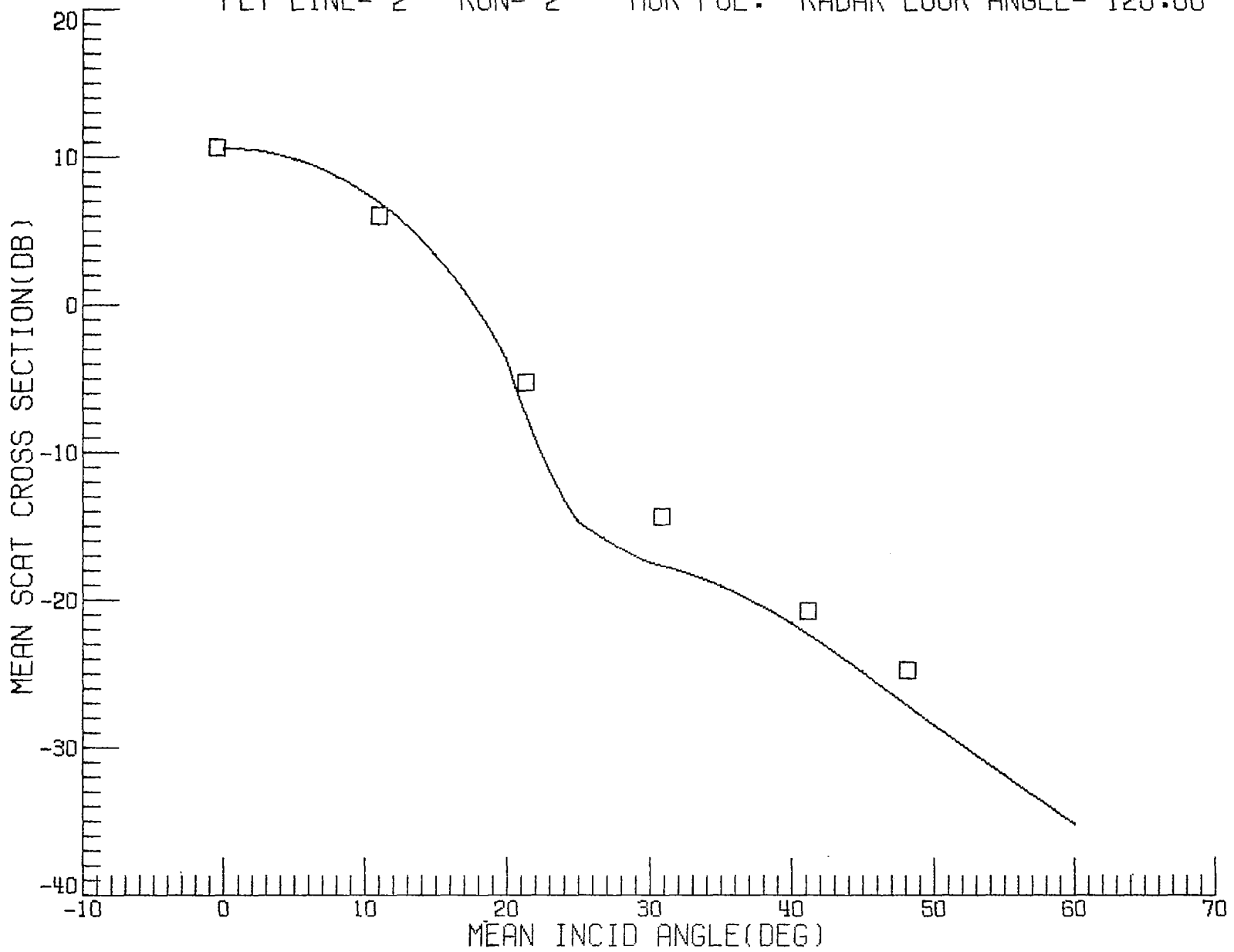
MISSION- 318 FLIGHT- 17 DATE- 9 9 1975 MODE- F.A.
FLT LINE- 2 RUN- 2 HOR POL. RADAR LOOK ANGLE- 120.00
MEAN SCAT CROSS SECTION(DB)
20
10
0
-10
-20
-30
-40
-10
0
10
20
30
40
50
60
70
MEAN INCID ANGLE(DEG)

DATA FOR A LINE

Flight 17, September 9, 1975

Line 3, Run 3, Downwind

Wind Speed = 12.1 m/s

Azimuth viewing angle relative to upwind = 177°

Small-Scale Parameters:

$a_0(\kappa_m) = 7.72 \times 10^{-6}$ cm^4

$q = 4.4$

$\kappa_c = 2.00$ cm^{-1}

Power Reflectivity at Nadir:

$R = 0.41$

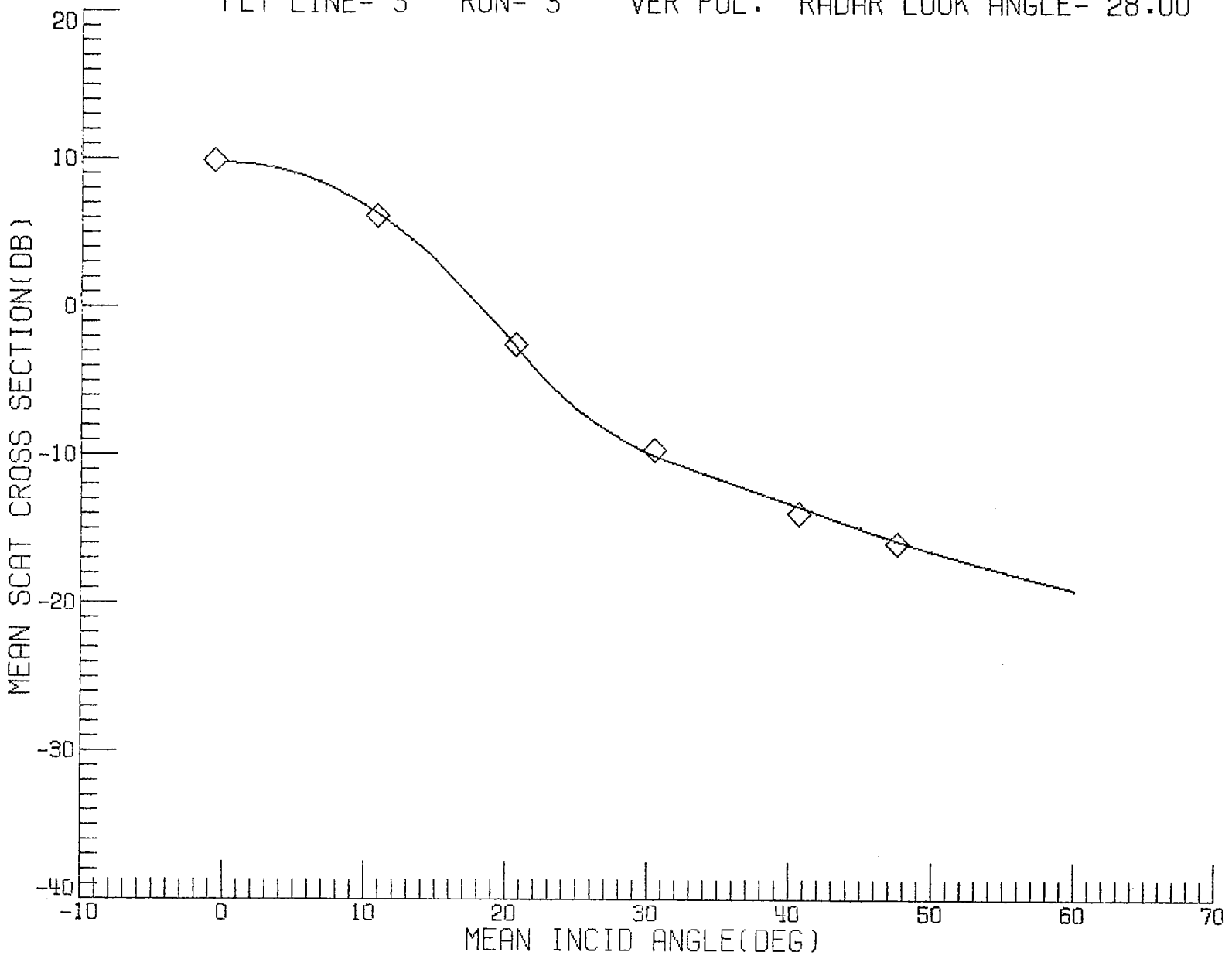
MISSION- 318 FLIGHT- 17 DATE- 9 9 1975 MODE- F.A.
FLT LINE- 3 RUN- 3 VER POL. RADAR LOOK ANGLE- 28.00
MEAN SCAT CROSS SECTION(DB)
20
10
0
-10
-20
-30
-40
-10
0
10
20
30
40
50
60
70
MEAN INCID ANGLE(DEG)

MISSION- 318 FLIGHT- 17 DATE- 9 9 1975 MODE- F.A.
FLT LINE- 3 RUN- 3 HOR POL. RADAR LOOK ANGLE- 28.00

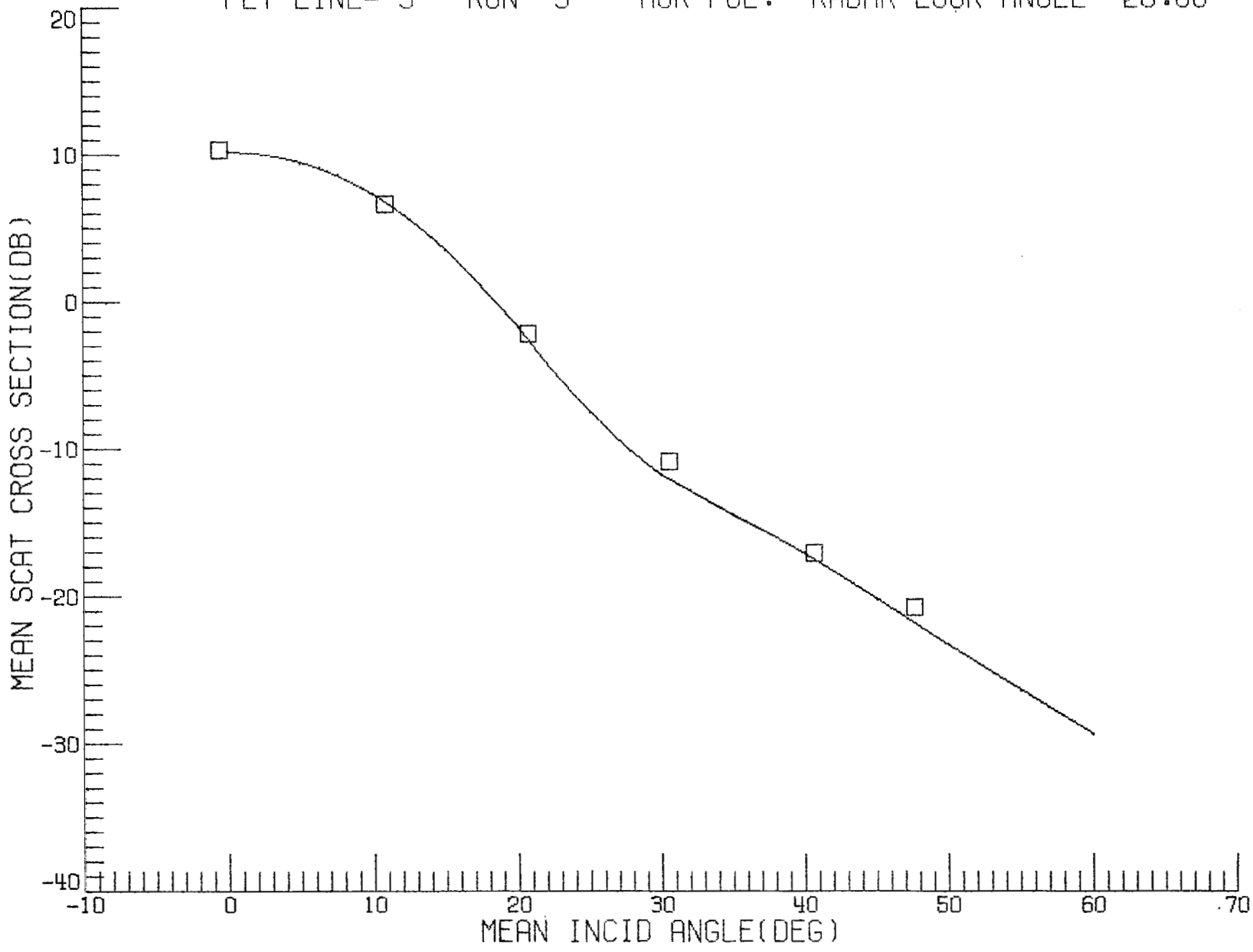

DATA FOR A LINE

Flight 17, September 9, 1975

Line 3, Run 4, Upwind

Wind Speed = 12.0 m/s

Azimuth viewing angle relative to upwind = 355°

Small-Scale Parameters:

$a_0(\kappa_m) = 8.24 \times 10^{-6}$ cm^4

$q = 4.1$

$\kappa_c = 1.80$ cm^{-1}

Power Reflectivity at Nadir:

$R = 0.40$

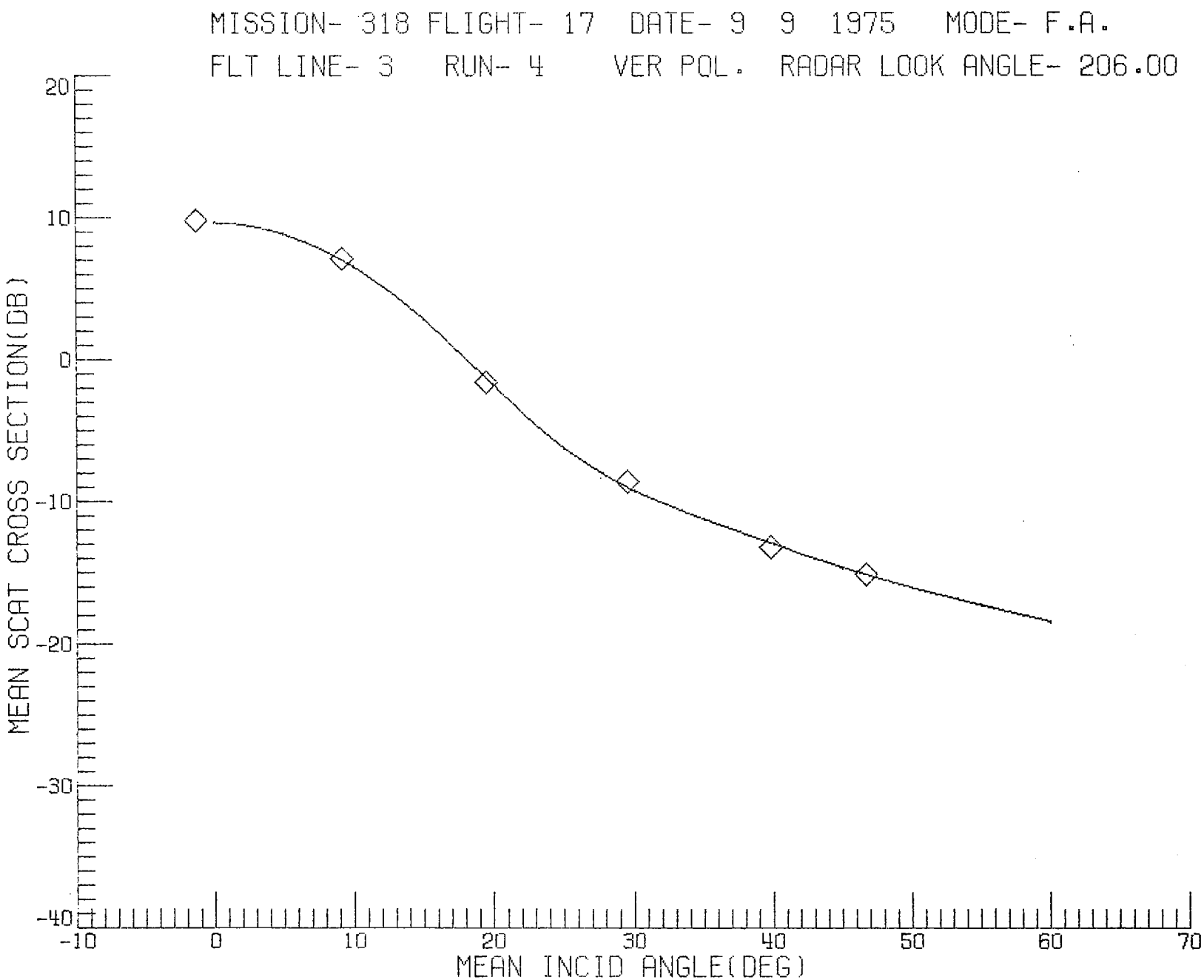
MISSION- 318 FLIGHT- 17 DATE- 9 9 1975 MODE- F.A.
FLT LINE- 3 RUN- 4 VER POL. RADAR LOOK ANGLE- 206.00
MEAN SCAT CROSS SECTION(DB)
20
10
0
-10
-20
-30
-40
-10
0
10
20
30
40
50
60
70
MEAN INCID ANGLE(DEG)

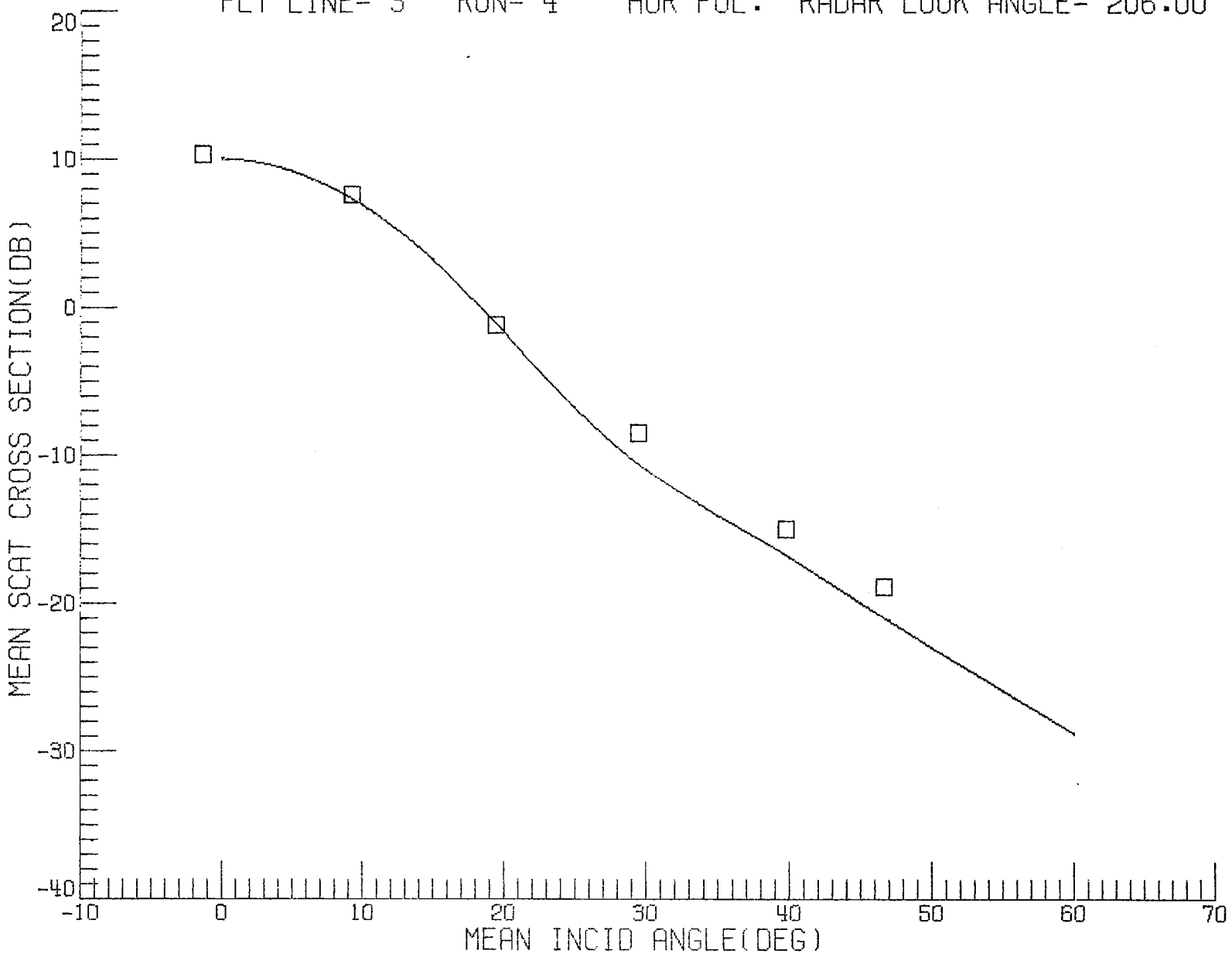
MISSION- 318 FLIGHT- 17 DATE- 9 9 1975 MODE- F.A.
FLT LINE- 3 RUN- 4 HOR POL. RADAR LOOK ANGLE- 206.00
MEAN SCAT CROSS SECTION(DB)
20
10
0
-10
-20
-30
-40
-10
0
10
20
30
40
50
60
70
MEAN INCID ANGLE(DEG)

DATA FOR OVERALL FLIGHT

Flight 19, September 10, 1975

Average Wind Speed = 7.7 m/s

Average Wind Direction (out of) = 245° east of North

Large-Scale Parameters:

$\langle S_u^2 \rangle^{\frac{1}{2}} = 0.14$

$\langle S_c^2 \rangle^{\frac{1}{2}} = 0.13$

$c_1 = -0.115$

$c_2 = -0.03$

$c_3 = 0.01$

$c_4 = 0.015$

$c_5 = -0.01$

Small-Scale Anisotropy Ratio:

$a_r = 0.67$

DATA FOR CIRCLES

Flight 19, September 10, 1975

Three circles for θ = 20°, 40°, and 65°

Wind Speed = 7.5 m/s

Small-Scale Parameters:

$a_0(\kappa_m) = 3.19 \times 10^{-6}$ cm^4

$q = 3.9$

$\kappa_c = 2.10$ cm^{-1}

Power Reflectivity at Nadir:

$R = 0.43$

MISSION- 318 FLIGHT- 19 DATE- 9 10 1975
FLT LINE- 4 RUN- 10 VER POL.
DATA CORRECTED TO 20.00° INCIDENCE ANGLE

□ = CORRECTED RADSCAT DATA
△ □ CALCULATED DATA

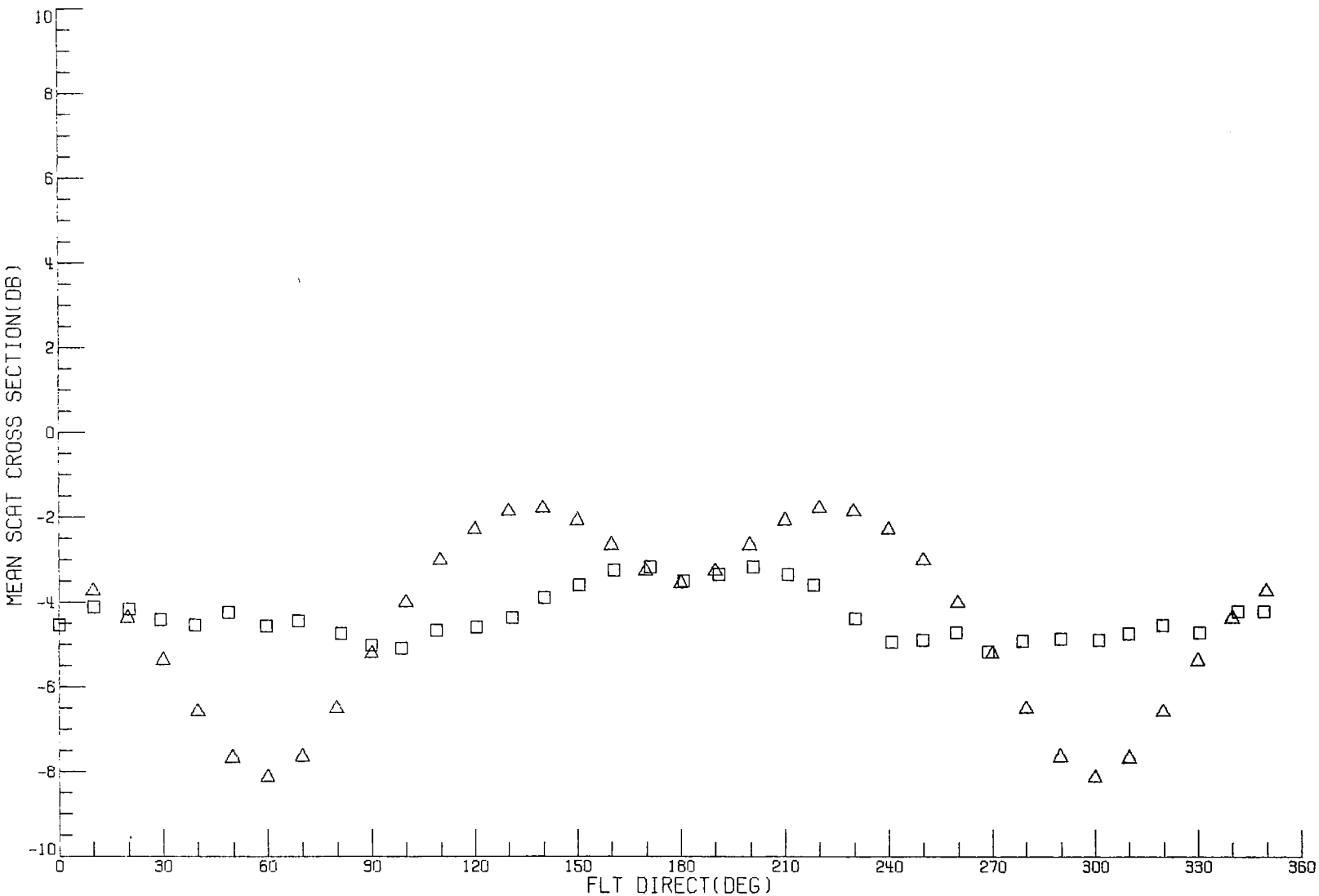

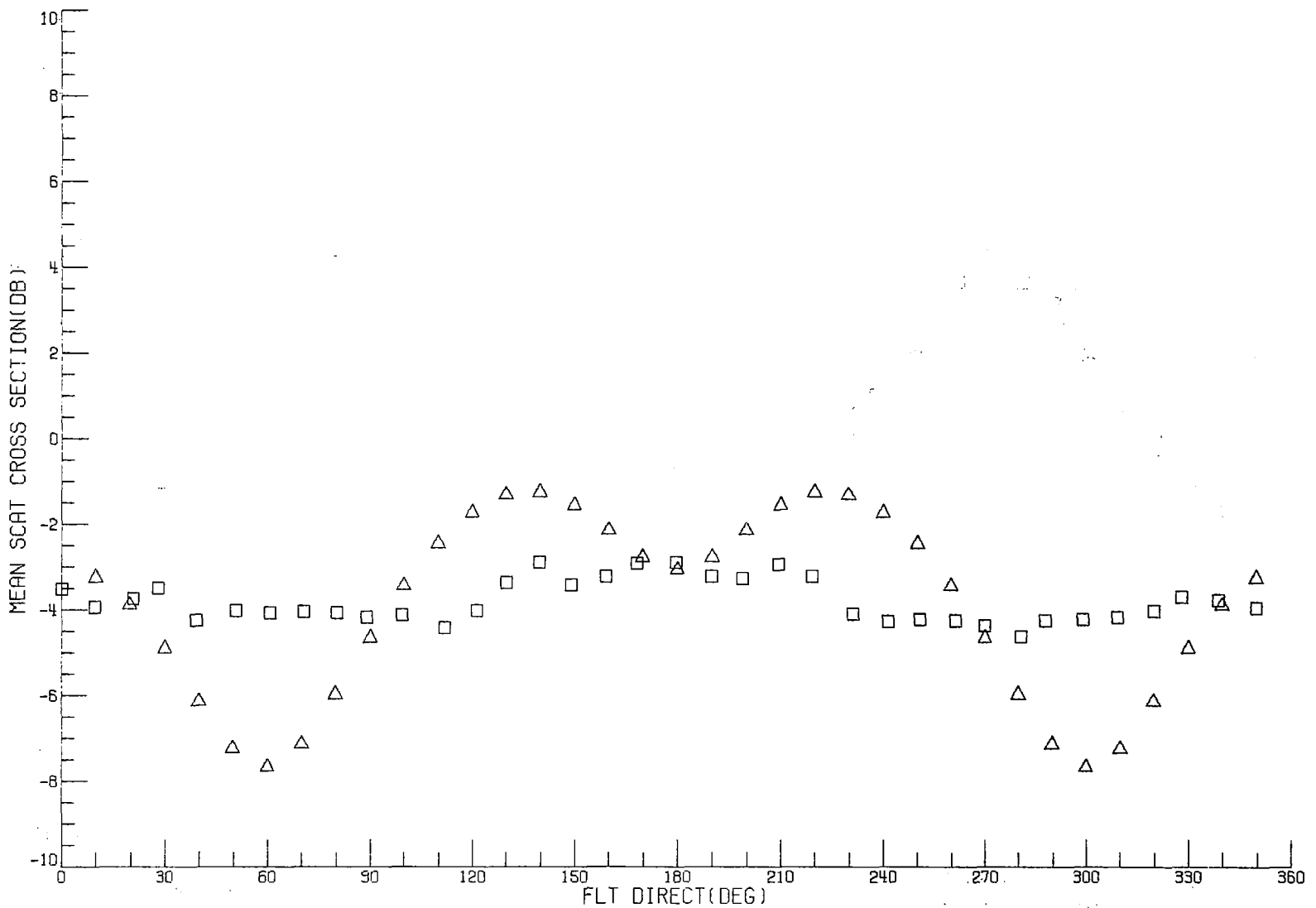
MISSION- 318 FLIGHT- 19 DATE- 9 10 1975
FLT LINE- 4 RUN- 10 HOR POL.
DATA CORRECTED TO 20.00° INCIDENCE ANGLE
□ = CORRECTED RADSCAT DATA
△ □ CALCULATED DATA
MEAN SCAT CROSS SECTION(DB)
10
8
6
4
2
0
-2
-4
-6
-8
-10
0
30
60
90
120
150
180
210
240
270
300
330
360
FLT DIRECT(DEG)

MISSION- 318 FLIGHT- 19 DATE- 9 10 1975
FLT LINE- 4 RUN- 13 VER POL.
DATA CORRECTED TO 40.00° INCIDENCE ANGLE

□ = CORRECTED RADSCAT DATA
△ = CALCULATED DATA

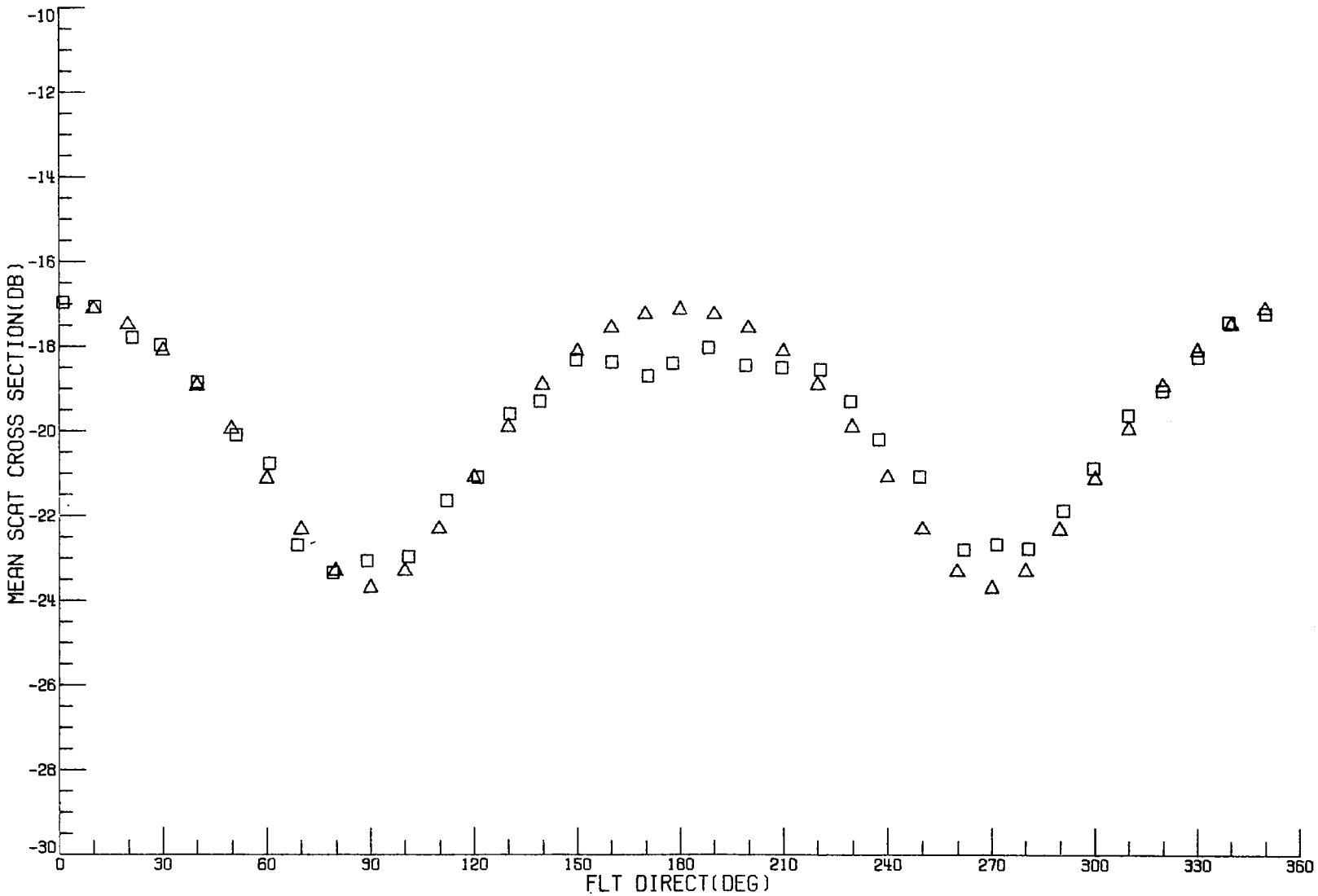

MISSION- 318 FLIGHT- 19 DATE- 9 10 1975
FLT LINE- 4 RUN- 13 HOR POL.
DATA CORRECTED TO 40.00° INCIDENCE ANGLE

□ = CORRECTED RADSCAT DATA
△ □ CALCULATED DATA

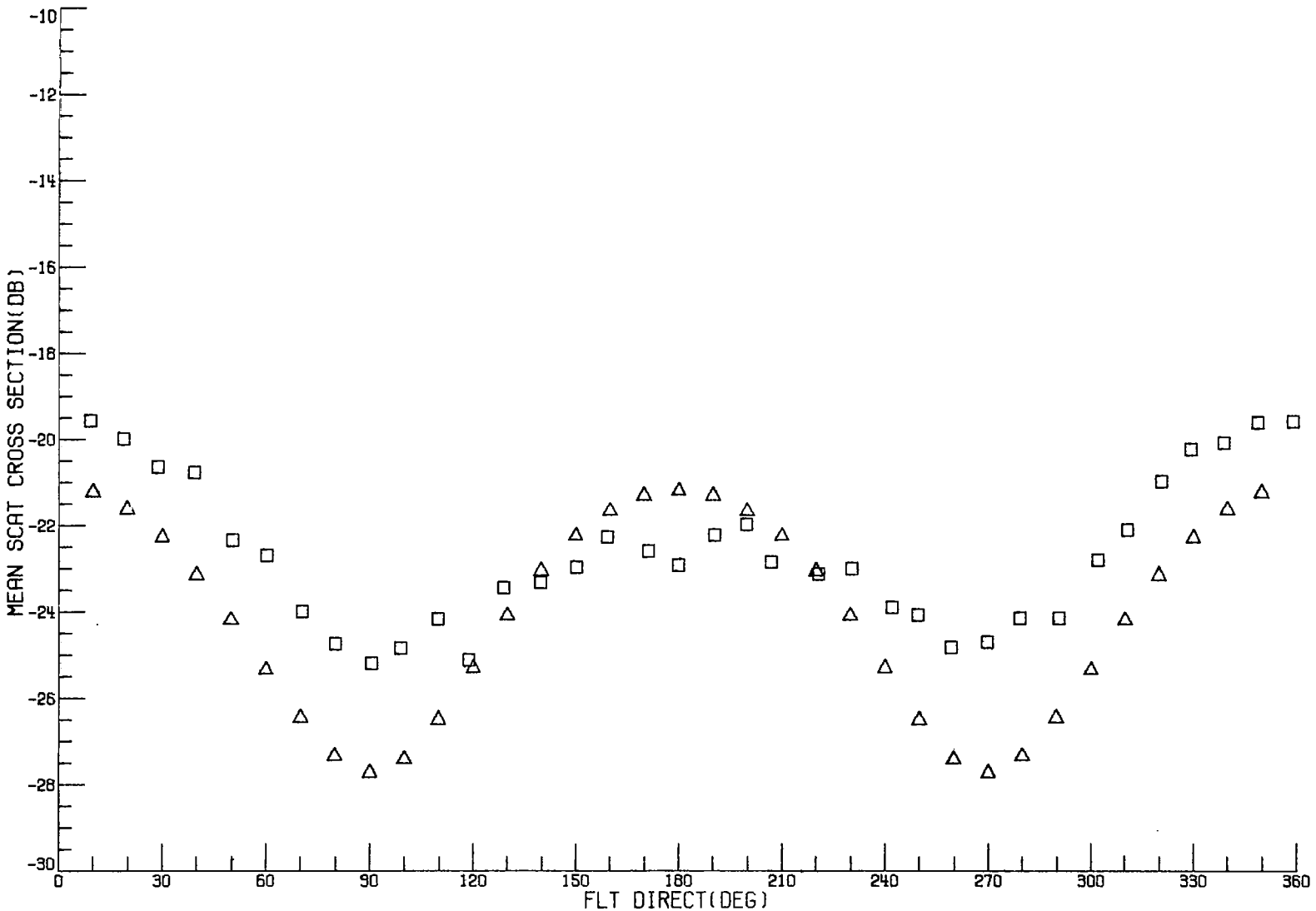

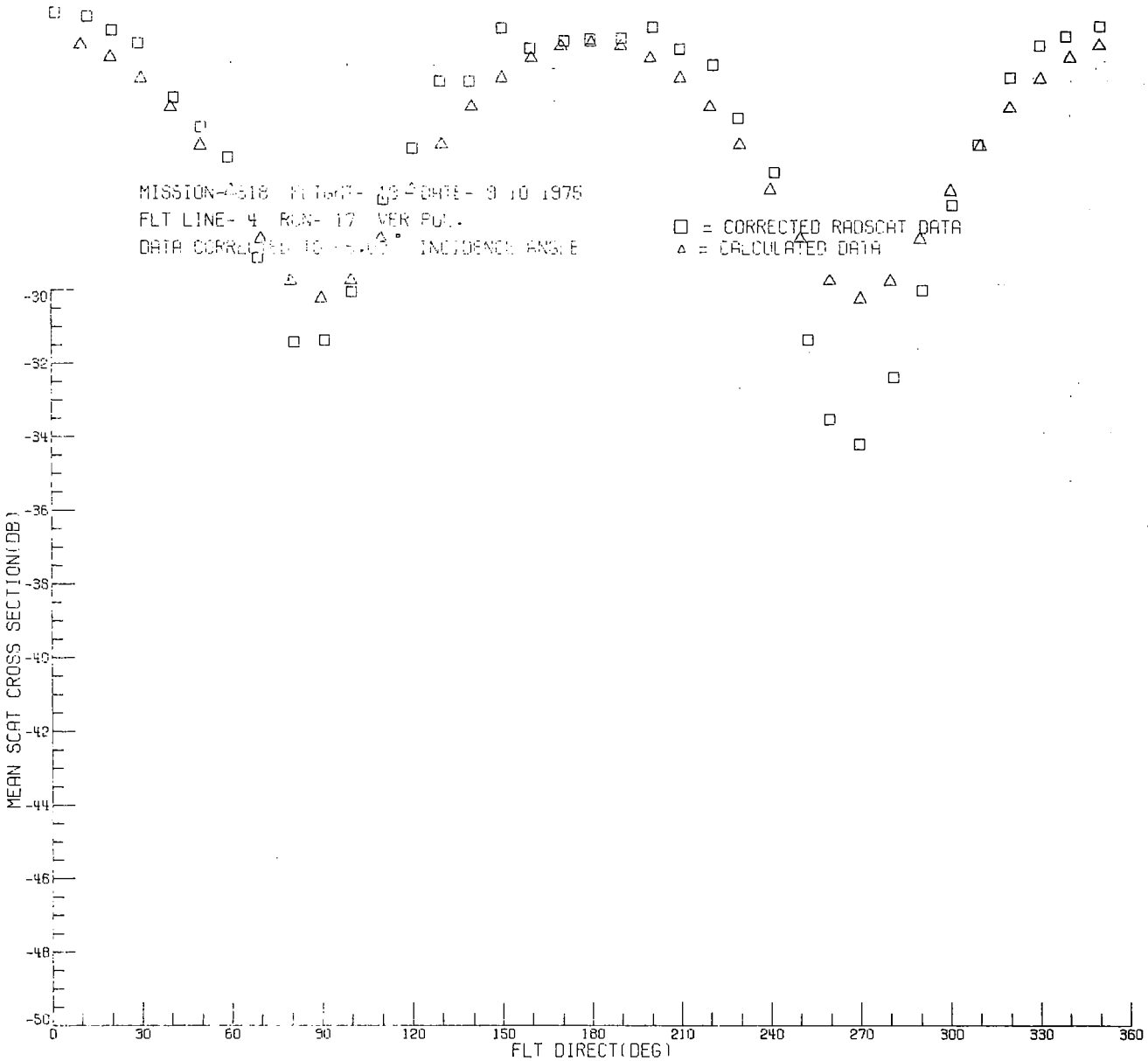
MISSION-A518
FLT LINE- 4 RUN- 17 VER POL.
□ = CORRECTED RADSCAT DATA
△ = CALCULATED DATA
MEAN SCAT CROSS SECTION(DB)
-30
-32
-34
-36
-38
-40
-42
-44
-46
-48
-50
0
30
60
90
120
150
180
210
240
270
300
330
360
FLT DIRECT(DEG)

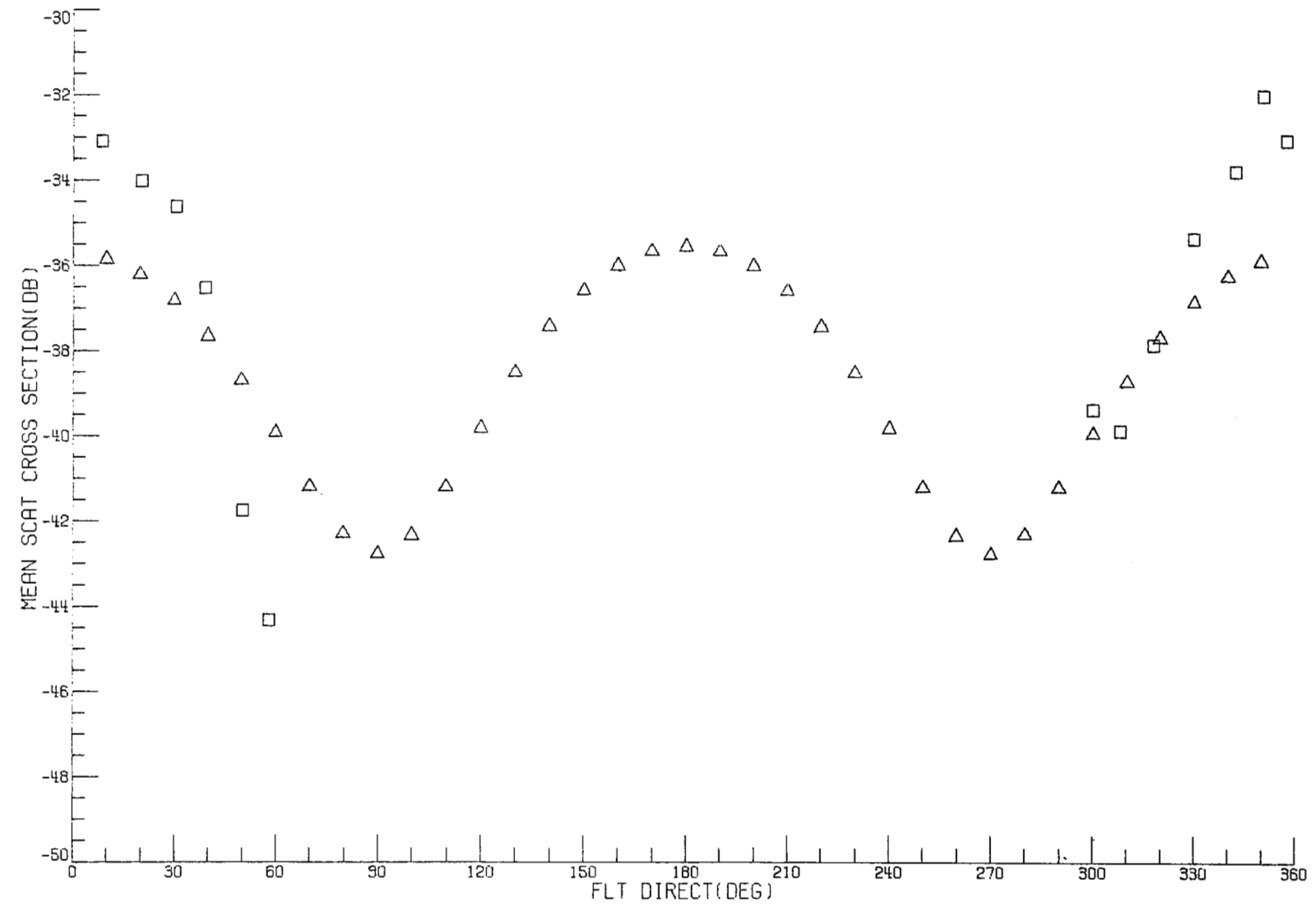
MISSION- 318 FLIGHT- 19 DATE- 9 10 1975
FLT LINE- 4 RUN- 17 HOR POL.
DATA CORRECTED TO 65.00° INCIDENCE ANGLE
CORRECTED RADSCAT DATA
CALCULATED DATA
MEAN SCAT CROSS SECTION(DB)
-30
-32
-34
-36
-38
-40
-42
-44
-46
-48
-50
0
30
60
90
120
150
180
210
240
270
300
330
360
FLT DIRECT(DEG)

DATA FOR A LINE

Flight 19, September 10, 1975

Line 2, Run 6, Crosswind

Wind Speed = 8.0 m/s

Azimuth viewing angle relative to upwind = 265°

Small-Scale Parameters:

$a_0(\kappa_m) = 4.98 \times 10^{-6}$ cm^4

$q = 7.3$

$\kappa_c = 2.50$ cm^{-1}

Power Reflectivity at Nadir:

$R = 0.44$

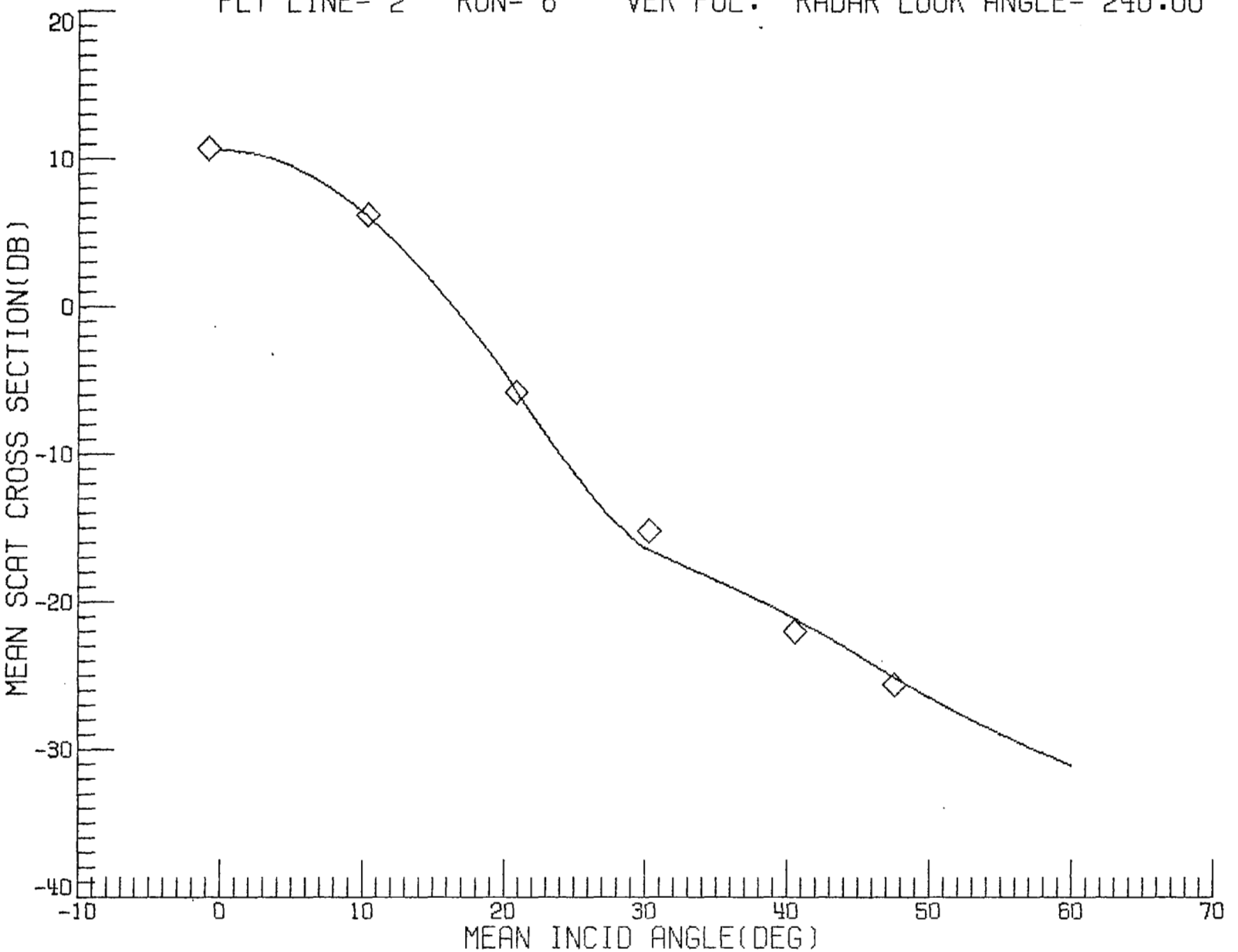
MISSION- 318 FLIGHT- 19 DATE- 9 10 1975 MODE- F.A.
FLT LINE- 2 RUN- 6 VER POL. RADAR LOOK ANGLE- 240.00
MEAN SCAT CROSS SECTION(DB)
20
10
0
-10
-20
-30
-40
-10
0
10
20
30
40
50
60
70
MEAN INCID ANGLE(DEG)

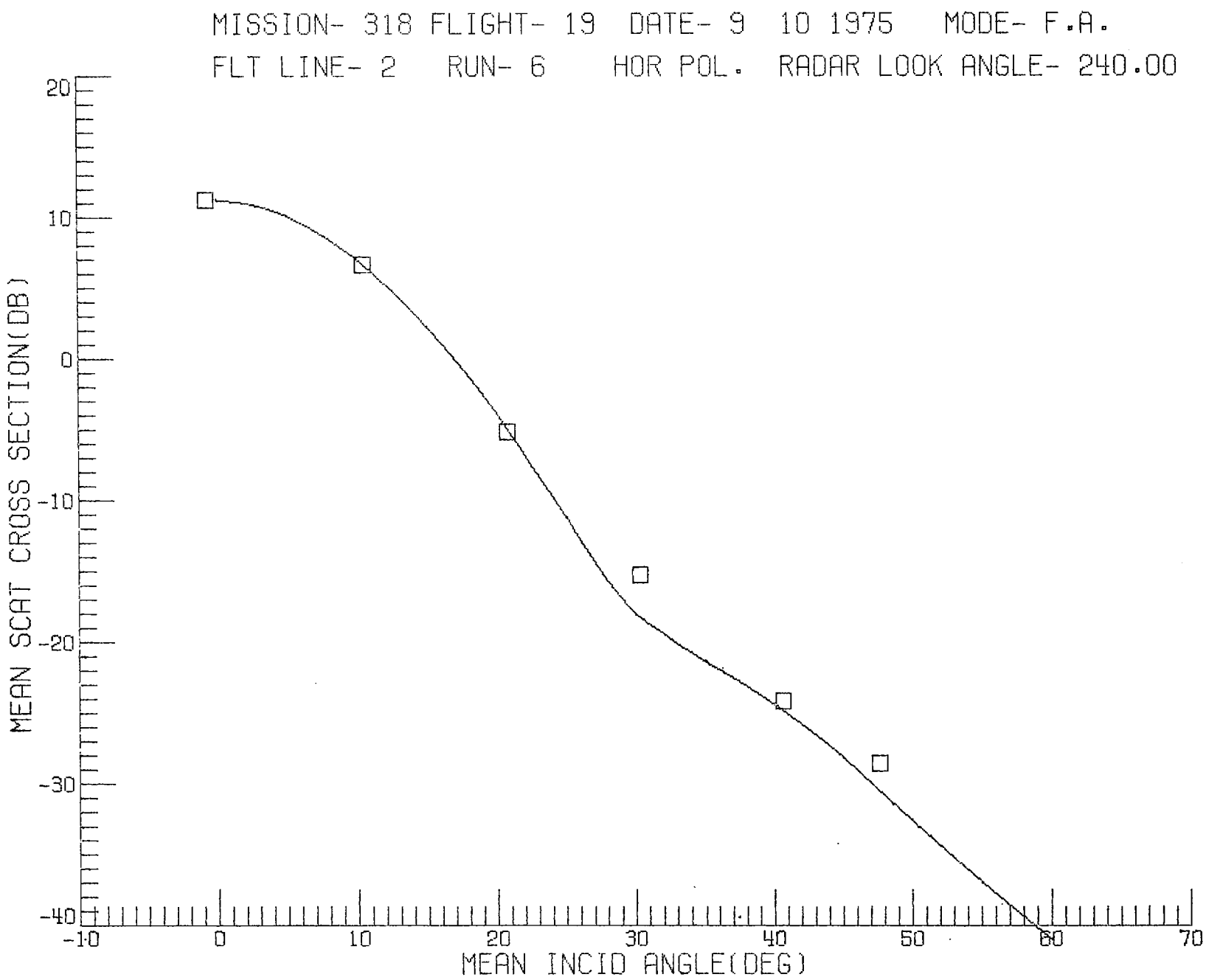
MISSION- 318 FLIGHT- 19 DATE- 9 10 1975 MODE- F.A.
FLT LINE- 2 RUN- 6 HOR POL. RADAR LOOK ANGLE- 240.00
MEAN SCAT CROSS SECTION(DB)
20
10
0
-10
-20
-30
-40
-10
0
10
20
30
40
50
60
70
MEAN INCID ANGLE(DEG)

DATA FOR A LINE

Flight 19, September 10, 1975

Line 3, Run 3, Downwind

Wind Speed = 7.7 m/s

Azimuth viewing angle relative to upwind = 179°

Small-Scale Parameters:

$a_0(\kappa_m) = 3.11 \times 10^{-6}$ cm^4

$q = 4.3$

$\kappa_c = 1.70$ cm^{-1}

Power Reflectivity at Nadir:

$R = 0.44$

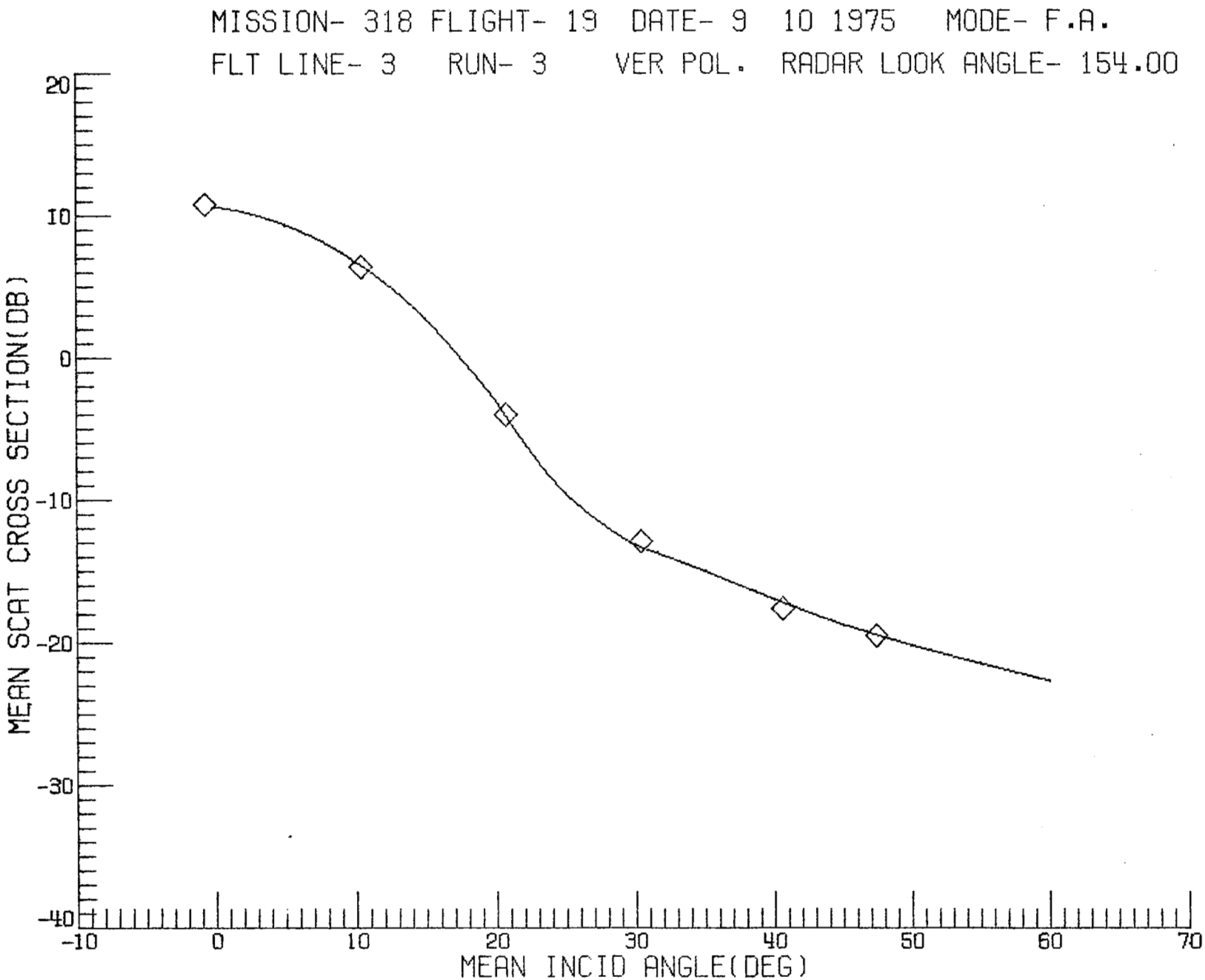
MISSION- 318 FLIGHT- 19 DATE- 9 10 1975 MODE- F.A.
FLT LINE- 3 RUN- 3 VER POL. RADAR LOOK ANGLE- 154.00
MEAN SCAT CROSS SECTION(DB)
20
10
0
-10
-20
-30
-40
-10
0
10
20
30
40
50
60
70
MEAN INCID ANGLE(DEG)

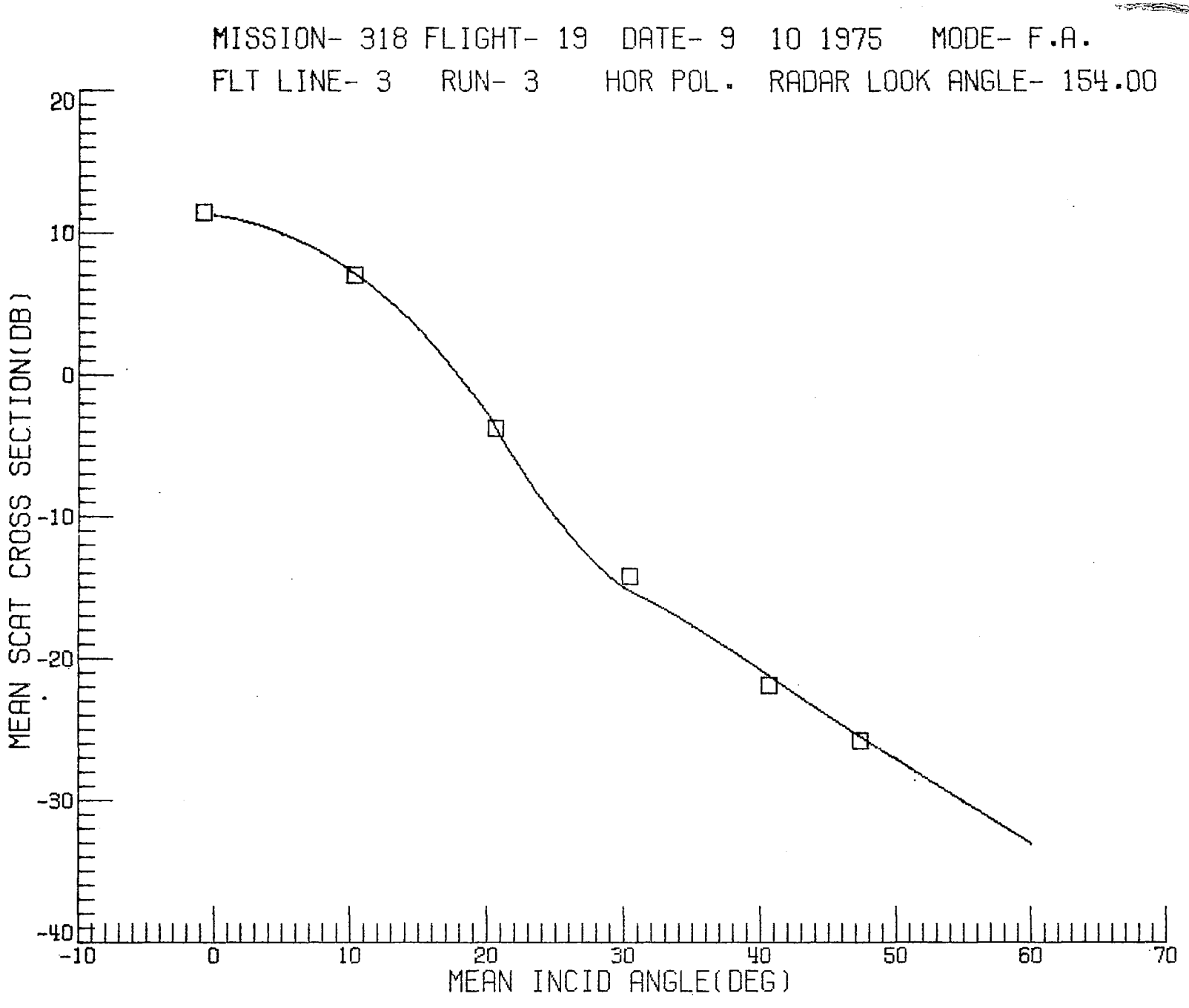
MISSION- 318 FLIGHT- 19 DATE- 9 10 1975 MODE- F.A.
FLT LINE- 3 RUN- 3 HOR POL. RADAR LOOK ANGLE- 154.00
MEAN SCAT CROSS SECTION(DB)
20
10
0
-10
-20
-30
-40
-10
0
10
20
30
40
50
60
70
MEAN INCID ANGLE(DEG)

REFERENCES

Cox, C., and W. Munk, Slopes of the sea surface deduced from photographs of sun glitter, Bul. Scripps Inst. Oceanog. 6, 401-488, 1956.

Phillips, O. M., The Dynamics of the Upper Ocean, Cambridge University Press, London, 1966.

Pierson, W. J., and R. A. Stacy, The elevation, slope, and curvature spectra of a wind roughened sea surface, Contract. Rep. NASA CR-2247, 1973.

Porter, R. A., and F. J. Wentz, Microwave radiometric study of ocean surface characteristics, Contract. Rep. 1-35140, Nat. Environ. Satell. Serv., NOAA, Washington, DC, July 1971.

Rice, S. O., Reflection of electromagnetic waves from slightly rough surfaces, Commun. Pure Appl. Math., 4, 351-378, 1951.

Ruck, G. T., ed., Radar Cross Section Handbook, Plenum Press, New York, 1970.

Wentz, F. J., Radar backscattering from a sea having an anisotropic large-scale surface, NASA CR-145278, 1977.